Anthropogenic and Climate Impacts on Groundwater Resources in the Lower Apalachicola-Chattahoochee-Flint River Basin

by

Subhasis Mitra

A dissertation submitted to the Graduate Faculty of
Auburn University
in partial fulfillment of the
requirements for the Degree of
Doctor of Philosophy

Auburn, Alabama
May 9, 2015

Keywords: Drought, Climate Variability, El Niño Southern Oscillation (ENSO), Groundwater, Irrigation

Approved by

Puneet Srivastava, Chair, Professor of Biosystems Engineering
Ming-Kuo Lee, Professor of Geology and Geography
Latif Kalin, Associate Professor, School of Forestry and Wildlife Sciences
David Blersch, Assistant Professor of Biosystems Engineering

Abstract

El Niño Southern Oscillation (ENSO) is one of the major climate variability cycles around the world and is responsible for droughts in the Southeast United States. These ENSO-induced droughts have been responsible for agricultural losses, water disputes and promotion of water restrictions in the Southeast. In the Apalachicola- Chattahoochee-Flint (ACF) River Basin, in addition to drought, rapid population growth, urban sprawl, and increased agricultural production are threatening the availability of freshwater resources and causing endangered species concerns. As a result, Alabama, Georgia, and Florida have been fighting over the allocation of ACF River Basin water for the past two decades. The water conflict heats up every time there is drought in the basin. This research was conducted to study the effects of ENSO-induced droughts and irrigation pumpage on groundwater levels and groundwater budget components of the Upper Floridan Aquifer (UFA) in the lower ACF River Basin. Results indicate that ENSO exhibits teleconnection with groundwater levels in the UFA. The teleconnection was more prominent during the winter season. The study also found that prolonged droughts severely affect groundwater levels and the groundwater recovery periods can be as much as 2 years. The groundwater model, MODular Finite-Element Model (MODFE), was used to study the effect of irrigation water withdrawal during droughts years of 2010 – 2012. The results showed that groundwater levels and stream-aquifer flux are affected by irrigation water withdrawal. Most of the irrigation water pumped is contributed by loss in aquifer storage and losses in stream-aquifer flux. The results also showed that irrigation during the year 2012

resulted in groundwater levels to fall by as much as 6 ft, and in areas with endangered species concerns. Finally, MODFE was also used to study the effect of possible future increased irrigation levels on groundwater levels and stream-aquifer flux in the study area during the drought water year of 2012. The effect of application of irrigation restrictions in vulnerable regions was also studied. Results showed that elevated irrigation levels severely affect groundwater levels in the vulnerable regions. Doubling of irrigation resulted in as much as 11 ft decline in groundwater levels in the Spring Creek subwatershed. Additionally, the study also found that irrigation water-withdrawal exhibits a linear relationship with stream-aquifer flux in the study area.

Acknowledgement

Many people have encouraged and helped me through my academic journey at Auburn and I'm forever grateful to them. I would like to express my sincere gratitude towards my advisor and mentor Dr. Puneet Srivastava for providing me this opportunity and for persevering as my advisor. I would also like to express my heartfelt gratitude to my dissertation advisory committee Dr. Latif Kalin, Dr. Ming-Kuo Lee and Dr. David Blersch for their help and time. I would also like to thank Lynn Torak for his tremendous help, support and feedback during the course of my research. I would specially like to thank Sarmistha Singh for her invaluable help and support. This dissertation would not have been possible without her. Special thanks to Nafiul Islam, Golbahar Mihrhosseini, Suresh Sharma, Sarah Richards, Ryan McGehee and many others for their help, encouragement and above all friendship during the course of this study. I would also like to thank all in the Biosystems Engineering Department at Auburn University for extending assistance and support during this research.

I am indebted to my parents for their unconditional love, support, encouragement and blessings throughout my life that instilled in me the confidence of pursuing even the hardest things and to harbor an optimistic approach.

To all my friends and family, this journey would not have been possible without your love and support.

Table of Contents

List of Tables

List of Figures

List of Abbreviations

ACF	Apalachicola-Chattahoochee-Flint River basin
AMO	Atlantic Multi-Decadal Oscillation
CMRA	6 Consecutive 3-Month Running Average
DEWS	Drought Early Warning System
ENSO	El Niño Southern Oscillation
FR	Flint River
FRDPA	Flint River Drought Protection Act
GAEPD	Georgia Environmental Protection Division
GHZ	Geohydrologic Zone
GW	Groundwater Levels
GWB	Groundwater Budget
GWC	Groundwater Budget Components
HIM	Heavily Irrigated Months
ICH	Ichawaynochaway Creek Subwatershed
IR	Irrigated Scenario
KMC	Kinchafunee-Muckalee Creek Subwatershed
MODFE	MODular Finite Element Model
NAO	North Atlantic Oscillation

NCDC	National Climatic Data Center
NIDIS	National Integrated Drought Information System
NOAA	National Oceanic and Atmospheric Administration
NI	Non-Irrigated Scenario
PDO	Pacific Decadal Oscillation
SCW	Spring Creek Subwatershed
SST	Sea-Surface Temperature
UFA	Upper Floridan Aquifer
USCU	Upper Semi-Confining Unit
WTC	Wavelet Coherence Transform
WY11	Water Year 2011
WY12	Water Year 2012
XWT	Cross Wavelet Transform

Chapter 1

Introduction

1.1 Background

Water resources around the world are under major stress. An ever increasing global population and increased irrigated agriculture is putting a lot of stress on the freshwater resources such as rivers, lakes and underground aquifers. During the past 50 years, total human water consumption has increased by almost three-fold, and by 2025, five out of eight people are projected to live under conditions of water scarcity (Postel et al. 1996). These existing water shortages can be exacerbated by interannual, decadal and multi-decadal climate variability cycles and climate change. Identification, understanding and quantification of this variability is important to minimize its consequences on water resources and agriculture (Climate Research Committee and National Research Council 1995). Time and again, various information sources such as visual observations, instrumental records, and paleoclimatic data have been witness to variability in the earth's climatic system on time scales ranging from years to decades to centuries. Understanding and determination of how these climate variations affect components of the hydrologic cycle and occurrences, intensities, and locations of extreme events is one of the major challenges for scientists and decision makers. Climate variability cycles, such as El Niño Southern Oscillation (ENSO), Pacific Decadal Oscillation (PDO), Atlantic Multi-Decadal Oscillation (AMO) and North Atlantic Oscillation (NAO) are responsible and also can alter the behavior of extreme events, such as hurricanes, floods, heat waves and droughts around the world (Intergovernmental

Panel on Climate Change, IPCC 2001). Due to limited understanding and knowledge of the physical mechanisms and their influences on hydrologic cycles it is important to study their impacts on water resources to be able to cope and better manage future water shortages resulting due to droughts induced by these climate variability cycles.

The Southeast because of very high evapotranspiration rate, increased demand by ever growing urban centers, and increased irrigated agriculture and intra-annual climate variability often suffers from low surface water availability during summer months and more so during droughts. Therefore, identification of the onset of a drought, its persistence and conclusion, from climate signals that are chaotic and exhibit annual, inter-annual, decadal, or much longer periods of variability, can be of extreme importance for better managing of scarce water resources. Therefore, this dissertation focuses on studying the effects of climate variability on groundwater hydrologic components in the southeastern United States. In this study, variability has been defined as fluctuations in climatic anomalies extending from monthly to seasonal and multi-annual scale, which are quantified via standard climate indices.

1.2 El Niño Southern Oscillation (ENSO)

El Niño Southern Oscillation (ENSO) is an ocean-atmospheric phenomenon caused by fluctuations in sea surface temperature (SST) and pressure along the equatorial pacific and is one of the major causes of climate variations and resulting climatic anomalies around the world. ENSO occurs with a predictable periodicity of 2-7 years, while retaining variability in its magnitude and climatic effects around the world (Cane, 2005). ENSO has three phases, a warm phase-El Niño, a cold phase-La Niña, and a Neutral phase. Walker (1924) coined the term 'Southern Oscillation' to describe pressure fluctuations between the Southeast Pacific subtropical

high-pressure cell (Philander and Rasmusson, 1985) and the North Australian—Indonesian low-pressure trough. The difference in pressure between Djakarta, Indonesia and between Easter Island in the Southeast Pacific is representative of the Southern Oscillation Index (SOI) (Walker and Bliss, 1926) and is defined as the normalized monthly mean pressure anomaly difference between Tahiti (18°S, 150°W) and Darwin (12°S, 131°E) (Chen, 1982). During the non- El Niño years, the pressure is higher than normal in the Southeast Pacific and lower than normal at the north Australia area representing a positive SOI. SOI is negative when the Southeast Pacific exhibits below-normal pressure and northern Australia exhibits above-normal pressure.

Due to the lack of clear understanding on the exact cause of El Niño, several theories have been proposed. A study conducted by Hickey (1975) showed that the El Niño phase correlated with the lowering in southeast trade winds near Peru resulting in the coastal upwelling of the cold subsurface waters to decrease leaving warm water at the surface. His study suggested that it is caused by a minimum in the meridional wind stress east of 120°W and a minimum in the zonal wind stress at longitudes west of 120°W.

The warm phase of ENSO- El Niño, meaning “little boy” or “Christ child” in Spanish, represents the phenomenon that starts at the beginning of the year (Christmas time). El Niño occurs when warm water drifts towards the east Pacific from the western Pacific region due to weakening of trade winds (Figure 1.1 a). This results in warm ocean surface water off the coast of South America, which increases the temperature of the water in the equatorial eastern Pacific. This change in ocean temperatures in the eastern Pacific region tends to change the weather of the region and has far reaching impacts around the world. The clouds and rainstorms associated with warm ocean water also shift toward the east pacific, thus bringing rain over the deserts of Peru which is supposed to occur over the tropical rain forests of Indonesia. This leads to forest

fires and drought in the one part of the Pacific (western) and flooding in other the part of the Pacific (South America).

La Niña meaning "The Little Girl" in Spanish is referred as anti-El Niño, or simply "a cold event" or "a cold episode." La Niña conditions are associated by strong trade wind blowing to the west leading to shallow equatorial thermocline in the east causing heat to concentrate in the western tropical pacific, strengthening convection and westerly winds that move back to the east (Figure 1.1 b). A strong Walker circulation (air circulation in the lower atmosphere) is introduced by these conditions. La Niña results in the periodic (every 3 to 5 years) cooling of ocean surface temperatures in the central and east-central equatorial Pacific.

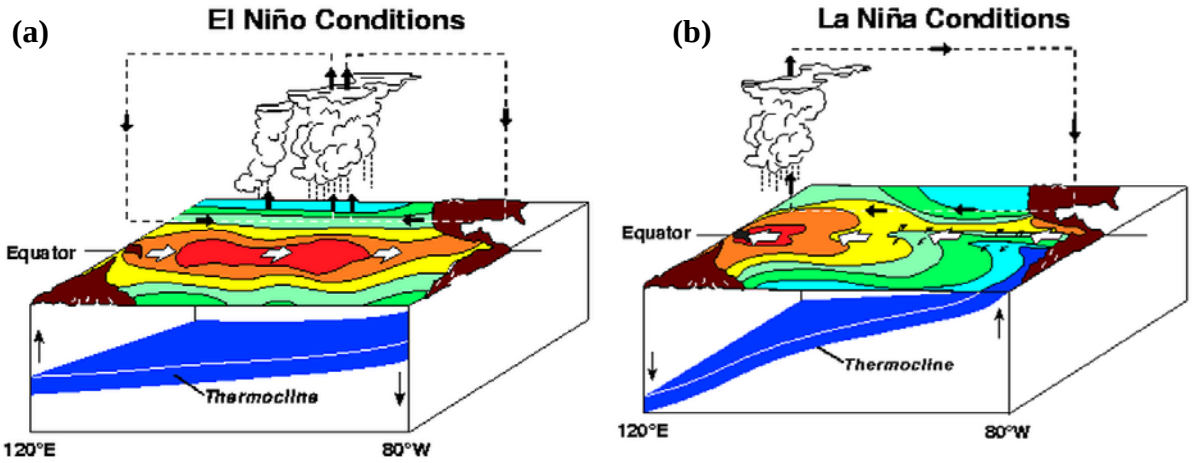

Figure 1.1 The ENSO phases of (a) El Niño and (b) La Niña.
(Source: http://www.pmel.noaa.gov/tao/elnino/el-nino-story.html)

ENSO has also been found to interact with other global climatic patterns, such as the Atlantic Multi-Decadal Oscillation (AMO), North Atlantic Oscillation (NAO) and Pacific Decadal Oscillation (PDO). Better understanding and quantification of these interactions could in the future lead to improved climate/weather forecasts and also be used in predicting climatic

events such as storms, droughts, heat waves and hurricane activity. A study conducted by Huang et al. (1998) found that warm ENSO events between 1900 and 1995 exhibit significant interaction with NAO.

Gershunov and Barnett (1998) showed that PDO moderated ENSO patterns thus suggesting interaction with different climatic cycles. Highly negative PDO is associated with a strong La Niña phase and highly positive PDO phases have been found to correlate with a strong El Niño phase. A study conducted by Newman et al. (2003) also showed that PDO and ENSO interact with each and also suggested that prediction of PDO might help with improved ENSO forecast.

1.3 ENSO Indices

Climate indices are quantitative measures that help in monitoring significant pattern and the state of a climate cycle, and are represented generally as time series. Indices have been developed for various climatic events such as hurricane activity, air pressure differences, sea surface temperatures and precipitation during monsoon seasons. Sea surface temperatures (SST) in specific areas around the world have been used to describe various climatic cycles. There are various indices based on different classes used to define the phase and strength of ENSO. Some of the indicators, such as Niño-1, Niño 2, Niño-3, Niño-4, Niño-3.4, Japan Meteorological Agency (JMA), and the modified JMA are based on sea surface temperatures recorded in different regions in the tropical Pacific Ocean calculated using 100-year SST anomaly dataset (Rasmusson and Carpenter 1982; Glantz 2001). Regions for Niño-1 and Niño 2 index have been found to be highly responsive to seasonal changes induced by El Niño. Changes in SST in Niño 4 region are influenced by longitudinal shifts of the east-west temperature gradients in the

equatorial region. The region of JMA index lies within the Niño-3 region (4°N-4°S and 150°-90°W) and is defined by spatial average of 5-month running mean of SST anomalies.

Other ENSO indicators such as Southern Oscillation Index (SOI) defined by the US Climate Prediction Center are based on the atmospheric (pressure) component of the ENSO cycle. SOI is based on the mean sea level atmospheric pressure difference between Eastern and Western Pacific (Troup 1965; Chen 1982; Ropelewski and Jones 1987). Prolonged negative SOI values have been found to be associated with warmer ocean water across the eastern tropical Pacific Ocean and representing El Niño phases whereas prolonged positive periods of SOI have been found to coincide with La Niña phases.

Other indices such as the multivariate ENSO index (MEI) (Wolter and Timlin 1993) and trans- Niño index (TNI) (Trenberth and Stepaniak 2001) are complex indicators and are based on combinations of different factors. Each of these ENSO indices use different regions for recording of the sea surface temperature or pressure and are tailored towards different regions around the world. The scientific community presently lacks consensus on the ENSO index that best defines the strength, duration and timing of the ENSO cycle. The MEI is a composite index that uses SST, sea-level pressure, cloudiness, zonal and meridional surface wind and surface air temperature (Wolter and Timlin, 1993). It has strong correlation with SST and SOI indices in identifying ENSO phases. The TNI index is defined as the scaled difference between sea surface temperature anomalies in the Niño 1+2 and Niño 4 regions. TNI has been found to be able to show the formation of ENSO phases but unable to capture their occurrence.

The Niño-3.4 index is based on the region of 5°N -5°S and 170°W - 120°W of the Pacific ocean (Trenberth and Hoar, 1996). In this region, the sea level temperature and pressure anomalies have been found to exhibit strong correlation with each other and also have been

found to bear most relevance with the Southeast United States. Therefore, Niño-3.4 index has been used in this study.

1.4 ENSO Impacts

The ENSO phenomenon has been found to have variable effects around the world (Molnar and Cane, 2007) and is linked to the regional precipitation-generating mechanisms (Waylen and Poveda, 2002). Studies have linked ENSO events with climate extremes around the globe (Ropelewski and Halpert 1987; Halpert and Ropelewski 1992). Temperature and precipitation patterns around the world have also been found to be majorly influenced by ENSO (Barsugli et al. 1999; McCabe and Dettinger, 1999). Equatorial South America experiences the most prominent signals of ENSO. In equatorial South America, El Niño phases results in below normal precipitation whereas the La Niña years are associated with above normal precipitation (Aceituno, 1988). El Niño phase has the opposite effects in eastern equatorial and southeast Africa where it results in greater than normal precipitation and cooler temperatures (Ropelewski and Halpert, 1987; Halpert and Ropelewski, 1992). Higher precipitation has been observed during La Niña years in northern Europe (Fraedrich and Muller, 1992). Historically, El Niño events have also been found to be linked with failed Indian monsoon (Ropelewski and Halpert, 1987; Kiladis and Diaz, 1989; Charles et al., 1997). In Australia, El Niño phases have been found to be linked with less winter precipitation in eastern Australia, whereas, La Niña years have been found to be wetter (Nicholls et al., 1996). Relationships have been found between El Niño and Indonesian droughts by Quinn et al. (1978).

In addition to influencing temperature and precipitation around the world (Chiew et al., 1998; Roy, 2006; Keener et al., 2007), ENSO have also been found to affect groundwater, streamflow,

monsoon, droughts, flood frequency and crop yield in different parts of the world (McCabe and Dettinger 1999; Kahya and Drakup, 1993; Gurdak et al., 2007; Rajagopalan and Lall, 1998; Piechota and Dracup, 1999; Kulkarni, 2000; Tootle et al., 2005; and Hansen et al. 2001).

Studies have found strong correlation between ENSO, precipitation and streamflow (Redmond and Koch, 1991; Eltahir, 1996; Berri and Flamenco, 1999; Simpson and Colodner, 1999). ENSO have been found to have strong correlations with temperature and precipitation in the North American continent as well. Studies have reported that the northern United States experiences less precipitation and warmer winters during El Niño events. These effects are reversed during the La Niña phase (Rasmusson and Wallace, 1983; Halpert and Ropelewski, 1992). Studies showing the effect the past ENSO events and its effects on the hydrologic cycle present a picture of what might happen in the present and future and above all also provide with a possibility of better forecast and managing of events such as droughts.

1.5 ENSO and the Southeast USA

The southeastern United States is a region with rapid population growth, increased agricultural production and expanding urban areas. The need to provide freshwater and nutrients to Apalachicola Bay to supply a struggling shellfish industry is causing increased pressure on water resources of this region, which is further exacerbated by climate variability experienced by this region. Climate variability in the Southeast is majorly influenced by ENSO (Enfield et al., 2001, Martinez, 2011). The El Niño phase of ENSO is characterized by cooler and wetter (than normal) winters, while the La Niña phase is characterized by warmer and drier winters (Kiladis and Diaz, 1989; Hansen and Maul, 1991; Schmidt and Luther, 2002) in the Southeast. ENSO has

also been found to affect rainfall, water quality, and streamflow in watersheds of Georgia and Florida (Sharda et al., 2012; Schmidt et al., 2001; Keener et al., 2010; Johnson et al., 2013). Another phenomenon that affects climate variability in the region is the Pacific Decadal Oscillation (PDO), a decades-long version of El Nino-like events that causes warm or cool ocean-temperature anomalies in the northeast and tropical Pacific (Zhang and others, 1997). PDO has been found to have a regulating effect on ENSO, with ENSO signals being amplified during a strong (warm) phase of PDO (Gershunov and Barnett, 1998a and 1998b). Climate anomalies are weakened during high PDO-La Niña and low PDO-El Niño events (or coincidences). NAO has also been found to affect temperatures in the region. During La Niña phase, temperatures are in the region are lower than normal during the negative (cool) phase of NAO. Since ENSO affects precipitation, temperature, and streamflow in the Southeast, it can be hypothesized that groundwater resources in this region are also affected by ENSO as infiltrating precipitation recharges aquifers, which in turn affects discharge to streams.

1.6 Droughts in the Southeast USA

Large seasonal to inter-annual climate variability cycles are responsible for frequent droughts in the Southeast US. Due to the dependence of the region on water recharge during the winter season, drier conditions in winter (La Niña) have an enormous impact on the overall water resources of the region. The Southeast suffers from low surface water availability during summer months even during non La Niña phases due to very high evapotranspiration rates, increased demand by growing urban centers, increased irrigated agriculture. Since the early 1980s, a series of droughts in the Southeast US have resulted in agricultural productivity losses, prompted water-use restrictions, and exacerbated water conflicts between neighboring states (e.g., the Tri-

State Water Wars; Southern Environmental Law Center). The La Niña phase of 1998 -1999 was associated with a drought, the effects of which persisted until 2000- 2001 in parts of Alabama, Georgia and Florida. Recently, the drought conditions during the winter of 2007 and during 2010 – 2012 in the Southeast, especially in the Georgia, have resulted in losses to region's agricultural sector. An estimate put forth by the University of Georgia's Center for Agribusiness and Economic Development mentions that the 2007 drought was responsible for reduced total agricultural economic output by as much as $1.3 billion in Georgia (CAED 2007).

1.7 Tri-State Water Dispute

The Tri-State Water dispute is a dispute over water use between the neighboring states of Alabama, Georgia and Florida. The major river basins in this conflict are the Apalachicola-Chattahoochee-Flint River basin (ACF) (Figure 1.2) and the Alabama-Coosa-Tallapoosa River Basin (ACT). The major challenges regarding the dispute are the diversion of water from Lake Lanier on the Chattahoochee River for consumption by the growing city of Atlanta and increase in irrigated agriculture in southwest Georgia.

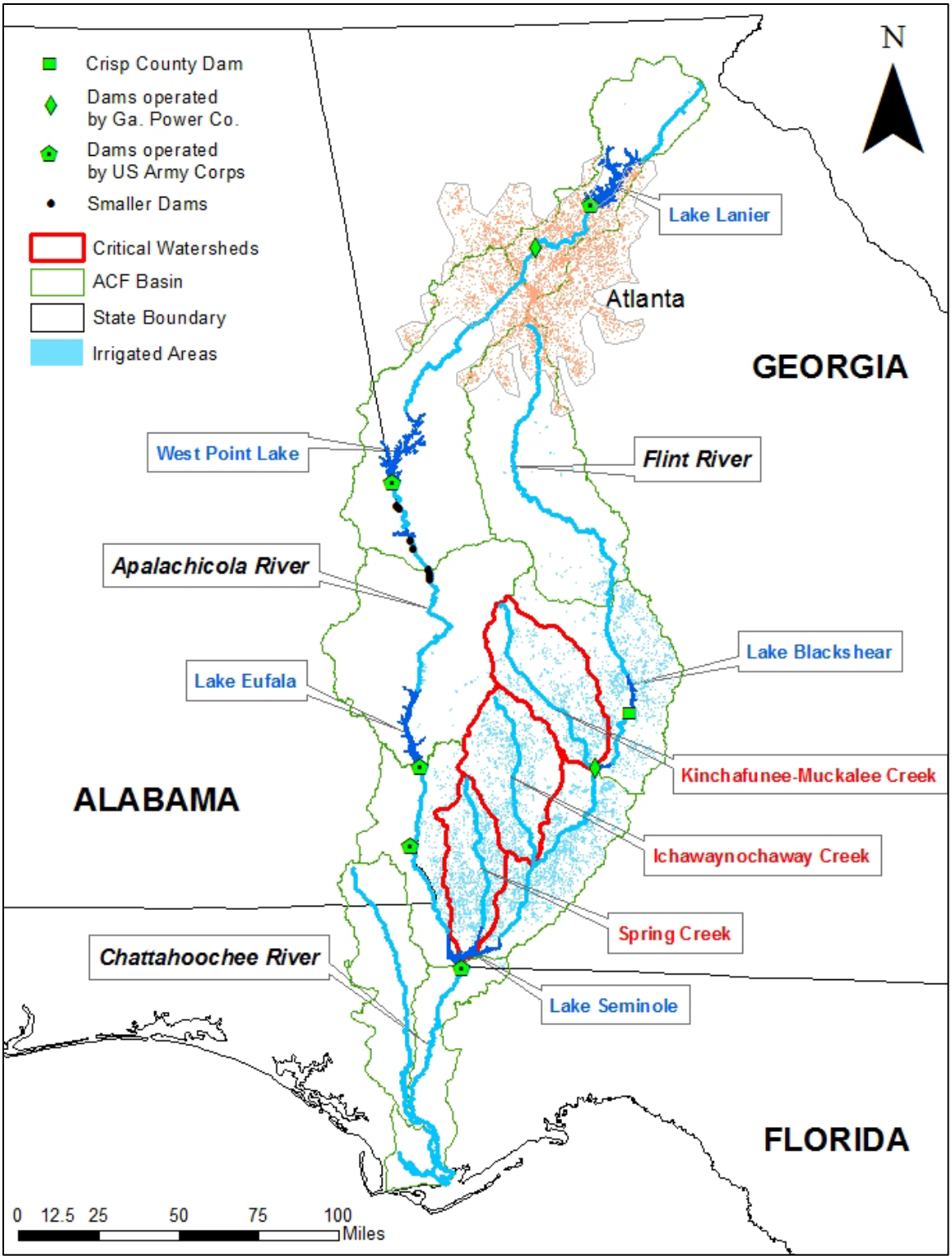

Figure 1.2 The ACF River Basin showing the irrigated acreage in southwest Georgia, the city of Atlanta, the lakes operated by USCOE on Chattachoochee River and the critical subwatersheds.

The dispute started in the early 1990s when Alabama and Florida filed a lawsuit against the US Army Corps of Engineers (USCOE) and Georgia over diversion of water from Lake Lanier and consequent decrease in flow levels in the Apalachicola River. A series of dams on the Chattahoochee River regulate its flow, and during droughts, lowering of flow levels in the Chattahoochee River result in lowering of flow levels at the downstream ends. In addition, increased irrigated agriculture in southwest Georgia from the Upper Floridan Aquifer during droughts also threatens flow in the Flint River due to the connection of the aquifer to the Flint River and its tributaries. This irrigation induced streamflow depletion in the Flint River and diversion of flow from Chattachoochee River during drought results in lowering of flow levels at the downstream Apalachicola River having environmental concerns and posing a threat to the shellfish industry in the Apalachicola Bay.

Attempts have been made to negotiate out of courts to reach mutually acceptable solutions to the problems. But talks broke down and the litigations resumed and are still pending in courts (as of 2014).

1.8 Drought Early Warning and Response System in the Southeast

The development of the Drought Early Warning and Response System (DEWS) for the Southeast has been tasked with the National Integrated Drought Information System (NIDIS). NIDIS is an interagency collaboration aimed at helping society manage droughts by shifting focus from reactive drought response to a proactive stance. NIDIS selected the ACF River basin as a priority project for the development of DEWS for the Southeast owing to the complexity of the water management issues and water conflicts in the region. Another organization that deals with droughts and other aspects of climate variability and risks associated with it in the Southeast

US is the Southeast Climate Consortium (SECC). NIDIS and SECC routinely conduct ACF River Basin Drought Assessment Webinars in which a number of drought indicators are used. Indicators derived from streamflows, precipitation, and lake levels are extensively used for determining the onset, persistence, and conclusion of droughts, while the use of groundwater levels as drought indicators has not been fully explored yet. Presently, the ACF River Basin Drought Assessment Webinars use groundwater levels from a single well in Upper Floridan Aquifer as a drought indicator. Since groundwater level fluctuations can vary enormously on a spatially variable scale, depending on geo-hydrologic conditions of the area, using a single well as drought indicator with respect to groundwater for the entire area can present an incorrect picture of status and severity of the drought in the area.

1.9 Groundwater and DEWS for the Southeast

Groundwater levels respond to prolonged seasonal and climatic time scales. At any given instance, a hydrologic or meteorological drought might end in the basin, but the groundwater levels might continue to show depleted levels, and due to stream-aquifer connection, parts of the basin (mainly in the Flint River Basin part of the ACF) might still continue to experience low streamflow conditions. Apart from time scales, groundwater level fluctuation is also spatially variable in the lower ACF, depending on the geo-hydrology (Torak and Jones, 2006). Groundwater levels showing more depleted levels in some areas (critical areas) compared to other, even though being in close-proximity, also suggest that some regions in the ACF might be more prone to groundwater extraction than others. These critical areas can further pose risks to flow in the Flint River during droughts if they are situated at close proximity to the river or if the river is in direct hydrologic connection to Upper Floridan Aquifer in those areas. Therefore,

groundwater levels at multiple locations, serving as drought indicators in the ACF, could present a more comprehensive picture of the status and severity of droughts in the area and help develop more robust and realistic indicators of droughts related to groundwater in the area. Therefore, in this study, identification of locations affected by ENSO-induced droughts can help identify wells that can be used as drought indicators for the NIDIS-SECC webinars.

1.10 Problem Statement

To address the issues related to irrigation induced streamflow reduction and development of DEWS for the ACF, and to ensure adequate streamflow in the Flint River, it is important to study the link between ENSO-induced droughts-groundwater and streamflow. Initially, the study will focus on establishing a relationship between ENSO-induced droughts and fluctuations in groundwater levels. Equally important will be to study aspects related to the onset, persistence and conclusion of drought impacts on groundwater at a spatially variable scale. Analysis of other aspects such as recovery periods and seasonal impacts of ENSO phases on groundwater levels would add great value to knowledge related to sustainability of groundwater resources in the area as well. As groundwater level fluctuates at very prolonged time scales, it would also be interesting to analyze specific drought events based on their longevity. After studying the ENSO-groundwater level relationship it would be important to focus on La Niña events and its relation to anthropogenic activities (irrigation) that is of prime concern in the area. It is important to note that impacts of drought events on groundwater levels (GWL) in the area have two aspects: 1. Climatic: Depleted GWL due to below average precipitation only and 2. Anthropogenic: Depleted GWL due to increased irrigation water withdrawal from the aquifer. Separating the impacts of the climatic and anthropogenic aspects will finally help in building a clearer picture

on the extent and role of irrigation water withdrawal towards depletion of flows in the Flint River. Further, identification of critical areas (areas where GWL are more prone to irrigation withdrawal) might help reduce the footprint of irrigation-induced streamflow depletion. Furthermore, to analyze the effect of future increases in irrigation pumpage and possible restrictions on irrigation on groundwater levels and groundwater budget components should also be studied.

1.11 Dissertation Objectives

The objectives of this dissertation are:

1. To study and quantify the effect of ENSO-induced climate variability on groundwater levels under different overburden conditions.
2. To quantify how pumping for irrigation exacerbates the effect of La Niña (droughts) on groundwater levels and groundwater budget components.
3. To analyze the effects of simulated irrigation levels on groundwater levels and groundwater budget components during a La Niña event.

1.12 Dissertation Organization

The primary focus of this dissertation is on the above laid objectives and includes 6 chapters. Chapter 1 includes introduction, review of literature, problem statement, and objectives of this study. In chapter 1, a brief description of ENSO and its impacts around the world and in the Southeast has been presented. In addition to that, the tri-state water dispute and the drought early warning systems for the Southeast have been discussed. Chapters 2 to 4 present the methodology and results of the three objectives listed above. In chapter 2, fluctuations in

groundwater levels to ENSO phases under different overburden conditions have been discussed. Chapter 2 also deals with the recovery periods and impacts of prolonged droughts on groundwater levels. The results of this chapter have already been accepted for publication in the journal *Transactions of ASABE* (Mitra et al., 2014). Chapter 3 deals with the effects of irrigation during droughts on groundwater levels and groundwater budget components and stream-aquifer flux. This chapter also looks at the contribution of each budget component to irrigation withdrawal. This chapter will be submitted to the Journal of Hydrologic Sciences. Chapter 4 presents the effect of elevated irrigation pumpage on groundwater levels and groundwater budget components in the event of droughts. This chapter will be submitted to the Journal of Hydrologic Sciences. Chapter 5 presents the major conclusions and findings of this study. Finally, Chapter 6 provides suggestions for future work.

Chapter 2

Effect of ENSO induced Climate Variability on Groundwater Levels in the Lower Apalachicola-Chattahoochee-Flint River Basin

2.1 Abstract

Rapid population growth, urban sprawl, and increased agricultural production in the Apalachicola- Chattahoochee-Flint (ACF) River Basin are threatening the availability of freshwater resources and greatly affecting supply of fresh water to the Apalachicola Bay that supports a struggling shellfish industry. As a result, Alabama, Georgia, and Florida have been fighting over the allocation of ACF River Basin water for the past three decades. The water conflict heats up every time there is drought in the basin. In the Southeast, droughts are mainly caused by the La Niña phase of the seasonal-to-interannual climate variability phenomenon El Niño Southern Oscillation (ENSO). Understanding and quantifying the impact of ENSO-induced climate variability on precipitation, soil moisture, stream flows, and groundwater levels can provide valuable information for sustainable management of water resources in this region. This study was undertaken to quantify the impact of ENSO on groundwater levels in the lower ACF River Basin, an area highly dependent on groundwater for agricultural water use. Twenty-one observation wells with 30 years of monthly groundwater level data were used to study the ENSO-groundwater level relationship. Wavelet analysis techniques were used to study the teleconnection between ESNO and groundwater levels, while the Mann-Whitney tests were conducted to quantify the impact. The effect of prolonged La Niñas on groundwater levels and

their corresponding recovery periods were also studied. Results indicate a strong relationship between groundwater level fluctuations and ENSO. This relationship was found to be stronger during the recharge season (December-April) as compared to the non-recharge or agricultural-irrigation season (May-November). The results obtained can be used to identify wells suitable for drought indicators in the study area.

2.2 Introduction

Natural climate variability phenomena such as El Niño Southern Oscillation (ENSO), North Atlantic Oscillation (NAO), and Pacific Decadal Oscillation (PDO) affects precipitation, temperature, and stream flows, and can significantly alter the behavior of extreme events such as hurricanes, floods, droughts, and cold waves (IPCC 2001). Among these, ENSO-induced climate variability is one of the major causes of natural variability in the global climate system (Diaz and Markgraf, 1992). Identification, understanding and quantification of this variability are important for minimizing its effect on water resources and agriculture (Climate Research Committee and National Research Council 1995).

ENSO is a complex ocean-atmospheric phenomenon that occurs in the equatorial Pacific and has three phases, namely, El Niño, La Niña and Neutral (oceanic component). El Niño and La Niña refer to the warm and cool phases, respectively, of sea surface temperatures in the central Pacific Ocean that leads to changes in climatic conditions around the world (Quinn 1994; Aceituno 1992). Numerous indices, namely, Niño-1+2, Niño-3, Niño-4 and Niño-3.4, have been derived based on the sea surface temperature (SST) anomalies. ENSO have been found to affect temperature and precipitation around the world (Chiew et al., 1998; Roy, 2006; Keener et al., 2007). Additionally, ENSO has also been shown to affect groundwater, streamflow, monsoon,

droughts, flood frequency and crop yield in different parts of the world (McCabe and Dettinger 1999; Kahya and Drakup, 1993; Gurdak et al., 2007; Chiew et al., 1998; Rajagopalan and Lall, 1998; Piechota and Dracup, 1999; Kulkarni, 2000; Roy, 2006; Keener et al., 2007; Tootle et al., 2005; and Hansen et al. 2001).

In the Southeast US, rapid population growth, urban sprawl, and increased agricultural production in the Apalachicola- Chattahoochee-Flint (ACF) River Basin are threatening the availability of freshwater resources and greatly affect the supply of fresh water to the Apalachicola Bay that supports a struggling shellfish industry. This stress on water resources of the basin is further exacerbated by large seasonal-to-interannual climate variability experienced by this region. Climate variability in the Southeast is mainly influenced by ENSO, which is the primary reason for droughts in the Southeast (Enfield et al. 2001). The El Niño phase of ENSO is characterized by cooler and wetter (than normal) winters, while the La Niña phase is characterized by warmer and drier winters (Kiladis and Diaz, 1989; Hansen and Maul, 1991; Schmidt and Luther, 2002). In the Southeast, ENSO has been found to affect rainfall, water quality, and streamflow in watersheds of Alabama (AL), Georgia (GA) and Florida (FL) (Sharda et al., 2012; Schmidt et al., 2001; Keener et al., 2010; Johnson et al., 2013). ENSO-induced droughts during 2000-01, 2007 and 2010-12 have not only caused losses in agricultural productivity but have also prompted water-use restrictions and have intensified long-term conflicts among competing water interests in neighboring states, i.e., the Tri-State Water Wars between the state of AL, GA and FL (Southern Environmental Law Center). Over the last two decades, the conflict has been marked by litigations and failed negotiations. The tri-state water conflict owes its seeds to the failure of the state of GA to maintain adequate streamflow levels in the Apalachicola-Flint River during drought events. One of the major aspects of the conflict is

the streamflow reduction in the Flint River (FR) during droughts due to increased pumpage for irrigation, municipal and industrial purposes from surface and groundwater sources in southwest Georgia.

Agriculture in southwest Georgia is heavily dependent on irrigation water withdrawals from surface and groundwater sources. In this region, groundwater sites outnumber surface water sites and groundwater withdrawal can run into hundreds of millions of gallons per day. During La Niña events, excessive irrigation from the Upper Floridan Aquifer (UFA), which is the major groundwater bearing unit, can not only cause lowering of groundwater levels in the aquifer but also reduction of streamflows due to the hydrologic connection between the UFA and FR. Additionally, unhindered exploitation of the groundwater resources in the UFA might also not be sustainable in the long term. Large groundwater withdrawal adversely affects groundwater levels, particularly during dry periods and in areas where the aquifer is overlaid by thick overburden conditions severely limiting aquifer recharge (Torak and Painter, 2006; Jones and Torak, 2006). This reduction in groundwater levels due to irrigation can cause further reduction in streamflow levels at places where the stream and aquifer are hydrologically connected. Irrigation-induced streamflow reduction in the FR also contributes to water quality degradation, high-temperature issues, and endangered/threatened species concerns in the Apalachicola River, situated downstream of the FR (Figure 2.1).

GA's major drought management policy, The Flint River Drought Protection Act (formulated to compensate farmers for not irrigating their crops in the events of droughts to avoid irrigation-induced streamflow reduction), has failed in solving the water conflicts in the region, owing to the infectiveness of the policy and lack of funds. *Due to the complexity of drought-water management issues, failure of present drought management policies, and*

importance of groundwater resources for agricultural, municipal and industrial purposes in the watershed, it is important to understand relationships between ENSO-induced droughts and groundwater levels in the area. In this study, link between ENSO-induced climate variability and groundwater levels in the lower ACF River Basin was explored using wavelet analysis. The non-parametric Mann-Whitney tests were used to quantify the impact. Effects of severe droughts on groundwater levels and recovery periods were also studied to present a complete picture of ENSO-induced droughts on groundwater levels in the area.

2.3 Materials and Methods

2.3.1 Study Area

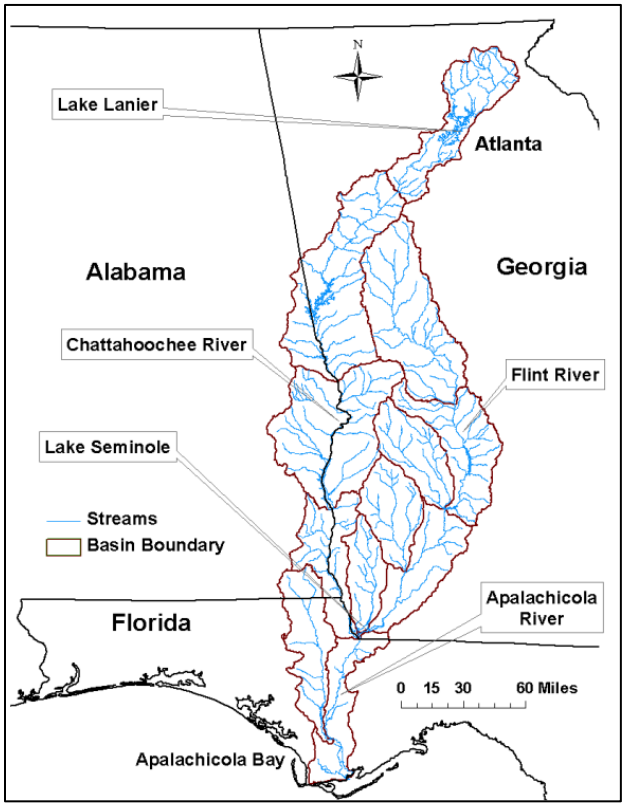

Figure 2.1 Apalachicola-Chattahoochee-Flint (ACF) River basin in AL, FL, and GA. Note: Most of the basin lies in GA, the Chattahoochee River forms the boundary between AL and GA, and the Chattahoochee and Flint Rivers meet in Lake Seminole at the GA-FL border to form the Apalachicola River.

The study area is located in the lower ACF River Basin in parts of southwestern Georgia, northwestern Florida, and southeastern Alabama (Figure 2.2). The climate of the lower ACF River Basin is humid subtropical with long summers and mild winters. The average annual temperature and precipitation in the study area is about 64^{o}F and 50 in, respectively. About 4,632 mi^{2} of land area recharges groundwater is contained in the karst UFA, which eventually contributes to surface water in the ACF River Basin. The UFA system is the major water-bearing formation of the region and consists of aquifers and semi-confining layers with four distinct hydrogeologic units, namely the surficial aquifer system, upper semi-confining unit (USCU), UFA, and lower confining unit (Torak and Painter, 2006). These hydrogeologic units are defined by differences in hydraulic characteristics and lithology, which might not coincide with the geologic-unit boundaries. The USCU lying above the UFA is the major source of vertical leakage to the UFA.

Groundwater levels in the UFA respond to seasonal climatic effects, such as changes in precipitation, temperature, and stream and lake stage, in addition to stresses such as groundwater withdrawal for agricultural, municipal and industrial purposes. Fluctuations in groundwater levels in the UFA also depend on aquifer thickness and location in the ACF River Basin, hydraulic characteristics of the USCU, proximity to surface streams or lake system, and pumping.

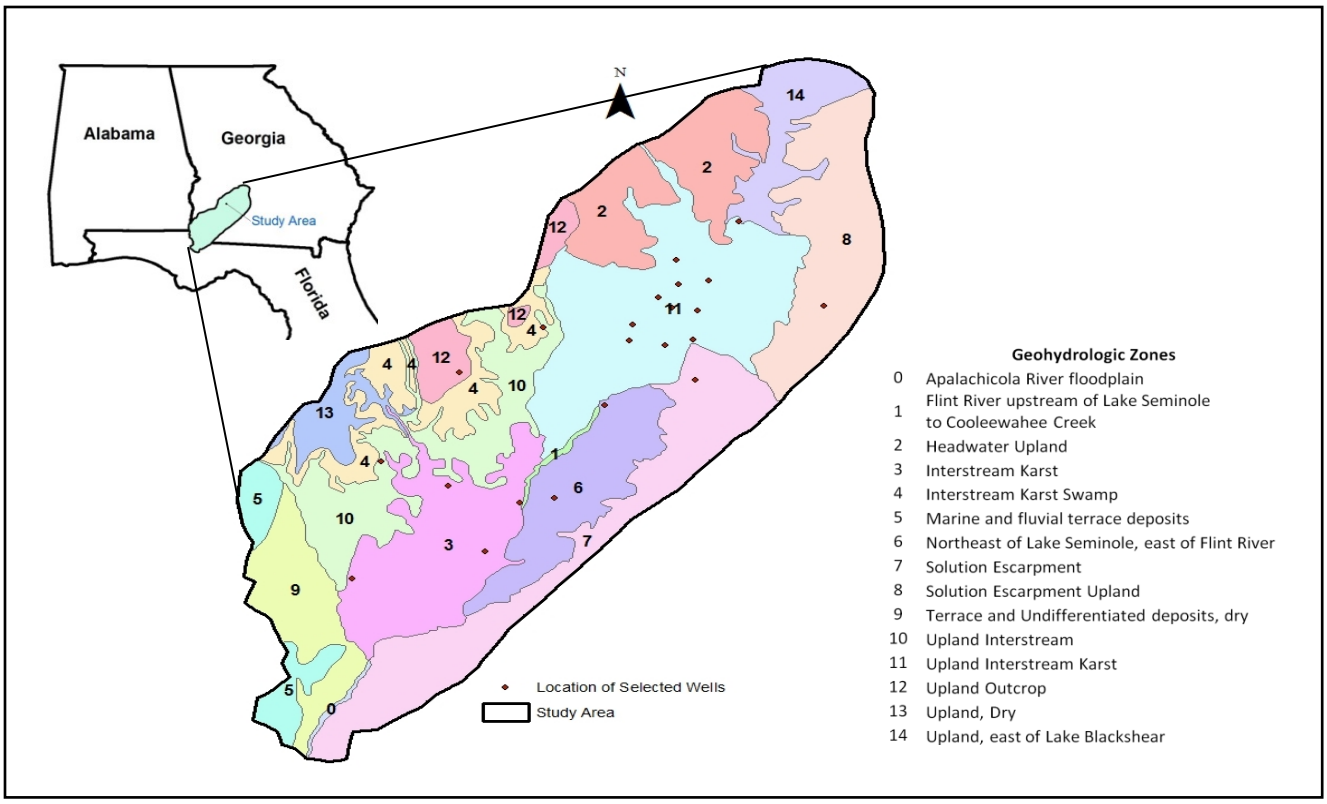

Figure 2.2 Location of the study area, observation wells, and geo-hydrologic zones. (Modified after Torak and Painter, 2006).

2.3.2 ENSO Index and Groundwater Level Data

The Niño-3.4 index provided by the National Oceanic and Atmospheric Administration's (NOAA) Climate Prediction Center (CPC) was used for the definition of the ENSO phase. This index is based on 3-month running mean of SST anomalies (ERSST.v3b) in the Niño 3.4 region (5^oN to 5^oS, 120^oW to 170^oW). The El Niño phase is defined when the Niño 3.4 index is above $+0.5^oC$ while the La Niña phase is defined when the Niño 3.4 index is below -0.5^oC. A neutral phase is defined when the Niño 3.4 index value is between -0.5^oC and $+0.5^oC$. For this study, the middle month of the 3-month running average value of the Niño 3.4 index was assigned to that month.

Daily groundwater (GW) level data for 21 observation wells (Appendix A.1) in the study area were obtained from the United States Geological Survey, Georgia. All the wells were in the

UFA, and the period of recorded data varied from 25 to 30 years. Time series of monthly groundwater level averages were calculated for each observation well. Finally, the period with the most complete monthly data for each well was used for the analysis. ENSO phase effects on monthly groundwater levels were studied using groundwater anomalies, which were calculated by subtracting the historical (period-of-record) average monthly GW levels from time series of monthly average GW levels. Thus, a negative anomaly represents a lower monthly GW level than historical (period-of-record) monthly average, or normal, GW levels; a positive anomaly indicates a higher than normal GW level. For the wavelet analysis, the wells with most complete data were used. Average GW levels for months having five or fewer missing daily values were calculated by ignoring the missing data and computing the average monthly GW levels.

2.3.3 Wavelet Analysis

Hydrological time series are statistically non-stationary (Coulibaly and Baldwin, 2005). The series may exhibit periodic signals that can vary in amplitude and frequency during the historical time period. Wavelet analysis examines the relationship between two time series to determine the prevailing modes of variability and their variation over the time period. In this study, wavelet analysis technique was used to quantify and visualize statistically significant changes in ENSO SST anomalies and GW level variance during the historical time period. Using the wavelet analysis, the magnitude and frequency of occurrence of ENSO phases and its relationship (co-variance, shared power, and phase correlations) to GW level anomalies can be detected over a multi-decadal time scale. Wavelet analysis was done for wells under three overburden conditions: (i) Well 08G001 - overburden below 50ft (shallow), (ii) Well 10G313 - overburden 50 – 100 ft (moderately deep aquifer) and (iii) Well 15L020 - overburden in excess

of 100ft (deep aquifer). The wavelet analysis was conducted to determine if GW levels respond to changes in ENSO SST anomalies. Below we provide brief explanations of the wavelet analyses performed in this study. More detail can be found in Torrence and Compo (1998).

2.3.4 Continuous Wavelet Transform (CWT)

The CWT analyses localize recurrent oscillations in time series by transforming it into time and frequency space. Any time series, x_n *(n = 0…..N-1)* with time spacing δt has a wavelet function $\Psi_0(\eta)$ with zero mean and is localized in time and frequency space. The choice of the wavelet function is determined by the data series. In this analysis, the Morlet Wavelet function is used whose function depends on a non-dimensional frequency, ω_o (default value 6), and non-dimensional time parameter, η.

$$\psi_0(\eta) = \pi^{-1/4} e^{-i\omega_0\eta} e^{-\eta/2} \tag{1}$$

The continuous wavelet transform $W_n(s)$ of a discrete sequence x_n, which is a scaled and translated version of $\Psi_0(\eta)$, is given by the following equation:

$$W_n(s) = \sum_{n'=0}^{n-1} X_{n'} \psi^* \left[\frac{(n'-n)\delta t}{s} \right] \tag{2}$$

where n' is the translated time index, n is the localized time index, s is the wavelet scale, Ψ is the normalized wavelet and (*) is the complex conjugate. The null hypothesis is that the signal is created by a static process with a background power spectrum (P_k), and the statistical significance of the wavelet power can be assessed relative to the null hypothesis. Time series can generally be modeled by a first order autoregressive (AR1) method (Grinsted et al., 2004). The equation of the Fourier power spectrum of an AR1 process (Allen and Smith, 1996) is given by:

$$P_k = \frac{1-\alpha^2}{\left|1-\alpha e^{-2i\pi k}\right|^2} \tag{3}$$

where, k is a Fourier frequency index, and α is autocorrelation at lag-1.

2.3.5 Cross-Wavelet Transform (XWT) and Wavelet Coherence Transform (WCT)

Although regions of high power can be seen in the WCT, a direct analysis of two time series will help in finding distinct regions of high shared power and thus significance. XWT examines whether regions in time frequency space with high common power have a consistent phase relationship, suggestive of casualty between the time series (Grinsted et al., 2004). For two time series, *X* and *Y*, with different wavelet transforms $W_{nX}(s)$ and $W_{nY}(s)$, the cross wavelet transform is defined as:

$$W_n^{xy}(s) = W_s^X(s) W_n^{Y*}(s) \tag{4}$$

where, $\left|W_n^{xy}(s)\right|$ is the cross-wavelet power and (*) represents the complex conjugate. In addition to XWT, WCT was used to evaluate the local co-variance of the two time series in time-frequency space, which may or may not exhibit high power. As XWT lose significance in visualizing shared power, WCT finds larger significant areas compared to XWT. The wavelet coherence transform for two time series (Grinsted et al., 2004) is given by:

$$R_n^2 = \frac{\left|S(s^{-1}W_n^{XY}(s)\right|^2}{S(s^{-1}\left|S(W_n^X(s)\right|^2).S(s^{-1}\left|S(W_n^Y(s)\right|^2)} \tag{5}$$

where, *S* is a smoothing operator for the wavelet function. This expression resembles the correlation coefficient indicating that wavelet coherence is actually correlation in time-frequency space. Statistical significance levels for the wavelet coherence were evaluated using Monte Carlo methods. XWT and WCT were performed on Niño 3.4 SST time series with GW level anomalies

for different overburden conditions, calculated to 95% significance levels. The software package used for CWT, XWT and WCT analyses was from the Matlab code developed by Aslak Grinsted (http://noc.ac.uk/using-science/crosswavelet-wavelet-coherence).

2.3.6 Groundwater Level Fluctuation and Climate Variability Analysis

Monthly GW level anomalies were sorted by La Niña phases and averaged by recharge (December to April) and non-recharge (May to November) months for all the observation wells. El Niño and La Niña phases of the ENSO cycle were analyzed to study the effects of drought periods on GW level anomalies. The year 2000-01 was especially analyzed to study the effects of strong La Niña events (prolonged droughts) on GW level anomalies. Non-parametric Mann-Whitney tests were used to evaluate the impacts of ENSO phases on the medians of GW level anomalies in the ACF. The Mann-Whitney tests assess whether the observations in one sample tend to be higher than another, makes no assumption of normality, and considers the same distribution for both the samples.

2.3.7 Recovery Periods

For this study, groundwater recovery was associated with the criteria of 6 consecutive 3-month running average (CMRA) of GW level anomalies above -0.25 ft after the end of the La Niña phase. Recovery period was calculated by the time required for the GW levels to meet the CMRA criteria after the end of the La Niña phase. Due to the lack of definitive criteria to study groundwater recovery, the CMRA criteria provided a good representation of the recovery periods. For the calculation of the recovery periods, two particular La Niña events years 1988–89

and 2000–01) were used, which represent short and prolonged La Niña (drought) occurrences, respectively.

2.4 Results and Discussion

2.4.1 Wavelet Analysis

The wavelet power spectra for Niño 3.4 SST, and GW level anomalies for wells 08G001 (shallow), 10G313 (moderately deep) and 15L020 (deep) are shown in Figure 2.3(a-d). As previously known (Wang and Wang, 1996; Torrence and Compo, 1998), SST power is concentrated within the band group of 3–7 years, although the dominant modes and magnitude tend to shift with time.

Groundwater levels in the ACF basin follow the distinct pattern of seasonality of precipitation in the Southeast USA. GW levels in the ACF basin reach a yearly maximum from late winter to early spring due to steady rain, low evapotranspiration, and low agricultural pumping in winter months. Groundwater levels start declining during the growing season due to decrease in recharge by precipitation and are at yearly lows during the mid-fall (Torak and Painter, 2006). Seasonal GW level fluctuations vary throughout of the study area (Torak and Painter, 2006). Groundwater levels fluctuate more where the USCU is thin (less than 30 ft) or absent, due to direct infiltration (where USCU is absent) and vertical downward leakage (recharge) from and (or) through the USCU. The wavelet power spectra used GW levels that spanned 1977–2012 for well 08G001 and 1976–2012 for wells 10G313 and 15L020. For wells 08G001 and 10G313, regions of high power relative to noise background, though not statistically significant, are seen in the wavelet power spectra in the 3–7 year periodicities (Figure 2.3b and 2.3c), which are similar to the periodicities in Niño 3.4 SST (Figure 2.3a). Both wells showed

strong power in the periodicities of 3–5 years and 4–7 years during 1982– 1990 and 1995–2005, respectively (Figure 2.3b and 2.3c), though the power is not statistically significant for well 08G001. High and significant power are seen in wells 08G001 and 10G313 in the 1–2 year period, which is perhaps related to seasonal storms or La Niña events during 1989–1990 and 1999–2001.

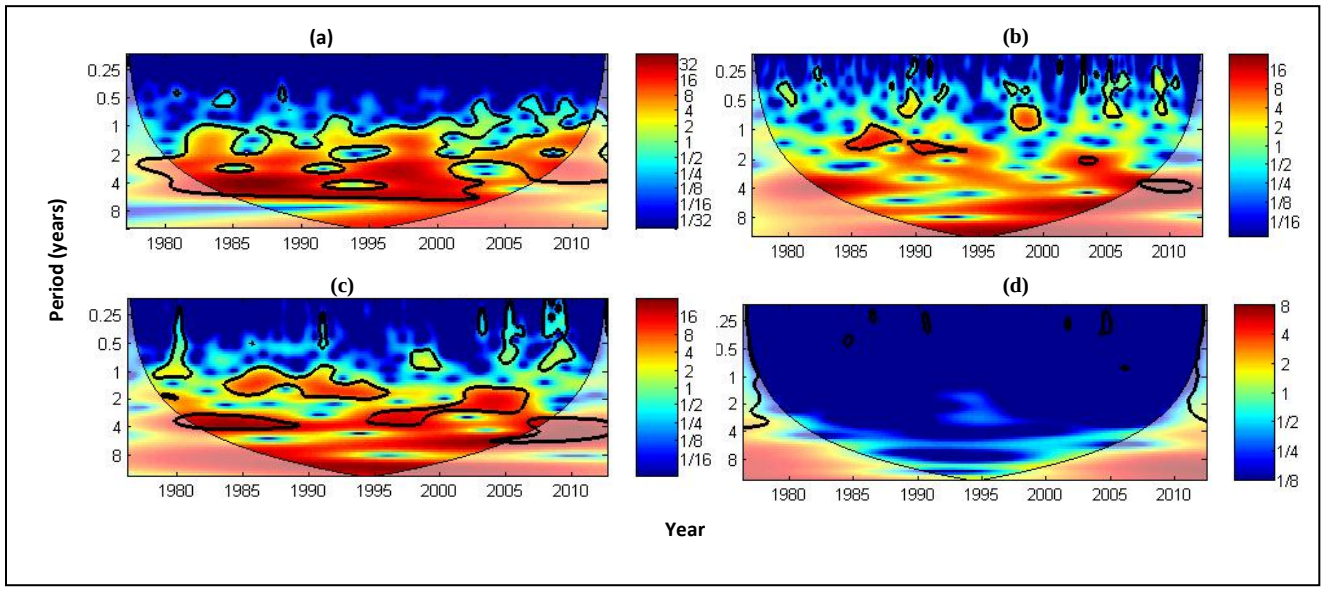

Figure 2.3 Significant Wavelet Power Spectra shown within the cone-of-influence for (a) monthly NIÑO 3.4 sea surface temperatures (^{o}C), (b) GW level anomalies (ft) for well-id 08G001, (c) GW level anomalies (ft) for well-id 10G313, (d) GW level anomalies (ft) for well-id 15L020. Cool colors (blues and white) indicate low wavelet power; warm colors (reds and oranges) indcate high wavelet power in. Black outlines indicate areas significant at the 95% confidence level.

High power was not seen in any periodicities for well 15L020 (Figure 2.3d). The high power 3–7- year periodicities observed in the wavelet spectra of well 08G001 and 10G313 and the lack of such power in well 15L020 suggests that GW levels in shallow and moderately deep overburden conditions exhibit ENSO teleconnection, while such a teleconnection is missing under deep overburden conditions.

2.4.2 Cross-Wavelet Analysis

Unlike wavelet power spectra, where two time series show high common power independently, cross wavelet spectrum analyzes the two time series directly. Significance levels for the cross wavelet transform between Niño 3.4 SST anomalies and monthly GW level anomalies are calculated against regions of red noise background delineated with thick black outlines in figures 2.4(a–c). The cross wavelet transform between SST and GW level anomalies indicates high shared power in areas that also share high power in the single wavelet spectra. That is, wells 08G001 and 10G313 shared high and significant power in periodicities of 3–5 years and 4–7 years from 1982– 1990 and 1995– 2005, respectively (Figure 2.4a and 2.4b). Both wells shared high power in the 3–7 year periodicities, and the significant areas within these periodicities are positively phase locked. This suggests causality between SST and GW level anomalies, which attest to ENSO being the major climate variability phenomenon in the Southeast USA.

The cross wavelet spectra for well 15L020 did not indicate shared high and significant power in any period. It can be inferred from this lack of shared high and significant power in the cross wavelet spectra that GW levels under deep overburden conditions are not affected by ENSO because of the high thickness of USCU having low water bearing properties, which restricts recharge of the UFA by vertical leakage in seasonal response to ENSO-produced variations in precipitation.

2.4.3 Wavelet Coherence Transform

WCT for Niño 3.4 SST and GW level anomalies for wells under different overburden conditions are shown in figure 2.4(d-f).

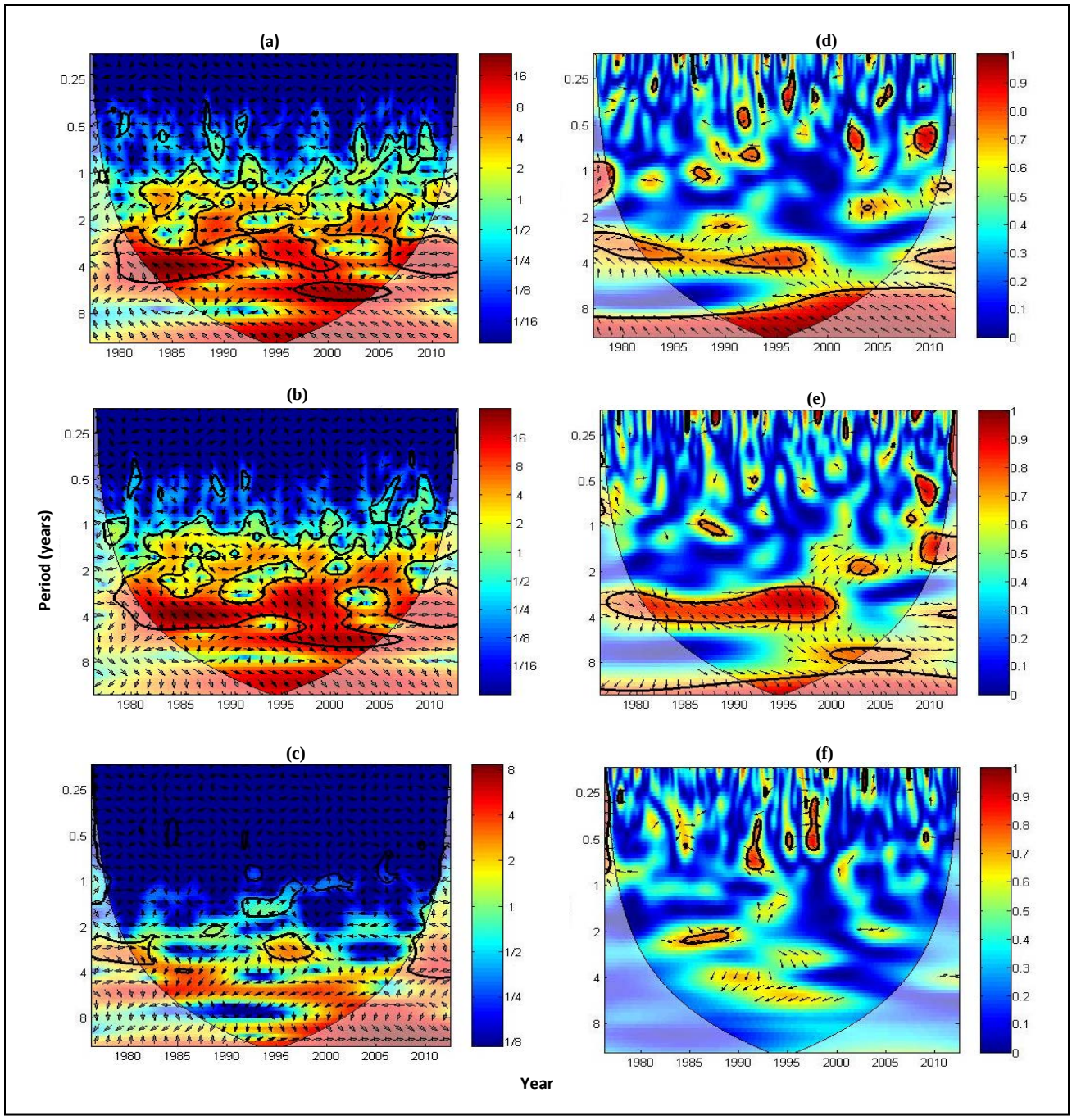

Figure 2.4 Cross Wavelet Spectrum between NIÑO 3.4 sea-surface temperatures and monthly GW level anomalies (ft) for wells (a) 08G001, (b) 10G313, and (c) 15L020. Wavelet Coherence Analysis between NIÑO 3.4 sea-surface temperatures and monthly GW level anomalies (ft) for wells (d) 08G001, (e) 10G313, and (f) 15L020. Black figures outlines indicate significant areas to 95% confidence. Arrows indicate variable's phase relationship. Arrows pointing anti-clockwise represents anti-phase behavoir, while clockwise arrows indicates in-phase behavior.

Significant commonality in cross wavelet transform spectra and wavelet coherence transform analysis does not necessarily translate to casualty, as significant correlation between the two variables being investigated could occur by chance. Although small significant areas in wavelet coherence transform likely can occur by chance and would not necessarily indicate causality, large areas of significance are unlikely due to chance and should be further examined for relations between the two series.

WCT for Niño 3.4 SST and GW level anomalies for well 08G001 (Figure 2.4d) delineate small areas having high and significant power corresponding with 3–7-year periodicities and phase locked positively. These small but significant areas also shared high power in the cross wavelet spectrum (Figure 2.4a) in a phase locked condition, inferring a causal relation between SST and groundwater level anomalies. More areas having high and significant power were prevalent in the WCT for well 10G313 (Figure 2.4e) than for well 08G001 (Figure 2.4d). For well 10G313, the WCT indicates high and significant power with 3–4-year periodicities and phase locked during 1982– 2000. These areas of shared power in WCT also shared power in the cross wavelet spectra (Figure 2.4b) further supporting causality. WCT for well 15L020 (Figure 2.4f) did not indicate significant areas of high power, inferring a non-causal relation. The results of wavelet power spectra, XWT, and WCT demonstrates that groundwater levels in wells 08G001 and 10G313 exhibit ENSO teleconnection in shallow and moderately deep overburden conditions, while groundwater levels under deep overburden conditions (well 15L020) do not show any such relation. This relationship was also validated wavelet analysis results on other long term wells. Those wells also showed significant areas of high power with for XWT and WCT suggesting causality between the ENSO and groundwater level anomalies.

2.4.4 Mann-Whitney Tests

In the previous sections, teleconnections between GW level anomalies and ENSO phases were inferred from wavelet analysis. Further analysis of 21 wells identified a high level of significant difference (p-value < 0.01) between the El Niño and La Niña phase GW level anomalies for all wells, except for well 15L020 (Table 2.1).

Table 2.1 Mann Whitney test results for ENSO phases and monthly GW level anomalies during the entire period of record. P values are significant at 0.01

Well-ID	El Niño[a] (ft)	La Niña[a] (ft)	Diff[c] (ft)	p
06F001	1.35	-3.96	5.30	0.0000
09F520	0.31	-0.62	0.93	0.0000
09G001	1.01	-2.02	3.03	0.0000
10G313	0.72	-2.82	3.54	0.0000
08G001	3.66	-5.50	9.16	0.0000
11J012	0.88	-1.56	2.44	0.0000
13J004	1.32	-1.53	2.85	0.0000
08K001	5.74	-2.42	8.16	0.0000
12K014	0.98	-1.56	2.54	0.0000
13K014	1.32	-2.41	3.73	0.0000
11K003	3.35	-1.52	4.87	0.0000
13L012	0.73	-1.55	2.28	0.0000
12L030	2.33	-2.56	4.88	0.0000
12L028	1.76	-3.19	4.96	0.0000
13L049	2.89	-3.68	6.57	0.0000
12M017	2.20	-1.38	3.58	0.0000
13M006	3.24	-1.62	4.86	0.0000
07H002	3.79	-2.76	6.56	0.0000
12L029	1.82	-2.24	4.07	0.0000
11K015	0.36	-2.03	2.39	0.0000
10K005	0.29	-0.19	0.48	0.0000
15L020*	0.60	-1.95	2.56	0.4129
Median	**1.36**	**-2.02**	**3.66**	

[a] *Values indicate the median for each well.*

[c] *Difference in median for El Niño and La Niña phase.*

* *Not significant wells.*

The median of GW level anomalies during the El Niño and La Niña phases were above and below average, respectively. Studies conducted by Ropelewski and Halpert (1986) found that El Niño and La Niña conditions were associated with above and below average precipitation, respectively, in the Southeast USA, which explains the results in Table 2.1 that considers connection between precipitation and groundwater levels in UFA. Well 08K001 showed the highest increase in the median of GW level anomalies during the El Niño phase, having a median GW level anomaly of 5.74 ft. The highest decline in GW levels during the La Niña is seen in well 08G001 with a GW level anomaly of -5.50 ft (Table 2.1). The differences in GW level anomalies for El Niño and La Niña phases varied for different wells with the highest difference of approximately 9 ft occurring in well 08G001, and a low of 0.48 ft occurring in well 10K005 (Table 2.1). The medians of monthly GW level anomaly for all wells during the El Niño and La Niña phases were 1.36 ft and -2.02 ft, respectively (Table 2.1).

The El Niño and La Niña phases affected GW level anomalies differently during recharge and non-recharge seasons, resulting in larger anomalies during the recharge season than during the non-recharge season, with a few exceptions (Table 2.2). It is important to note that ENSO phases predominantly influence winter precipitation in the Southeast USA (Sharda et al., 2012; Hanson and Maul, 1991; Schmidt et al., 2001), which explains the occurrence of larger differences in GW level anomalies during the recharge season compared to the non-recharge season.

The difference in GW level anomalies between the two ENSO phases during the recharge season is approximately 2.5 times that of the non-recharge season. All wells, except 15L020, showed significant differences in GW level anomalies during the recharge season, while 17 wells showed significant differences during the non-recharge season (Table 2.2).

Table 2.2 Mann Whitney test results of differences in median monthly GW level anomalies caused by El Niño and La Niña phases during recharge and non-recharge seasons. p values are significant at 0.05.

	Recharge				Non Recharge			
Well ID	**EL[b] (ft)**	**LN[c] (ft)**	**diff[a] (ft)**	**P value**	**EL[b] (ft)**	**LN[c] (ft)**	**diff[a] (ft)**	**P value**
06F001	5.40	-5.77	11.17	0.0000	0.10	-3.38	3.48	0.0001
09F520	1.44	-0.83	2.27	0.0000	-0.23	-0.29	0.06	0.3801*
09G001	3.01	-2.72	5.73	0.0000	0.59	-1.66	2.25	0.0000
10G313	1.91	-3.37	5.29	0.0000	-0.30	-2.40	2.10	0.0026
08G001	7.31	-7.93	15.23	0.0000	2.18	-4.35	6.53	0.0000
11J012	2.08	-2.41	4.49	0.0000	0.56	-0.89	1.45	0.0000
13J004	2.22	-3.37	5.59	0.0000	0.31	-0.75	1.05	0.1152
08K001	4.54	-2.21	6.75	0.0000	6.27	-3.30	9.56	0.0000
12K014	2.56	-2.79	5.35	0.0000	0.41	-1.08	1.48	0.0001
13K014	3.12	-3.40	6.52	0.0000	0.69	-1.69	2.39	0.0000
11K003	4.61	-3.23	7.84	0.0000	2.06	-0.86	2.92	0.0376
13L012	2.19	-2.38	4.57	0.0000	0.57	-0.94	1.51	0.0010
12L030	3.64	-2.77	6.42	0.0000	1.47	-2.45	3.92	0.0019
12L028	4.02	-4.06	8.08	0.0000	0.51	-3.17	3.68	0.0136
13L049	6.31	-4.42	10.73	0.0000	1.17	-2.82	3.99	0.0006
12M017	2.94	-1.96	4.90	0.0000	1.06	-0.71	1.77	0.0285
13M006	3.35	-1.51	4.86	0.0000	2.93	-1.73	4.66	0.0000
07H002	3.78	-2.47	6.25	0.0000	3.81	-4.16	7.97	0.0000
12L029	3.14	-2.87	6.01	0.0000	1.02	-1.78	2.81	0.0040
11K015	3.34	-3.21	6.54	0.0000	-0.41	-1.26	0.86	0.9206*
10K005	0.33	-0.39	0.73	0.0000	0.26	0.08	0.19	0.0311
15L020	0.7	-3.91	4.61	0.1559*	0.53	1.28	-0.75	0.7482*
Median	**3.13**	**-2.83**	**6.13**		**0.58**	**-1.68**	**2.32**	

* *Not significant wells.*

[a] *Difference in median monthly groundwater level anomalies for El Niño and La Niña phase.*

[b] *Values indicate the median monthly groundwater level anomalies for each well for the El Niño phase.*

[c] *Values indicate the median monthly groundwater level anomalies for each well for the La Niña phase.*

Figure 2.5 shows a map of distribution of differences in GW level anomalies during recharge and non-recharge seasons corresponding with the different ENSO phases. The distribution of differences in GW level anomalies during recharge and non-recharge seasons corresponding to the two ENSO phases varies considerably by geohydrologic zone (Figure 2.5).

The figure shows that during non-recharge seasons, wells in the geohydrologic zones (GHZ) of Solution Escaprment (well 13J004) and Solution Escarpment Upland (well 15L020) did not show any significant difference. In contrast, significant differences in groundwater anomalies were exhibited during the recharge season in wells located in the Solution Escarpment but not in the Solution Escarpment Upland. Except for wells 09F520 and 11K015 during the non-recharge season, all wells in the Upland interstream karst and Interstream karst GHZs show significant difference in both the seasons. The variation in differences in GW level anomalies during the two ENSO phases throughout the GHZs indicates that overburden conditions alone do not contribute to fluctuations in GW levels.

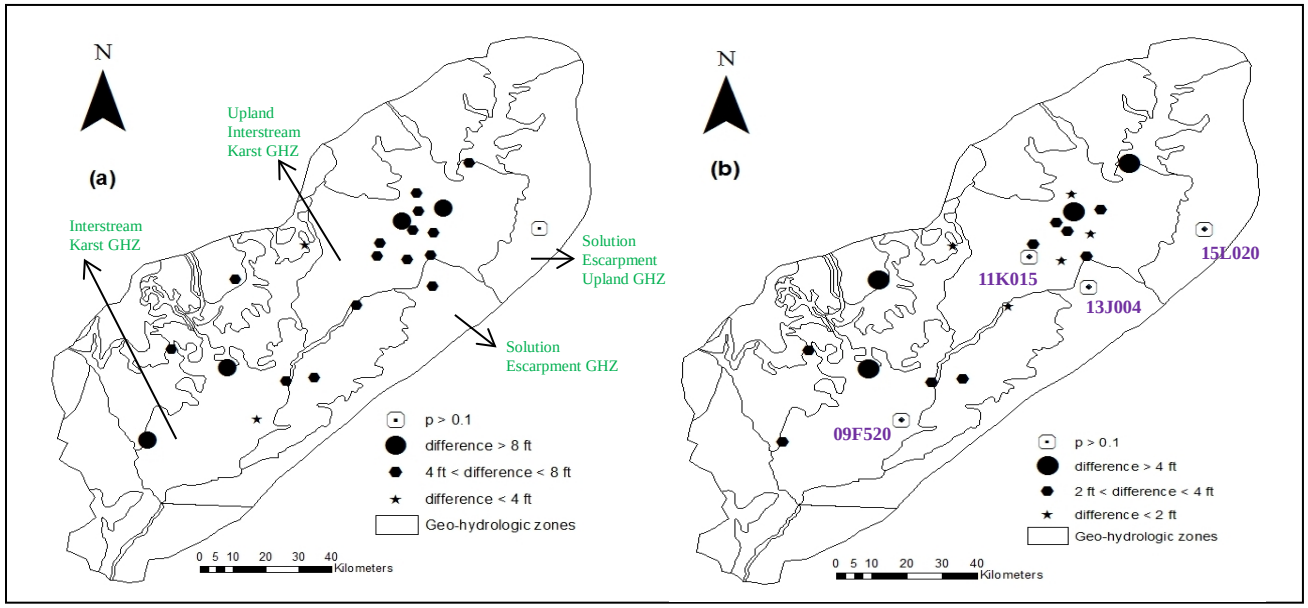

Figure 2.5 Map of the distribution of differences in groundwater level anomalies produced by El Niño and La Niña phases during **(a)** recharge and **(b)** non-recharge seasons.

This suggests that factors, such as, proximity to streams and lakes and the distribution of GW withdrawal for irrigation, municipal and industrial use also play an important role in the development of GW level anomalies. These factors uniquely combine at every location with

uncertainty in hydraulic properties of the Upper Floridan Aquifer system that govern vertical leakage, regional GW flow and storage, and GW and surface-water exchange, and hence add uncertainty to recharge of the UFA.

Table 2.3 shows the mean GW level anomalies during the average La Niña phase and for year 2000-01 (representing severe La Niña event). Comparison of mean GW level anomalies resulting from average and severe La Niña phase events indicates that severe La Niña events, such as the one occurred during 2000-2001, yield, on an average, twice the negative anomalies as those resulting from an average La Niña phase (Table 2.3). Unlike an average La Niña phase (where GW level anomalies differ during recharge and non-recharge season), GW level anomalies associated with the severe La Niña phase of 2000-01 exhibited similarities in magnitude during the recharge and non-recharge seasons. Groundwater levels in nearly all wells yielded larger negative anomalies during the severe La Niña phase than during the average La Niña phase. Maximum negative GW level anomalies for the years 2000–01 were nearly 3.25 to 5.12 times larger than anomalies associated with average La Niña phases during recharge and non-recharge seasons. Negative GW level anomalies exceeded −10 ft at 8 wells and −5 ft at 20 wells. In wells 08G001, 08K001 and 13M006, negative groundwater level anomalies exceeded −15 ft during 2000–01, which demonstrates the effect of a severe and prolonged La Niña phase on groundwater levels (Table 2.3).

GW level depletion during prolonged droughts is not only caused by decreased precipitation but also because of increased agricultural pumpage. The results in Table 2.3 demonstrate the combined effect of these two aspects on GW levels in the area. Such drastic fall in GW levels can lower streamflows in the Flint River and prohibit meeting the minimum flow requirements in the Flint and Apalachicola rivers.

Table 2.3 Comparison of monthly average GW level anomalies for severe (2000-01) and average La Niña phase during recharge and non-recharge seasons.

Well ID	Recharge		Non Recharge		Minimum-2000-01
	Average	Severe	Average	Severe	
06F001	-5.20	-4.49	-2.86	-4.24	-10.44
09F520	-1.11	-3.23	-0.19	-3.16	-5.13
09G001	-2.00	-3.34	-1.35	-3.00	-5.22
10G313	-2.90	-6.70	-2.15	-6.38	-9.60
08G001	-5.83	-8.83	-3.68	-7.90	-14.31
11J012	-1.93	-2.52	-0.98	-2.07	-4.64
13J004	-2.54	-5.91	-0.94	-5.92	-8.13
08K001	-3.58	-3.02	-3.48	-6.19	-15.26
12K014	-2.49	-3.32	-1.13	-2.62	-6.01
13K014	-2.76	-3.64	-1.57	-3.03	-6.31
11K003	-3.21	-8.47	-1.26	-7.37	-13.66
13L012	-1.88	-2.57	-0.84	-2.70	-5.11
12L030	-2.28	-3.79	-1.65	-3.83	-6.71
12L028	-3.56	-6.21	-2.09	-4.73	-10.13
13L049	-3.57	-6.13	-2.12	-5.38	-8.50
12M017	-1.69	-2.21	-1.13	-1.39	-8.84
13M006	-1.93	-2.06	-3.01	-3.93	-17.43
07H002	-2.56	-3.19 [a]	-1.77	-2.18[a]	-5.83
12L029	-3.79	-3.70	-3.76	-4.96	-10.44
11K015	-3.78	-9.07	-1.03	-7.15	-14.38
10K005	-0.51	-0.32 [a]	-0.49	-1.93 [a]	-5.48
Mean	**-2.81**	**-4.42**	**-1.78**	**-4.29**	**−9.12**

[a] *for year 2000 only*

2.4.5 Recovery Period

Recovery in GW levels following La Niña events vary according to the severity of the phase. On average, the severe La Niña phase during 2000–01 required significantly longer recovery time (22 months) than for the short duration La Niña event during 1988–89 (2 months) (Table 2.4). During 2000–01, GW levels tended to recover during the end of the La Niña phase (March 2001), although not always exhibiting positive anomalies. With the onset of the growing season in April 200,1 however, GW levels declined to further low levels as a result of increased

irrigation and evapotranspiration demands. The recovery period for wells during 2000–01 varied from 18–26 months, except for wells 12M017 and 07H002, which recovered within a month, thus meeting the 6 consecutive 3-month running average criteria. However, GW levels in these two wells also fell below normal with the onset of pumping during the growing season.

Table 2.4 Comparison of recovery periods (months) for prolonged (2001) and short (1989) La Niña phases.

Well-ID	Year 2001	Year 1989	Well-ID	Year 2001	Year 1989
06F001	18	1	13L012	25	0
09F520	23	2	12L030	26	2
09G001	25	2	12L028	26	6
10G313	24	8[z]	13L049	26	1
08G001	18	1	12M017	1[b]	1
11J012	24[a]	1	13M006	25	1
13J004	28[z]	9[z]	07H002	0[b]	2[z]
08K001	18[a]	0	12L029	25	1
12K014	24[a]	1	11K015	25	8[z]
13K014	24[a]	1	10K005	25	0
11K003	25	2	**Mean**	22	2

[a] *showing positive anomalies for a brief period time at the end of La Niña phase (March 2001) but not meeting the 6 consecutive 3-month running average criteria.*

[z] *did not meet the 6 consecutive 3-month running average criteria.*

[b] *meet the 6 consecutive 3-month running average criteria followed by negative anomalies due to the onset of the growing season (April 2001).*

The recovery time for wells during the short-duration La Niña phase of 1988–89 varied from 0 to 9 months (Table 2.4). Recovery time for wells 10G313, 13J004, 12L028 and 11K015 exceeded 5 months even though all other wells exhibited recovery period of 2 months or less. This again can be explained by the unique hydraulic characteristics at each well location, which is responsible for inconsistent GW level fluctuations and recovery throughout the study area. Results of Table 2.3 and 2.4 show that GW resources are vulnerable during severe La Niña events and it is important that when severe La Niña is forecasted, dependence on GW needs to be

reduced immediately. Considering the UFA-FR connectivity, reducing dependence on GW for irrigation during severe La Niñas might help ensure minimum levels of streamflow in the river.

2.4.6 Probability Analysis

Table 2.5 presents the probabilities of GW level anomalies for El Niño and La Niña phases of ENSO for different observation wells.

Table 2.5 Probabilities of groundwater level anomalies for El Niño and La Niña phase of the ENSO. Probability is represented by "P" followed by the values in the brackets. P(>0) represents the probability of groundwater level anomalies being higher than 0 ft.

	El Niño				La Niña			
	Recharge		Non-Recharge		Recharge		Non-Recharge	
Well_Id	P (>0)	P(>5)	P (>0)	P(>5)	P (<0)	P(<-5)	P (<0)	P(<-5)
06F001*	71.43	51.43	51.85	20.37	88.89	57.78	83.33	27.78
09F520	68.63	7.84	47.37	10.53	66.18	1.47	52.87	3.45
09G001	72.97	32.43	62.50	8.93	72.92	12.50	74.07	0.00
10G313*	68.89	28.89	46.15	23.08	72.00	34.00	67.86	28.57
08G001*	76.74	62.79	61.29	33.87	79.17	66.67	76.79	41.07
11J012	65.79	34.21	61.02	5.08	83.33	4.17	71.43	0.00
13J004*	74.36	35.90	57.63	11.86	62.50	39.58	55.36	28.57
08K001*	89.74	48.72	79.66	59.32	55.32	34.04	69.64	46.43
12K014	69.23	30.77	64.41	5.08	83.33	16.67	73.21	0.00
13K014*	72.97	35.14	56.90	15.52	83.33	22.92	76.79	3.57
11K003*	74.36	43.59	66.10	27.12	66.67	41.67	55.36	30.36
13L012	64.29	28.57	64.52	8.06	79.17	4.17	64.29	1.79
12L030	75.00	40.63	62.00	10.00	75.56	17.78	75.00	16.67
12L028*	71.88	40.63	52.94	21.57	80.00	40.00	73.17	21.95
13L049*	78.13	56.25	60.42	20.83	81.82	38.64	79.17	25.00
12M017	74.36	20.51	57.14	25.00	79.17	4.55	56.36	12.73
13M006	82.05	12.82	72.41	31.03	80.85	8.51	65.45	23.64
07H002*	69.23	43.59	72.88	40.68	57.78	37.78	81.82	40.00
12L029*	73.68	39.47	56.36	25.45	85.11	21.28	76.79	14.29
11K015	65.63	31.25	46.00	12.00	70.00	43.33	60.98	19.51
10K005	62.50	0.00	72.92	0.00	74.47	0.00	48.08	5.77

* *Wells showing relatively higher values of probabilities for P(>5) and P(<5).*

For the historical data, all the wells showed high probability of groundwater levels being above and below average during the El Niño and La Niña phases, respectively, in both the recharge and non-recharge months. All the wells showed higher than 50% chance of groundwater levels being above and below average for El Niño and La Niña phases, respectively, for the recharge months. The probability of GW level anomalies being higher than 5 ft (P(>5)) and lower than -5 ft (P(<-5)) for El Niño and La Niña phases respectively were considerably different for different wells. Wells 06F001, 08G001 and 11K003 showed higher values for P(>5) and P(<5) during the recharge period which suggest that these wells show higher fluctuations to ENSO phases. The sensitivity of these wells to ENSO phases can be used as important indicators of the condition of groundwater resources in the study area with respect to ENSO phases and hence in ultimately developing a procedure for short-term groundwater level prediction. The groundwater levels in these wells can serve as indicators to mark the onset of ENSO phase impacts on groundwater resources in the study area.

2.5 Summary and Conclusion

This study used wavelet analysis and the non-parametric Mann Whitney test to identify and quantify the teleconnection between ENSO and GW levels in the lower Apalachicola-Chattahoochee-Flint river basin. Wavelet analysis was used to find teleconnection between Niño 3.4 sea surface temperature anomalies and GW level anomalies, while the Mann-Whitney test was used to quantify this this teleconnection. Analysis of GW level fluctuations in the event of a severe drought (prolonged La Niña phase) was also performed to estimate recovery periods.

Results of wavelet analysis indicated that wells representing shallow and moderately deep overburden conditions respond to ENSO in the periodicities of 3–7 years. The well in deep

overburden condition did not respond to short-term climate fluctuations indicating that GW levels under deep overburden conditions are not affected by ENSO. Mann-Whitney test found significant differences (p-value<0.01) in GW level anomalies between the two phases of ENSO, El Niño and La Niña, for all wells, except the one in deep overburden condition. GW levels were higher than long-term average during El Niño phases while lower than average during La Niña phases. The results of the Mann-Whitney tests confirmed the results of the wavelet analysis. Analysis for recharge and non-recharge periods indicated that ENSO-phase induced anomalies were approximately 2.5 times greater during the recharge season than during for the non-recharge season, which is in agreement with previous studies that indicate the predominant effect of ENSO on winter precipitation and temperature in the Southeast USA. Comparison of La Niña phases representing severe (2000–01) and average conditions indicated that during recharge and non-recharge seasons average GW levels dropped approximately twice during the severe La Niña as compared to the average La Niña event. Unlike the average La Niña phase, where GW level anomalies are large during the recharge season, the severe La Niña event during 2000–01 produced similar GW level anomalies for both the recharge and non-recharge seasons, which could be due to increased irrigation during non-recharge season stemming from prolonged drought conditions. Recovery times for the severe La Niña during 2000–01 were significantly longer (22 months vs. 2 months) than those during the short La Niña of 1988–89.

The results of this study illustrated that La Niña does severely impact GW levels in the study area, especially during severe events. The prolonged recovery periods during severe droughts validates the point that GW level fluctuates at a different time scale as compared to soil moisture and stream flows. Therefore, the study suggests that GW levels should also be used (in combination with precipitation deficit, soil moisture, stream flows and others) as an indicator of

drought in this area. It was also found that the role of irrigation cannot be ignored for such large recovery periods because GW level depletions during droughts are caused not only by the lack of precipitation, but also because of increased irrigation pumpage. It was also found that GW levels are affected by local geohydrologic characteristics. Therefore, in order to use GW levels as an indicator of drought in this region, a number of wells in different geologic formations and overburden conditions should be used. Further, although ENSO forecasts (e.g., those issued by NOAA Climate Prediction Center and International Research Institute at Columbia University) can be used to forecast GW levels, reduce irrigation pumpage based on those forecasts, and maintain stream flows in Flint and Apalachicola Rivers, ENSO forecasts should be combined with a detailed GW model and irrigation water withdrawal projections to develop an effective GW level forecasting methodology and/or tool. Such a modeling effort will also help identify critical areas where timely reductions in irrigation water withdrawal will help maintain stream flows. This would help solve complex water management issues and conflicts (i.e., the Tri-State Water War) in this region.

Chapter 3

Effects of Irrigation Pumpage during droughts on Groundwater Levels and Groundwater Budget Components in the Lower Apalachicola-Chattahoochee-Flint River Basin

3.1 Abstract

Rapid population growth in the city of Atlanta and increased irrigated-agricultural production in southwest Georgia are threatening the availability of freshwater resources in the Apalachicola-Chattahoochee-Flint (ACF) River Basin and greatly affecting supply of fresh water to the Apalachicola Bay that supports a struggling shellfish industry. Since 1990s, Alabama, Georgia, and Florida have been fighting over the allocation of ACF Basin's water. The water conflict heats up every time there is drought in the basin. This study was conducted to quantify the effect of irrigation pumpage on groundwater resources and Flint River in the lower ACF and southwest Georgia. The groundwater model MODular Finite-Element Model (MODFE) developed by USGS was used to simulate the effect of irrigation on groundwater (GW) levels in the Upper Floridan Aquifer, groundwater budget, and stream-aquifer flux. The model was used to simulate the drought years of 2010 to 2012. To understand the effect of irrigation pumpage on GW levels, the model simulated two scenarios, i.e., irrigated and non-irrigated. The comparison of the results of the two scenarios showed that stream-aquifer flux are a major discharge source from the aquifer and irrigation can cause as much as 10% change in stream-aquifer flux. The results also show that storage loss, recharge and discharge from upper semi-confining unit and

stream-aquifer flux are the major water sources contributing towards irrigation pumpage in the study area. The study also found that GW levels can fall by as much as 6 ft due to irrigation pumpage.

3.2 Introduction

Climate variability and climate change are the most important phenomena affecting water resources around the world. Among these, managing the effects of climate variability on water resources is the most important challenge in the short term. Various climate variability cycles such as El Niño Southern Oscillation (ENSO), Pacific Decadal Oscillation (PDO), North Atlantic Oscillation (NAO) and Atlantic Multi-decadal Oscillation (AMO) affect hydrologic cycles and can significantly alter the behavior of extreme events such as hurricanes, droughts, cold waves, and floods (IPCC 2001). Therefore, it is important to identify and understand the risks of such cycles on water resources and agriculture, and build risk mitigation strategies to help societies cope with their effects (Climate Research Committee and National Research Council 1995).

ENSO is an ocean-atmospheric phenomenon and is caused due to fluctuations in sea-surface temperatures in the equatorial pacific. ENSO has three phases, namely, El Niño, La Niña and Neutral (oceanic component). El Niño and La Niña refer to the warm and cool phases, respectively, of sea surface temperatures that lead to changes in climatic conditions around the world (Quinn 1994; Aceituno 1992). ENSO-induced climate variability is one of the major variability cycles in the global climate system (Diaz and Markgraf, 1992). ENSO phases have been found to have strong influence on precipitation and temperature around the world (Chiew et al., 1998; Keener et al., 2007; Roy, 2006). Additionally, studies have found ENSO influence on groundwater, streamflow, flood frequency, water quality, droughts, monsoon and crop yield in different parts of the world (McCabe and Dettinger 1999; Kahya and Drakup, 1993; Gurdak et

al., 2007; Chiew et al., 1998; Rajagopalan and Lall, 1998; Piechota and Dracup, 1999; Kulkarni, 2000; Roy, 2006; Keener et al., 2007; Tootle et al., 2005; and Hansen et al. 2001).

In the Southeast United States, precipitation and weather patterns are majorly influenced by ENSO induced climate variability, and it is also the primary reason for droughts in this region (Enfield et al. 2001). The El Niño phase of ENSO is associated with wetter and cooler (than normal) winters, while the La Niña phase is characterized by drier and warmer winters and are responsible for droughts in the region (Kiladis and Diaz, 1989; Hansen and Maul, 1991; Schmidt and Luther, 2002). Studies have shown that rainfall, water quality, streamflow and GW levels in watersheds of the Southeast are majorly affected by ENSO (Sharda et al., 2012; Schmidt et al., 2001; Keener et al., 2010; Johnson et al., 2013; Mitra et al., 2014).

Since 1980's, the Southeast has witnessed rapid population growth, urban sprawl, and increased agricultural production in the Apalachicola-Chattahoochee-Flint (ACF) River Basin (Figure 3.1) that are threatening the availability of freshwater resources and greatly affecting supply of fresh water to the Apalachicola Bay that supports a struggling shellfish industry. This stress on water resources of the ACF basin has been further exacerbated by recurrent ENSO-induced droughts experienced by this region. Droughts caused due to La Niña phases during 2000-01, 2007 and 2010-12 have caused losses in agricultural productivity, prompted water-use restrictions, and have intensified long-term conflicts between the neighboring states, i.e., the Tri-State Water Wars between the states of Alabama (AL), Georgia (GA) and Florida (FL) (Southern Environmental Law Center). Over the last two decades, the conflict has been marked by litigations and failed negotiations, making the ACF one of the most contentious river basins of the US. The Tri-state water conflict started during the early 1990's due to the failure of the state of GA to maintain adequate streamflow levels in the Chattahoochee-Flint River system during

droughts. Streamflow reduction in the Flint River (FR) during droughts due to increased pumpage for irrigation, municipal and industrial purposes from surface and groundwater sources in southwest Georgia is one of the major aspects of the ongoing conflict.

Agriculture in southwest Georgia is heavily dependent on irrigation water withdrawals from surface and groundwater sources where groundwater sites outnumber surface water sites by five to one. Groundwater withdrawal in the region can run into hundreds of millions of gallons per day. During droughts (caused mainly by La Niña), excessive irrigation from the Upper Floridan Aquifer (UFA), which is the major groundwater bearing unit, can not only result in lowering of GW levels but also reduction of streamflows levels in the FR. Additionally, exploitation of the groundwater resources in the UFA might also be unsustainable in the long term. A recent study conducted by Mitra et al. (2014), conclusively showed that GW levels in the UFA are affected by droughts events. Prolonged droughts have greater impact on GW levels and their recovery periods than short term ones. In addition to droughts, large groundwater withdrawals adversely affect GW levels, particularly during dry periods and in areas where the aquifer is overlaid by thick overburden conditions severely limiting aquifer recharge (Torak and Painter, 2006; Jones and Torak, 2006). This irrigation induced reduction in GW levels can further lead to reduction in streamflow levels at places where the stream and aquifer are hydrologically connected, thereby contributing to water quality degradations, high-temperature issues, and endangered/threatened species concerns in the Apalachicola River, situated downstream of the FR (Figure 3.1). Therefore, the objective of this research is to understand the effects of irrigation pumpage on GW levels and other groundwater budget components during droughts.

3.3 Study Area

The study area is the lower Apalachicola-Chattahoochee-Flint (ACF) River Basin located in parts of southwestern Georgia, northwestern Florida, and southeastern Alabama (Figure 3.1). The climate in the lower ACF River Basin is humid subtropical with long summers and mild winters. The average annual precipitation and temperature in the study area is about 50 inches and 64^{o}F, respectively. About 4,632 mi^{2} of land area recharges groundwater contained in the karst Upper Floridan Aquifer (UFA), which eventually contributes to surface water in the ACF River Basin.

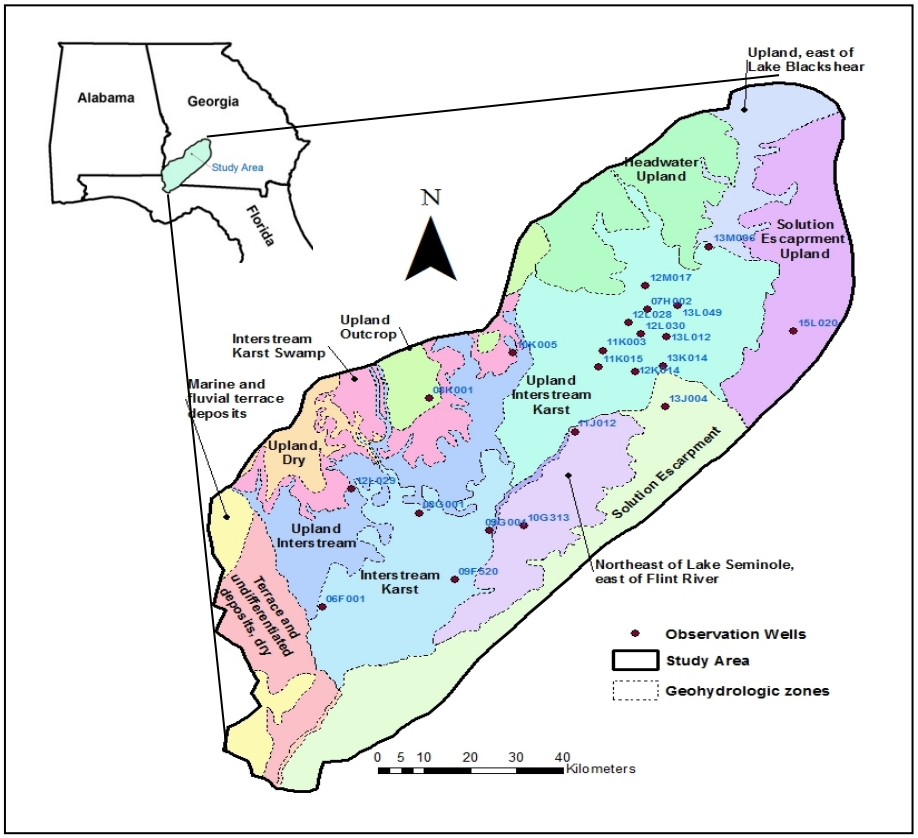

Figure 3.1 Location of the study area, long term observation wells and geohydrologic zones in them. Text in blue represents the well-id and those in black represent names of geohydrologic zones.

3.4 Upper Floridan Aquifer

The Upper Floridan Aquifer (UFA) system is the major water bearing aquifer in the region. UFA consists of four hydrologic units namely surficial aquifer system, upper semi-confining unit (USCU), UFA and lower confining unit (Torak and Painter, 2006). The hydrologic units are created by the differences in lithology and hydrologic characteristics within a geologic unit. The USCU lying above the UFA is the major source of vertical leakage to the UFA. The overlying USCU consists of layers clayey (below) and sandy (above) layers. During droughts, the upper sandy layer completely dewaters and the lower clayey layer acts as a source of recharge to UFA. GW levels in the UFA respond to seasonal climatic effects of droughts, precipitation, lake level changes and stream-stage. Fluctuations in water levels in the UFA also depend on the thickness and location specific hydraulic characteristics of the overlying USCU, groundwater irrigation withdrawal for agricultural, industrial, and municipal purposes, and also proximity to surface streams or lake system.

3.5 Methodology

3.5.1 USGS MODular Finite-Element Model (MODFE)

The groundwater model, MODFE (Cooley 1992; Torak 1993a,b), was used to understand and study the impacts of droughts and irrigation pumpage on GW levels and stream-aquifer exchange. MODFE is a finite element groundwater model developed by USGS. The model has been used in the past to simulate and understand the complex and interconnected stream-lake-aquifer system in the lower ACF (Figure 3.1).

3.5.2 Governing Equation

The equations in MODFE consist of partial differential equations that are related with appropriate initial and boundary conditions that describe the physics of fluid flow in porous media. Groundwater flow in the Upper Floridan Aquifer is governed by the following two-dimensional flow equation:

$$\frac{\partial}{\partial x}\left(T_{xx}\frac{dh}{dx}+T_{xy}\ \frac{dh}{dx}\right)+\ \frac{\partial}{\partial y}\left(T_{yx}\frac{dh}{dx}+T_{yy}\ \frac{dh}{dx}\right)+R(H-h)+W+P=S\frac{\partial h}{\partial t} \qquad (1)$$

where, *(x,y)* are the cartesian coordinate directions, *t* is time, *h(x,y,t)* is the aquifer hydraulic head, *H(x,y,t)* is the hydraulic head of the USCU, *R(x,y,t)* is the vertical hydraulic conductance (vertical hydraulic conductivity divided by thickness) of USCU, *W(x,y,t)* is the unit areal recharge or discharge rate (infiltration), *P(x,y,t)* are point source or sinks, *S(x,y,t)* is the storage coefficient and symmetric transmissivity is written in matrix form as

$$\begin{bmatrix} T_{xx}\ (x,y,t) & T_{xy}\ (x,y,t) \\ T_{yx}\ (x,y,t) & T_{yy}\ (x,y,t) \end{bmatrix} \qquad (2)$$

For approximation of the governing equation, initial and boundary conditions, MODFE uses the Garlerkin finite-element method with triangular elements and linear coordinate functions in space (Cooley, 1983; Zienkiewich, 1977). More details about initial and boundary conditions can be found in Jones and Torak (2006) and MODFE manuals (Torak, 1992).

3.5.3 Finite Element Mesh

A finite-element mesh, a network of triangular elements, is the basic component of MODFE representing the geometry of the study area. MODFE uses inputs (aquifer properties, climatic and anthropogenic stresses) to the finite-element mesh to simulate approximate solutions to the governing equation at the intersection of the element sides, which are called nodes. A

finite-element mesh developed by Jones and Torak (2006) was used for this study. The mesh for the study area consists of 37,587 elements and 18,951 nodes. More details about the finite element mesh can be found in Jones and Torak (2006).

3.5.4 Model Inputs

Data into MODFE are input under various input classes. These classes are assigned on the basis of different simulation approaches of the respective input parameters in the class. For example, irrigation is simulated as specified-flux boundary (class) at the nodes (simulation approach), whereas, parameters related to flow across streambeds are simulated as head-dependent flux boundaries (class) at the nodes and/or elements.

The model input parameters can also be classified as static and dynamic. The static input parameters are temporally constant and are representation of the aquifer, stream-lake system and USCU properties and their variation spatially. The static input parameters are model geometry, transmissivity of UFA, vertical leakage coefficients of the USCU and lakes, streambed conductance, storage coefficients of UFA, specific yield and head at the UFA updip limit (Figure 3.2). All the static input parameters were retained from the Jones and Torak (2006) model. Two parameters, vertical leakage from USCU and aquifer transmissivity, were changed slightly within the limits during calibration to account for the change in irrigation pumpage calculation procedure to meet the desired calibration criteria. The dynamic input parameters change temporally in the model and are representation of the temporal stresses in a transient simulation. The dynamic input parameters are municipal and irrigation pumpage, head at the USCU, stream and lake stage and infiltration. The dynamic input parameters act as monthly stresses, and along with boundary and initial conditions, solve for groundwater levels at nodes using the partial

differential groundwater equation (Equation 1) in the model. The input parameters and their respective input classes are summarized below.

3.5.5 Specified-Head Boundary at UFA Updip Limit

Specified head boundaries (SHB) represent areas where the hydraulic head remains constant (or change little) temporally. The location of the model boundary near the updip limit (Figure 3.2) represents unconfined conditions for UFA where the aquifer is at the land surface and is thin enough not to be considered as a water source. Water levels in this area do not fluctuate appreciably on yearly basis (Jones, 2006), thereby, classified as SHB. For this study, the hydraulic head distribution at the updip limit from the Jones (2006) model was retained.

3.5.6 Specified-Flux Boundaries

Specified-Flux Boundaries (SFB) represent areas where exchange of water is input and simulated in the model on the basis of a specified value that remains constant throughout that stress period (month) but might change in the subsequent stress period. Two types of SFB functions were used in the model on the basis of simulation approach namely; aerially-distributed functions applied at elemental areas and point functions applied at node points. Direct infiltration of precipitation was simulated using elemental SFB, and irrigation/municipal pumpage and off-channel spring flow were simulated using nodal SFB.

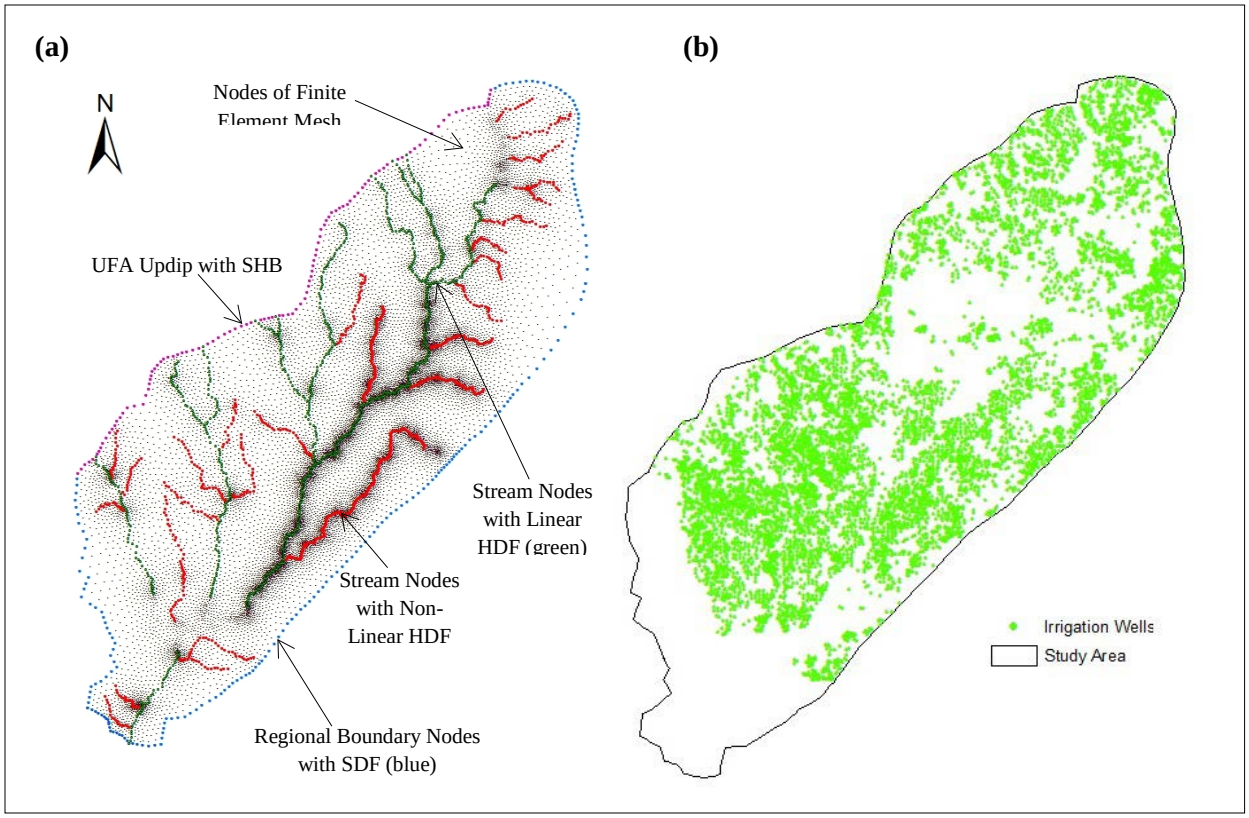

Figure 3.2 (a) The finite element mesh and the associated types of boundary nodes in the study area and **(b)** location of irrigation wells in the study area.

3.5.7 Irrigation/Municipal Pumpage and Springs

Irrigation water withdrawal is the major anthropogenic activity affecting groundwater resources in the study area. There are approximately 4000 irrigation wells in the model area (USGS). Irrigation pumpage were simulated as SFB at the model nodes. Monthly telemetered irrigation depth maps and irrigation acreage maps, procured from USGS, Georgia, were used to calculate irrigation pumpage on a nodal basis. Irrigation flux was calculated by multiplying irrigation depths with irrigated acreage and the flux value was assigned to the nearest node in the finite element mesh.

The municipal pumpage of 26 Mgal/d for the entire simulation period were simulated as SFB point discharge functions in the area was retained from the model conditions of Jones and

Torak (2006) as they are based on the records of Georgia Environmental Protection Division (GAEPD). Off-channel springs discharge of 0.39 Mgal/d which represents springflow in the identical manner as point withdrawals from wells was input as a constant value (SFB point discharge function) for the entire simulation period owing to the unavailability of time-varying data. The combined pumpage of municipal pumpage and springflow is extremely small compared to the total irrigation pumpage in the area and therefore unavailability of data is unlikely to introduce substantial error to the model.

3.5.8 Infiltration

Infiltration rates to the UFA vary on a seasonal basis. Mean annual recharge is about 10 inches per year (20 percent of mean annual rainfall) and 6 inches per year during late summer (Hayes et al., 1983). Mean monthly precipitation data was collected from 14 stations inside the study area from the National Climate Data Center (NCDC) (Appendix C.1). Infiltration was derived from precipitation on the basis of a seasonally varying conversion rate of 10, 20 and 30 percent of precipitation, allowing MODFE to simulate variable recharge in accordance to the variable infiltration rates in the region. Long duration precipitation from frontal passages is represented by conversion of 30 percent of precipitation to simulated infiltration during the fall and winter months (October to February) (Torak and Painter, 2006 and Jones et al., 2006). Similarly, low infiltration rates of 10 percent of average monthly rainfall are simulated corresponding to summer convective storms which are of usually high intensity and short duration (Jones et al., 2006) (April to August). March and September being transition months, in which both types of storms can occur, a conversion rate of 20 percent of average monthly precipitation was used for calculation of simulated infiltration (Jones and Torak, 2006) (April to

August). It is to be noted that MODFE in itself does not have an in-build mechanism to calculate infiltration from rainfall, due to which the above mentioned assumptions were made to simulate infiltration stresses.

It is also important to note that the USCU is unable to act as a source of recharge in areas where it is absent and where the thickness of the USCU is below 30 ft (Jones and Torak, 1996). In these areas, precipitation was allowed to infiltrate directly to UFA (due to absence or small thickness of the USCU) and vertical hydraulic conductance was assigned a zero value to simulate zero vertical leakage to/from USCU. Therefore, recharge through infiltration to the UFA was allowed in the areas only where the USCU is absent or thickness is less than 30 ft.

3.5.9 Head-Dependent Flux Boundaries (HDFB)

One of the major aspects of recharge and discharge from the UFA is the head-dependent flux boundaries (HDFB). Recharge and discharge to/from USCU, lakes and streams are controlled by the HDFB. Similar to SFB, there are two general types of HDFBs based on simulation approach namely: aerially-distributed functions applied across element areas and linear functions applied across element sides. Regional groundwater flow into and out of model area (except UFA updip) and flow across streambeds were simulated using linear head dependent flux boundaries, whereas, vertical leakage from the overlying USCU and lake beds were simulated using aerially-distributed flux boundary.

3.5.10 Regional GroundWater Flow

Regional groundwater flow across model boundaries (except UFA updip) was simulated across element sides corresponding to the nodes at the model boundaries. Groundwater at the

model boundary is allowed to flow across the boundary as the difference in the external head (controlling head) and the computed hydraulic head at the boundary nodes and by the value of leakage coefficients that accounts for the thickness of UFA and hydraulic conductivity of the area outside the model. Each node defining an element side on the boundary are aligned along the boundary and has an external head (H_B) associated with it. The external head at the boundary node represents the head at a distance from the node that helps the model simulate inflow/outflow in the model area. Since the model boundaries (except UFA updip) represent a groundwater divide, values in the area do not change appreciably on a monthly basis, and changes in hydraulic heads at the boundary nodes due to seasonal and anthropogenic stresses control the inflow/outflow to the study area. Thus the region external to the model area is not simulated *per se*, rather only the flow rate is calculated from/to the external area. The mathematical expression for nodal flow across an element side defined by nodes *k* and *l*, at the model boundary is expressed as:

$$Q_B = (1/2)\ \alpha\ L_{kl}\ (H_{Bi} - h_i),\ i = k\ or\ l \tag{3}$$

L_{kl} is the length of the element side and α is defined as

$$\alpha = \frac{Kb}{L} \tag{4}$$

K and *b* are average hydraulic conductivity and thickness of the aquifer between the model boundary and H_B. A distance of 3 mi was used for *L* to separate external head H_B from the model boundary. Values of the external head were interpolated from the potentiometric surface maps of the UFA for May 2010 published by Kinnaman and Dixon (2011). The values of α for regional boundaries were retained from the model of Jones (2006).

3.5.11 Flow across Streambeds

Simulation of flow across streambeds is with HDFB and is similar to the representation of regional flow. However for streambed flux the value of α is defined as

$$\alpha = \frac{K_r W_r}{b_r} \tag{5}$$

where, K_r is vertical hydraulic conductivity of the streambed, W_r and B_r is streambed width and thickness, respectively. For flows across streambeds controlling head, H_{Bi}, in equation 3 is the stream stage (or lake level), for the associate node *i* (=*k or l*) of the element side on the boundary. The nodes/elements representing streambed are aligned along the stream or other water feature. This linear HDFB is applied to streams that are perennial streams and have flow throughout the year.

A non-linear form of HDFB condition is used to simulate ephemeral or small streams that go dry if the water level goes below the altitude of the streambed. The boundary condition is non-linear as streambed leakages in these streams are dependent on the relative positions of the altitude of the bottom of the streambed, z_r, and nodal aquifer head, h_i. Therefore, for node *i* (=*k or l*) on an element side representing a surface water feature as non-linear HDFB, leakage is given by

$$Q_{ri} = \begin{cases} C_{ri}\,(h_{ri} - h_i), & h_i > Z_{ri} \\ C_{ri}\,(h_{ri} - z_{ri}), & h_i > Z_{ri} \end{cases} \tag{6}$$

where, Q_{ri} is the volumetric flow rate, C_{ri} is the coefficient, h_{ri} is stream stage and z_{ri} is the altitude of streambed bottom. α values for the present model were used from model of Jones (2006). α values at certain reaches were changed within limits during calibration owing to the different procedure used in calculation of irrigation for this model. Stream stage values, H_{Bi}, for all the streams in the model area were calculated from 13 stream gauging stations and two lake

stages obtained from U.S. Army Corps of Engineers, Mobile District, Mobile, Alabama, (Appendix B.1) (USCOE and Crisp County Power Commission). The stream stage data for all nodes representing a stream were obtained by interpolating the data from these 13 gauging stations. Interpolation of the stream stage data was based on the local variations in slope (obtained from contour maps) of the stream surface data.

3.5.12 Vertical Leakage across USCU and Lake-Beds

Vertical leakage to/from the USCU and lake Seminole and Blackshear were simulated using a non-linear leakage function expressed by *R(H-h)* in equation 1 and is simulated in areas where the USCU thickness is greater than 30 ft. The volumetric flow rate, Q_{ai}, across nodes *i* of the UFA from/to USCU is expressed as

$$Q_{ai} = \begin{cases} C_{ai}\,(H_i - h_i), & h_i > z_{ti} \\ C_{ai}\,(H_i - z_{ti}), & h_i > z_{ti} \end{cases} \quad (7)$$

where, Q_{ai} is the flow rate for the steady vertical leakage, C_{ai} is the nodal vertical leakage coefficients, h_i is the nodal hydraulic head in the UFA, H_i is the nodal head in the USCU, z_{ti} is the nodal altitude of the top of UFA or base of USCU. The maximum rate of recharge to the UFA is limited by equation 7 when the aquifer head drops below the base of USCU whereas discharge from the aquifer to the USCU is not limited by the non-linear function. Nodal heads for USCU, H_i, are calculated as a proportion of the thickness of USCU which varies seasonally for each geo-hydrologic zone (GHZ). For the simulation of a droughts (La Niña event) as in this study (May 2010 – September 2012), the saturation proportion of the USCU for each GHZ is the representation of the thickness of the sandy clay or clay layer in USCU for the respective zone which remains saturated even when the upper sandy layer completely dewaters (Torak and

Painter, 2006). This lower clayey layer that remains saturated acts as a source of recharge and discharge from/to the UFA. Due to lack of head data in USCU (only 6 wells in the entire study area) and since the simulation of a La Niña period for study are similar to the drought conditions simulated by Jones and Torak (2006) (March 2001 – February 2002), the proportional saturation values for all the months from the previous study were retained.

It is important to note that static input parameters such as leakage coefficients of USCU, transmissivity, and specific yields are highly spatially heterogeneous and are measured at specific points thereby resulting in lack of spatially extensive data. Therefore, spatial interpolation techniques such as krigging and conditional simulation were used by Jones and Torak (2006) for spatial representation of the data. These techniques fill the gaps in the unmeasured areas, but may lack accuracy as these techniques might not be able to capture the location specific spatial heterogeneity of the parameters, thus introducing errors in the model on a location specific basis while being consistent on a regional scale. These errors will also be manifested in the simulation of nodal hydraulic heads from equation 1 by MODFE. More detailed explanation about the model input parameters and simulation techniques can be found in the MODFE manual (Torak, 1992) and USGS scientific investigation reports by Jones and Torak (2006) and Torak et al (1996).

3.5.13 Transient Simulation (May 2010 - September 2012) and Model Validation

Simulating and understanding the groundwater conditions in the absence of irrigation stresses is the key in understanding the effects of irrigation on groundwater resources in the study area. Groundwater models, such as MODFE, present us with such opportunities to simulate groundwater conditions without irrigation and studying its effects (keeping rest of the stresses

same). Therefore, for this study, the La Niña event of 2010 as drought was selected to study the coupled effects of droughts and irrigation on GW levels and stream-aquifer fluxes in the region. The La Niña event of 2010 started from mid-2010 and continued until mid-2012. This La Niña event was selected because it was responsible for severe drought in the Southeast and also because robust irrigation data were available for the period. Therefore, for this study, the model was used to simulate the drought period of May 2010 to September 2012 to understand the effect of irrigation pumpage. Two scenarios namely: Irrigated (IR) and Non-Irrigated (NI) were simulated for the drought period and the results from the two scenarios were compared to better understand the coupled effects of irrigation and droughts. The simulation of the NI scenario helped us quantify groundwater conditions in the absence of irrigation and helped us quantify the effect of irrigation on stream-aquifer fluxes and GW levels.

Since the model setup used for the study was same as from Jones and Torak (2006) (which was calibrated), and most of the model parameters were retained (except dynamic stress), not much effort was needed to calibrate the model. Still, for the transient simulation, GW level data and stream-aquifer flux data for July 2011 was compared to the model output of that month to validate the model. For initial conditions the published USGS potentiometric surface maps for May - June 2010 was used (Kinnaman and Dixon, 2011). The month of July 2011 was used because data from 159 wells were available (Appendix A.2). For the rest of the months, such extensive data were not available.

The criteria for accepting simulated GW level were based on the accuracy of GW level measurements and model input parameters. The average accuracy of GW level measurements is 4.7 ft and conservatively model input parameter (aquifer geometry) has an average accuracy similar to measured GW levels (Jones and Torak, 2006). Combining the two potential errors, the

the Root Mean Square Error (*RMSE*) of the model should be close to 6.7 ft for the simulated values at the end of the month. The *RMSE* is defined as

$$RMSE = \left[\frac{1}{N}\sum_{i=1}^{N}(h_{i\,sim} - h_{i\,mes})^2\right]^{1/2} \quad (8)$$

where, N is the number of residuals (Simulated – Observed), and $h_{i\,sim}$ and $h_{i\,mes}$ are the simulated and measured hydraulic heads, respectively.

Stream aquifer flux was calibrated across 17 stream reaches following Torak et al. (1996). Observed stream-aquifer fluxes were obtained by averaging the measured streamflow data across measured upstream and downstream ends. 21 USGS streamflow gauging stations were used for calculation of target flow across stream reaches which were used for calibration of stream-aquifer flux (Appendix B.2). These fluxes were compared to simulated model outputs at the end of the month. An error factor (EF) was applied to account for the fluctuations in daily stream flow data. A target range having a lower and upper limit of stream-aquifer fluxes were calculated using the EF. The lower and upper limits, $Flux_{min}$ and $Flux_{max}$, of the target range are defined as

$$Flux_{min} = (Q_d - EF \,.\, Q_d) - (Q_u + EF \,.\, Q_u) \quad (9)$$

$$Flux_{max} = (Q_d + EF \,.\, Q_d) - (Q_u - EF \,.\, Q_u) \quad (10)$$

where, Q_d is the measured streamflow at the downstream end and Q_u is the measured streamflow at the upstream end. Estimated flux, *qm*, is the average of $Flux_{max}$ and $Flux_{min}$. Simulated fluxes were compared with corresponding target range and measured fluxes, *qm*, for evaluation of model acceptance. It is to be noted that stream-aquifer fluxes can vary significantly on a daily basis. Therefore, it is impossible to compare the observed fluxes for a single day to the simulated fluxes. The concept of target range allows us to have a certain range beyond which the fluxes are

not expected to vary on a daily basis. More details about model calibration can be obtained from Jones and Torak (2006) and Torak et al, (1996).

3.6 Results and Discussion

3.6.1 Model Validation

The root mean square error (RMSE) of the groundwater level residuals obtained was 8.58 ft (Table 3.1) which was close to the acceptable limits of 6.7 ft.

Table 3.1 Validation statistics of the residuals for the simulated model for July 2011.

Root Mean Square Error	Standard Deviation (STD)	Range (R*)	STD/R	Average
8.58 ft	8.40 ft	234.31 ft	0.04	2 ft

**Range of simulated groundwater levesl.*

The RMSE of the present model is close to the October 1999 model (RMSE of 8.18 ft) by Jones and Torak (2006). The ratio of standard deviation and range were well below 0.01, which is considered good (Table 3.1). Table 3.2 shows the simulated stream-aquifer flow, observed flow and the associated target ranges for various stream reaches for July 2011.

The simulated stream-aquifer flows for all the stream reaches were within the target range except for reach number 15 and 16 (Muckalee Creek). The fluxes in the reach 16 also did not meet the required target range for the October 1999 model by Jones and Torak (2006). The validation results show that the model was performing satisfactorily to simulate groundwater flow in the study area. The model was able to simulate GW levels within the acceptable error limits and also simulate stream-aquifer fluxes within the respective target ranges for most of the reaches.

Table 3.2 Simulated stream-aquifer flow, Measured flow, and associated target ranges for stream reaches for July 2011. All the flow values are in cubic feet per second.

Reach Number	EF[c]	Stream Reach	Simulated Flux (qs)	Target Flux[a]		Estimated Flux[b] (qm)
				$Flux_{min}$	$Flux_{max}$	
1	0.1	Big Cypress Creek near Newton, Ga.	0.00	0.00	0.00	0.00
2	0.1	Big Slough at Ga. 179 near Pelham, Ga.	0.00	0.00	0.00	0.00
3	0.1	Big Slough at Ga. Hwy. 97 near Bainbridge, Ga.	0.00	0.00	0.00	0.00
4	0.1	Long Branch near Colquitt, Ga.	0.00	0.00	0.00	0.00
5	0.1	Aycocks Creek below Colquitt, Ga.	0.00	0.00	0.00	0.00
6	0.1	Gum Creek (U.S. Hwy. 280) at Coney, Ga.	40.72	37.62	45.98	41.80
7	0.1	Cedar Creek near Cordele, Ga.	0.25	0.00	0.00	0.00
8	0.1	Swift Creek near Warwick, Ga.	6.69	6.69	8.17	7.43
9	0.1	Jones Creek near Oakfield, Ga.	1.18	1.09	1.33	1.21
10	0.1	Abrams Creek near Oakfield, Ga.	3.50	3.35	4.09	3.72
11	0.1	Mill Creek near Albany, Ga.	7.18	6.80	8.32	7.56
12	0.1	Cooleewahee Creek near Newton, Ga.	0.30	0.29	0.35	0.32
13	0.1	Spring Creek at Ga. Hwy. 200 at Damascus, Ga.	-3.04	-3.26	-2.66	-2.96
14	0.1	Spring Creek at U.S. 27, at Colquitt, Ga.	98.58	65.22	99.18	82.20
15	0.1	Dry Creek at Hentown, Ga.	5.53	27.98	38.82	33.40
16	0.1	Muckalee Creek below Leesburg, Ga.	17.74	-81.50	-28.50	-55.00
17	0.1	Spring Creek near Reynoldsville, Ga.	63.65	52.88	100.72	76.80

[a] *Target flux, $Flux_{min}$ and $Flux_{max}$ are calculated using equation 9 and 10.*

[b] *Estimated fluxes are derived from USGS streamflow gauging stations.*

[c] *Error factor obtained from Jones and Torak (2006).*

3.6.2 Groundwater Budget for Water Year 2011

Accurate representation of groundwater resources and understanding the effects of irrigation requires a complete analysis of the groundwater components (GWCs) of the water cycle. Seasonal precipitation patterns of the Southeast USA also manifests in GW levels in the

UFA. Seasonal GW level fluctuations vary throughout of the study area (Torak and Painter, 2006; Mitra et al., 2014). GW levels reach a yearly maximum from late winter to early spring due to high and steady rain and low evapotranspiration. Thereafter, GW levels start declining during the growing season due to decrease in recharge because of lack of precipitation and are at yearly lows during mid-fall (Torak and Painter, 2006). Since GW levels drive GWCs and vice-versa, GWCs also follow a distinct pattern of seasonality (Table 3.3).

Table 3.3 and Table 3.4 show the simulated recharge and simulated discharge of each GWC of UFA for water year 2011 (WY 11) for irrigated (IR) and non-irrigated (NI) scenarios, respectively. The groundwater budget (GWB) presents a complete picture of the groundwater resources in the region. Figure 3.3 shows the percentage contribution of each GWC to the water budget for WY 11 for IR and NI scenarios and presents a comparison of the change in each component due to irrigation as a percent of GWB. This was calculated by finding the percentage contribution of each component (recharge and discharge) to the total recharge and discharge in the study area. The average monthly recharge through infiltration to the UFA for WY 11 was about 320 million gallons per day (Mgal/d) (Table 3.3). Infiltration as a component is not expected to change with irrigated and non-irrigated scenarios. Infiltration increased during the late fall and decreased considerably during the summer months. The highest and lowest average daily infiltration was for the months of February 2011 and May 2011 with a value of 826 Mgal/d and 38 Mgal/d (Table 3.3), respectively. The contribution of infiltration as a recharge component to the water budget varied from 2% to 11% for the WY 11 (Figure 3.3).

Irrigation for WY 11 varied largely on a monthly basis with an average monthly irrigation rate of 97 Mgal/d (including the non-irrigated months). Irrigation for WY 11 was far lower than the irrigation during the March 2001-02 period (Jones and Torak, 2006) and WY 12

(Table 3.3). Irrigation withdrawal was highest (479 Mgal/d) during July 2011 and lowest (7 Mgal/d) for March 2011(Table 3.3). The contribution of irrigation to GWB varied from 1% in the month of May 2010 to as high as 7% for July 2011 (Figure 3.3). This suggested that irrigation pumpage is a major component in the entire GWB for the study area and can significantly affect the recharge and discharge components (especially through streams).

Regional flow through the model boundary also accounted for a significant portion of recharge and discharge to/from the UFA. The average daily recharge and discharge for WY 11 through regional flow amounted to 588 Mgal/d and 460 Mgal/d (Table 3.3), respectively. The percentage contribution of regional flow to the GWB was approximately 15% and this did not vary much for IR and NI scenarios (Figure 3.3) suggesting that regional flows were not affected by irrigation pumpage. On a seasonal basis, recharge to aquifer from regional flows decreased and discharge through regional flow from aquifer increased during the late fall and early winter months (November to December) while the fluxes reversed during the rest of the years (Table 3.3). This happened because during late winter and early spring GW levels in the study area rise (due to recharge through precipitation) and thereby resulting in efflux from the study area. Whereas, during the summer months, GW levels are lower in the study area thereby causing an influx in the study area. Flux through aquifer outcrop was not a major source of recharge or discharge to UFA and accounted for only 2% to 3 % of the entire GWB (Figure 3.3).

Recharge and discharge through USCU is one of the major components of GWB. USCU is also the major source of recharge to the UFA and accounts for almost 66% of the total recharge to the UFA (Table 3.3). The average daily recharge and discharge through USCU for WY 11 was approximately 2208 Mgal/d and 960 Mgal/d, respectively (Table 3.3).

Table 3.3 Simulated recharge (to UFA) and discharge (from UFA) budget components under irrigated conditions for water year 2011.

Budget Components	2010			2011									WY 10
	Oct	Nov	Dec	Jan	Feb	Mar	Apr	May	June	July	Aug	Sep	Average
Recharge to UFA, in million gallons per day													
Infiltration	153	376	279	625	826	537	108	38	137	283	129	348	320
Regional Flow	614	552	544	540	530	542	558	612	633	638	648	650	588
Streams	44	33	40	43	57	60	62	40	38	49	43	41	46
Aquifer Outcrop	157	136	132	115	101	129	144	152	154	159	158	160	141
USCU	2114	2270	2373	2307	2210	2091	2172	2163	2195	2235	2190	2169	2208
Total	**3082**	**3368**	**3367**	**3631**	**3723**	**3359**	**3044**	**3006**	**3157**	**3364**	**3168**	**3368**	**3303**
Discharge from UFA, in million gallons per day													
Irrigation	271	0	0	0	0	7	66	13	69	479	41	217	97
Springs and Municipal Wells	30	30	30	30	30	30	30	30	30	30	30	30	30
Regional Flow	484	518	514	511	495	463	450	436	427	413	409	403	460
Streams	2229	2174	2147	2111	1949	1949	1940	2240	2284	2061	2147	2144	2115
Aquifer Outcrop	32	34	33	40	49	34	28	26	25	25	24	24	31
USCU	952	1011	950	1001	1022	1046	963	930	912	902	899	930	960
Net Storage Loss or Gain	-916	-398	-305	-62	178	-171	-434	-669	-591	-545	-383	-381	-390
Total	**3082**	**3368**	**3367**	**3631**	**3723**	**3359**	**3044**	**3006**	**3157**	**3364**	**3168**	**3368**	**3303**

Table 3.4 Simulated recharge (to UFA) and discharge (from UFA) budget components under non-irrigated conditions for water year 2011.

Budget Components	2010			2011									WY 10
	Oct.	Nov.	Dec.	Jan.	Feb.	Mar.	Apr.	May	June	July	Aug.	Sep.	Average
Recharge to UFA, in million gallons per day													
Infiltration	153	376	279	625	826	537	108	38	137	283	129	348	320
Regional Flow	611	551	544	540	529	542	558	612	632	630	645	646	587
Streams	40	31	38	42	56	59	60	39	37	44	40	36	43
Aquifer Outcrop	141	128	126	109	93	124	141	150	152	150	157	153	135
USCU	2075	2256	2362	2296	2194	2083	2155	2158	2177	2154	2171	2139	2185
Total	**3020**	**3343**	**3349**	**3612**	**3697**	**3345**	**3021**	**2998**	**3136**	**3261**	**3141**	**3321**	**3270**
Discharge from UFA, in million gallons per day													
Irrigation	0	0	0	0	0	0	0	0	0	0	0	0	0
Springs and Municipal Wells	30	30	30	30	30	30	30	30	30	30	30	30	30
Regional Flow	487	520	515	512	496	464	451	437	429	421	414	409	463
Streams	2291	2206	2170	2132	1973	1961	1963	2253	2312	2173	2200	2218	2154
Aquifer Outcrop	32	35	33	42	53	35	28	26	25	26	24	25	32
USCU	969	1018	955	1008	1032	1050	970	932	918	929	904	942	969
Net Storage Loss or Gain	-790	-466	-354	-111	113	-196	-421	-680	-578	-319	-432	-303	-378
Total	**3020**	**3343**	**3349**	**3612**	**3697**	**3345**	**3021**	**2998**	**3136**	**3261**	**3141**	**3321**	**3270**

Recharge and discharge through USCU accounted for approximately 45% of the entire GWB (Figure 3.3). Recharge and discharge through USCU also varied on a seasonal basis. Stream-aquifer flux is one of the major components of the entire GWB. The entire contribution of stream-aquifer flux to the GWB was approximately 30% (Figure 3.3) and is the major source of discharge from UFA. The total average stream recharge and discharge to and from UFA for WY 11 was 46 Mgal/d and 2115 Mgal/d respectively (Table 3.3). Recharge and discharge through streamflow tended to change due to irrigation. For Irrigated months (Oct 2010 and Jan to Sep, 2011), application of irrigation resulted in increased recharge from and decreased discharge to the streams from UFA (Table 3.3 and Table 3.4).

Figure 3.3 shows that two components, namely, flux through USCU and stream-aquifer flux, change considerably as a percentage of GWB when there is significant withdrawal for irrigation.

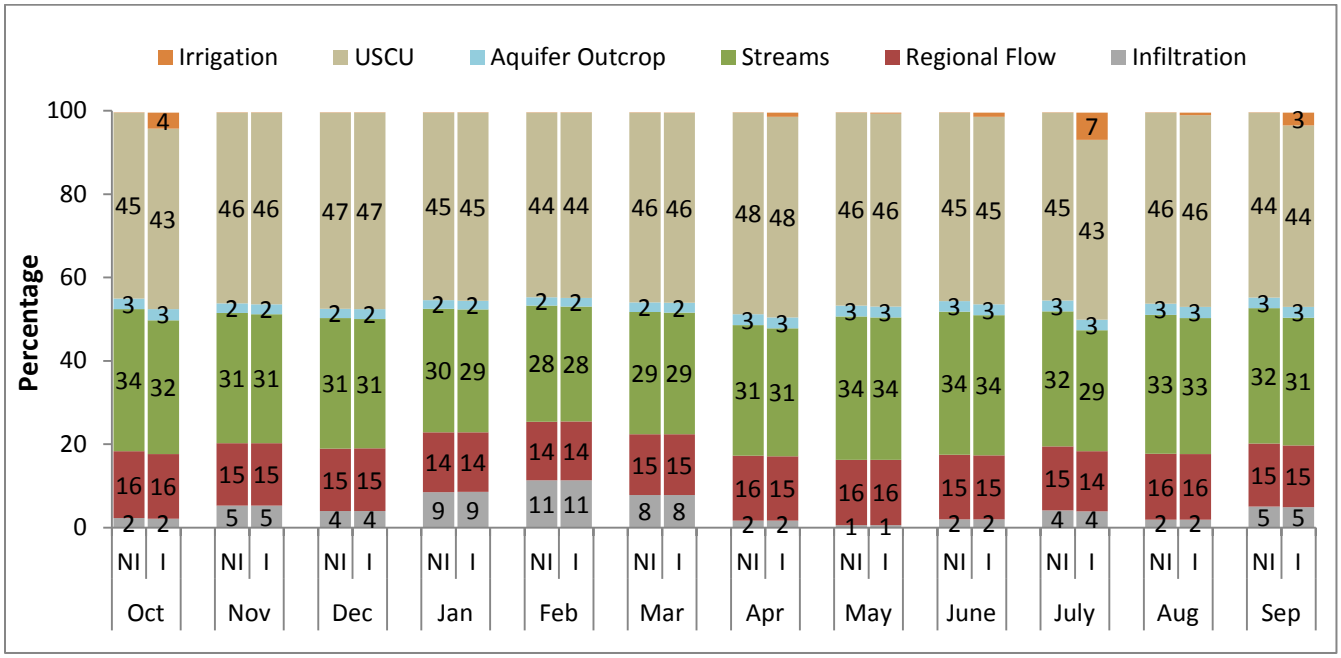

Figure 3.3 Percentage changes in simulated recharge and discharge components due to irrigation pumpage for water year 2011. "I" and "NI" represents irrigated and non-irrigated scenarios, respectively.

These two GWC are also the major source and sink to the UFA, and also represent a major component in the entire GWB (Figure 3.3). For Oct 2010 and July 2011, the contribution of stream-aquifer fluxes and USCU flux, changed by more than 2% (Figure 3.3). Change in storage (gain and loss) also followed seasonality in the UFA. Storage loss was lower during the late winter and early spring than during the summer months (Table 3.3). Irrigation resulted in increased storage loss from the aquifer except for the non-irrigated months and March 2011 and May 2011 (Table 3.3 and Table 3.4). The average daily loss in storage for the UFA was 390 Mgal/d for WY 11. The results above exemplify that apart from seasonality, irrigation pumpage plays an important role in the overall state of groundwater resources in the study area.

3.6.3 Groundwater Budget for Water Year 2012

Table 3.5 and Table 3.6 show simulated recharge (to UFA) and discharge (from UFA) budget components for water year 2012 under IR and NI scenarios, respectively. Figure 3.4 shows percentage contribution of each GW component to the water budget for IR and NI scenarios for WY 12. There was more irrigation pumpage during WY12 than WY 11. Therefore, comparison of GWB of WY11 and WY 12 helps us understand the effect of increased irrigation on GWC, and stream-aquifer fluxes, in particular. The total average irrigation for the WY12 was 425 Mgal/d (Table 3.5) as compared to just 97 Mgal/d (including non-irrigation months) in WY11 (Table 3.3). Irrigation increased dramatically during the growing season and ranged between 533 Mgal/d to 893 Mgal/d (Table 3.5) which was about 7% to 12% of the GWB (Figure 3.4), and peaking during May 2012. All GWC for WY 12 ranged similar to values as during WY 11 except for discharge to stream, recharge from USCU, and storage losses (Tables 3.3 and 3.5). The percentage contribution of the groundwater components to GWB was also similar as in WY

11 (Figures 3.3 and Figure 3.4). Average discharge to stream decreased from 2,115 Mgal/d during WY 11 to 2,002 Mgal/d in WY 12, while average recharge from USCU increased from 2,208 Mgal/d during WY 11 to 2,327 Mgal/d (Tables 3.3 and 3.5). For WY 12, monthly discharges to the streams were lower than during the same months for WY 11 because of increased irrigation. Storage loss in WY 12 was lower than WY 11 with average storage loss being 390 Mgal/d for WY 11 compared to 241 Mgal/d for WY 12 (Tables 3.3 and 3.5).

Table 3.5 Simulated recharge (to UFA) and discharge (from UFA) budget components under irrigated conditions for water year 2012.

Budget Components	2011			2012									WY 11
	Oct	Nov	Dec	Jan	Feb	Mar	Apr	May	June	July	Aug	Sep	Average
Recharge to UFA, in million gallons per day													
Infiltration	519	419	511	491	593	324	97	148	237	238	320	386	357
Regional Flow	654	595	596	577	597	609	647	680	682	688	690	696	643
Streams	45	40	47	47	44	79	67	62	63	53	54	63	55
Aquifer Outcrop	154	143	134	126	115	157	170	177	178	180	177	179	158
USCU	2148	2314	2402	2363	2305	2267	2364	2379	2367	2373	2327	2318	2327
Total	**3521**	**3512**	**3690**	**3604**	**3653**	**3436**	**3346**	**3447**	**3526**	**3532**	**3568**	**3642**	**3540**
Discharge from UFA, in million gallons per day													
Irrigation	194	0	0	0	0	533	655	893	769	745	577	734	425
Springs and Municipal Wells	30	30	30	30	30	30	30	30	30	30	30	30	30
Regional Flow	398	441	444	448	435	397	383	370	368	363	362	354	397
Streams	2121	2133	2123	2004	2047	1814	1943	1980	1956	1990	1967	1946	2002
Aquifer Outcrop	25	29	32	36	43	26	23	22	22	21	21	21	27
USCU	930	984	947	968	961	941	868	844	833	829	839	855	900
Net Storage Loss or Gain	-177	-103	115	119	137	-305	-557	-693	-452	-446	-228	-298	-241
Total	**3521**	**3514**	**3690**	**3605**	**3653**	**3435**	**3345**	**3446**	**3526**	**3532**	**3568**	**3642**	**3540**

Except for winter months, all other months showed loss of storage with the highest storage loss occurring during May 2012 (Table 3.5). Due to higher irrigation in the WY 12 than WY 11, the comparison of WY 11 and WY 12 budgets shows that increase in irrigation can lead to greater changes in stream-aquifer flux and flux through the USCU.

Table 3.6 Simulated recharge (to UFA) and discharge (from UFA) budget components under non-irrigated conditions for water year 2012.

Budget Components	2011			2012									WY 11
	Oct.	Nov.	Dec.	Jan.	Feb.	Mar.	Apr.	May	June	July	Aug.	Sep.	Average
Recharge to UFA, in million gallons per day													
Infiltration	519	419	511	491	593	324	97	148	237	238	320	386	357
Regional Flow	649	593	594	576	595	598	630	656	659	664	669	671	630
Streams	39	37	44	45	42	66	54	44	45	39	40	44	45
Aquifer Outcrop	148	141	132	125	114	145	154	157	157	159	157	156	145
USCU	2097	2300	2391	2353	2297	2164	2230	2189	2184	2192	2168	2144	2226
Total	**3452**	**3491**	**3672**	**3589**	**3641**	**3296**	**3164**	**3194**	**3283**	**3292**	**3355**	**3401**	**3403**
Discharge from UFA, in million gallons per day													
Irrigation	0	0	0	0	0	0	0	0	0	0	0	0	0
Springs and Municipal Wells	30	30	30	30	30	30	30	30	30	30	30	30	30
Regional Flow	405	445	447	450	437	410	401	394	391	387	384	381	411
Streams	2196	2176	2154	2026	2064	1921	2084	2192	2166	2208	2164	2163	2126
Aquifer Outcrop	26	30	32	37	43	29	25	25	25	25	25	25	29
USCU	958	989	950	971	964	997	935	919	914	908	909	939	946
Net Storage Loss or Gain	-163	-178	59	75	102	-91	-312	-366	-242	-265	-157	-137	-140
Total	**3452**	**3492**	**3673**	**3590**	**3641**	**3295**	**3163**	**3194**	**3283**	**3292**	**3355**	**3401**	**3403**

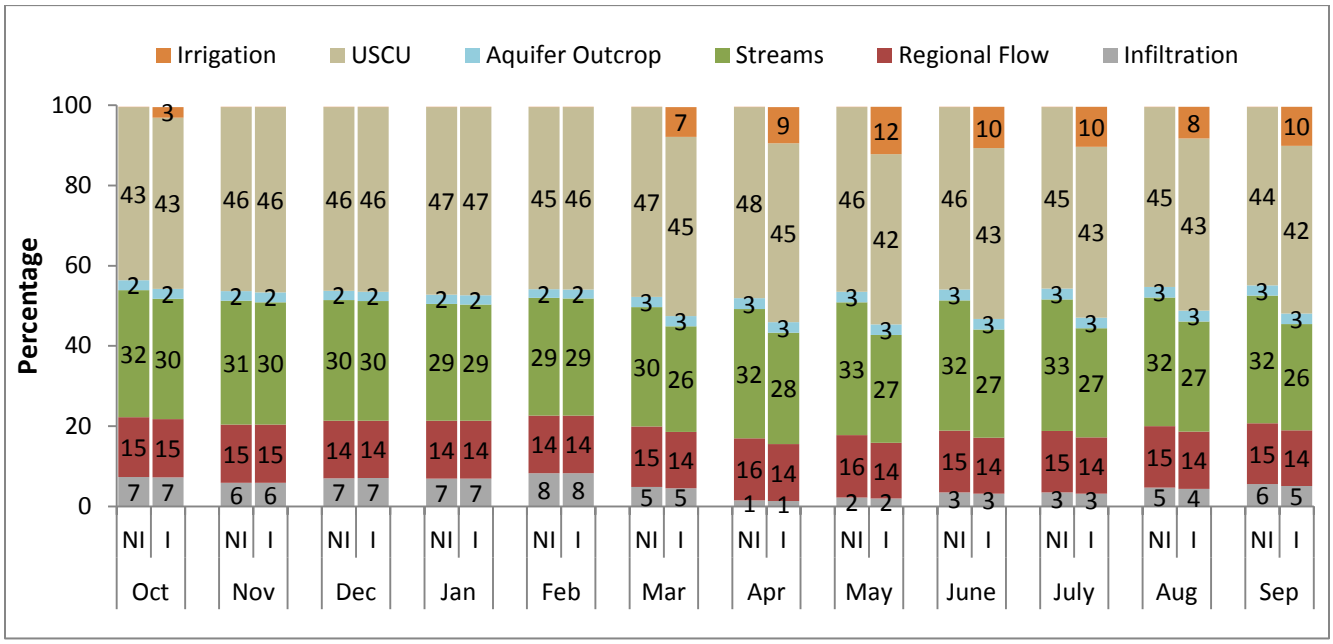

Figure 3.4 Percentage changes in simulated recharge and discharge components due to irrigation pumpage for water year 2012. "I" and "NI" represents irrigated and non-irrigated scenarios, respectively.

Similar to WY 11 (Figure 3.3), stream-aquifer flux and flux through USCU changed significantly as a percentage of GWB during heavily irrigated (HIM) months (Sep 2011 and March to Sep 2012) for IR and NI simulations (Figure 3.4).

3.6.4 Change in Groundwater Component for Water Year 2011

Table 3.7 shows the percentage change in each GWC (recharge and discharge) due to irrigation pumpage for WY 11. Recharge to the UFA through stream increased by more than 10% due to irrigation, when monthly average irrigation was more than 150 Mgal/d.

Table 3.7 Percentage change in simulated recharge (to UFA) and discharge (from UFA) budget components due to irrigation pumpage for water year 2011.

Percentage change in flux from Recharge Components of UFA												
Components	**2010**			**2011**								
	Oct.	**Nov.**	**Dec.**	**Jan.**	**Feb.**	**Mar.**	**Apr.**	**May**	**June**	**July**	**Aug.**	**Sep.**
Infiltration	0	0	0	0	0	0	0	0	0	0	0	0
Regional Flow	1	0	0	0	0	0	0	0	0	1	0	1
Streams	10	6	5	4	3	2	3	1	2	12	7	13
Aquifer Outcrop	11	6	5	5	8	4	2	1	1	6	1	5
USCU	2	1	0	0	1	0	1	0	1	4	1	1
Percentage change in flux from Discharge Components of UFA												
Regional Flow	-1	0	0	0	0	0	0	0	0	-2	-1	-2
Streams	-3	-1	-1	-1	-1	-1	-1	-1	-1	-5	-2	-3
Aquifer Outcrop	-1	-3	-3	-4	-9	-2	-2	-1	0	-2	-1	-2
USCU	-2	-1	-1	-1	-1	0	-1	0	-1	-3	-1	-1
Decreased Storage Gain or Increased Storage Loss	-16	15	14	44	-58	13	-3	2	-2	-71	11	-26

Recharge from stream to aquifer during the winter months (November to February) also increased by 3% to 6% for IR scenario (compared to non-irrigated scenario) as the effect of irrigation during the previous months persist resulting in lower GW levels. Decrease in discharge to streams ranged from 3% to 5% for months with more than 150 Mgal/d of irrigation (Table 3.7). This small change in streamflow discharge had a significant impact on streamflow since it

is a major discharge component in the GWB (Figure 3.3). In addition to increased recharge and decreased discharge, there was increased storage loss as well, when compared to NI scenario. For months with high irrigation, increase in storage loss ranged from 16 % to 71% (Table 3.7) due to irrigation. Whereas, during the winter months or months with less irrigation, there was net increase in storage. In percentage terms, changes in recharge and discharge through aquifer outcrop values are high, but these values are not significant considering their small contribution to GWB (Table 3.7). Recharge and discharge through USCU also changed considerably during months with high irrigation. Recharge through USCU increased by 1% to 4% and discharge decreased by 1% to 3% (Table 3.7). It should be noted that changes in discharge to stream from aquifer and recharge from stream to aquifer results in changes in streamflow. Although the actual values of the streamflow and their changes were not calculated by the model, the changes in stream-aquifer fluxes give a good idea of baseflow changes, which is important during drought periods since streams are mainly sustained by baseflow during droughts.

3.6.5 Change in Groundwater Component for Water Year 2012

Table 3.8 shows percentage change in each GWC (recharge and discharge) due to irrigation pumpage for WY 12. During the irrigated months, the increase in recharge from stream to UFA ranged from 14% to 42% (Table 3.8). Simultaneously, we also see decrease in discharge to the stream from UFA (Table 3.8) due to irrigation. The decrease in stream discharge was approximately 10% during May 2012 to September 2012, suggesting that irrigation significantly affects stream-aquifer flux in the study area. Comparison of WY 11 (Table 3.7) and WY 12 (Table 3.8) also illustrate the fact that increased irrigation pumpage affects stream-aquifer flux in the study area. Also, there was significant change in aquifer outcrop and USCU

recharge/discharge and the changes were higher than during the WY 11 (Table 3.7). Table 3.8 also shows that there was significant increase in storage loss in IR scenario (compared to the NI scenario). Overall, we see a greater change in GWC in WY 12 as compared to WY11, suggesting that increased irrigation pumpage has significant impact on all the GWC in the study area.

Table 3.8 Percentage change in simulated recharge (to UFA) and discharge (from UFA) budget components due to irrigation pumpage for water year 2012.

Components	2011			2012								
	Oct.	Nov.	Dec.	Jan.	Feb.	Mar.	Apr.	May	June	July	Aug.	Sep.
Percentage change in flux from Recharge Components of UFA												
Infiltration	0	0	0	0	0	0	0	0	0	0	0	0
Regional Flow	1	0	0	0	0	2	3	4	4	4	3	4
Streams	14	8	7	5	4	20	25	42	38	36	35	42
Aquifer Outcrop	4	2	1	1	1	8	11	12	13	13	13	15
USCU	2	1	0	0	0	5	6	9	8	8	7	8
Percentage change in flux from Discharge Components of UFA												
Regional Flow	-2	-1	-1	-1	0	-3	-5	-6	-6	-6	-6	-7
Streams	-3	-2	-1	-1	-1	-6	-7	-10	-10	-10	-9	-10
Aquifer Outcrop	-6	-3	-2	-2	-1	-10	-10	-12	-13	-15	-15	-18
USCU	-3	-1	0	0	0	-6	-7	-8	-9	-9	-8	-9
Decreased Storage Gain or Increased Storage Loss	-8	73	-49	-37	-25	-70	-44	-47	-46	-40	-31	-54

3.6.6 Contribution to Irrigation for Water Year 2011

Tables 3.9 and 3.10 show contribution of simulated increased recharge and decreased discharge components of UFA due to irrigation pumpage and/or increased storage gain for WY 11 and WY 12, respectively. The values in the table are calculated by calculating the difference in the water budget components for IR and NI simulations. The table, therefore, represents how much increased recharge and decreased discharge are caused by irrigation withdrawal when comparing the IR and NI scenarios. It should be noted those months during which there is increased storage gain, when comparing the IR and NI simulations, the storage gain was added to the irrigation withdrawal to attain water balance. For example, during the month of March 2011,

irrigation withdrawal was 7 Mgal/d and increased storage gain was 25 Mgal/d (Table 3.9). These two values were combined (for water balance) to get a value of 32 Mgal/d which was then balanced by the recharge and discharge components (Table 3.9).

Table 3.9 Simulated increase in recharge and decrease in discharge components of UFA due to irrigation pumpage for water year 2011.

Irrigation Withdrawal and Increased Storage Gain in millions of gallons per day								
Month*	**2010**	**2011**						
	Oct.	**Mar.**	**Apr.**	**May**	**June**	**July**	**Aug.**	**Sep.**
Irrigation	271	7	66	13	69	478	41	217
Increased Storage Gain	0	25	0	11	0	0	0	0
Total of Irrigation and/or Increased Storage Gain	**271**	**32**	**66**	**24**	**69**	**478**	**90**	**217**
Simulated Change in Recharge Components of UFA due to Irrigation Withdrawal (Mgal/d)								
Infiltration	0	0	0	0	0	0	0	0
Regional Flow	3	0	1	1	1	8	3	4
Streams	4	1	2	1	1	5	3	5
Aquifer Outcrop	16	5	3	2	1	9	2	7
USCU	39	8	17	6	18	81	19	31
Total	**62**	**14**	**22**	**8**	**21**	**103**	**27**	**46**
Simulated Change in Discharge Components of UFA contributing to Irrigation Withdrawal and Increased Storage Gain (Mgal/d)								
Increased Storage Loss	126	0	12	0	13	226	0	78
Regional Flow	3	1	1	1	1	9	5	7
Streams	62	12	22	13	27	112	53	74
Aquifer Outcrop	0	1	1	0	0	1	0	0
USCU	18	5	7	2	6	28	5	12
Total	**209**	**18**	**43**	**15**	**47**	**375**	**63**	**170**

Table 3.9 also shows that during high irrigated months of October 2010, July 2011 and September 2011 most of the irrigation water was contributed from USCU and stream-aquifer flux. During October 2010, comparing the IR and NI simulation showed that out of 271 Mgal/d of irrigation withdrawal 62 Mgal/d were met by increase in recharge from stream, whereas, for July and September 2011 these values are 103 Mgal/d and 46 Mgal/d, respectively. In table 3.9 we also see that USCU is a major recharge component contributing to irrigation withdrawal. Increased storage loss is also one of the major components contributing to irrigation withdrawal,

thus indicating drop in GW levels (Table 3.9). In the discharge components, most of the water is found to be contributed by decreased stream-aquifer flux (Table 3.9). During the months of October, July and September, discharge from the aquifer to the streams decreased by 209, 375, and 170 Mgal/d, respectively (Table 3.9). Table 3.9 shows that decreased discharge to stream was contributing to irrigation water withdrawal in the study area. In other words, stream-aquifer flux was one of the major factors contributing water for irrigation.

Table 3.10 Simulated increase in recharge and decrease in discharge components of UFA due to irrigation pumpage for water year 2012.

Irrigation Withdrawal and Increased Storage Gain in millions of gallons per day								
Month*	**2011**	**2012**						
	Oct.	**Mar.**	**Apr.**	**May**	**June**	**July**	**Aug.**	**Sep.**
Irrigation	194	533	655	893	769	744	577	734
Increased Storage Gain	0	0	0	0	0	0	0	0
Total of Irrigation and/or Increased Storage Gain*	**194**	**533**	**655**	**893**	**769**	**744**	**577**	**734**
Recharge Components of UFA contributing to Irrigation Withdrawal and Increased Storage Gain in millions of gallons per day								
Infiltration	0	0	0	0	0	0	0	0
Regional Flow	5	11	17	25	23	24	21	25
Streams	6	13	14	19	17	14	14	18
Aquifer Outcrop	7	12	17	19	21	21	20	23
USCU	51	103	134	190	182	181	158	174
Total	**69**	**140**	**182**	**252**	**243**	**240**	**213**	**241**
Discharge Components of UFA contributing to Irrigation Withdrawal and Increased Storage Gain in millions of gallons per day								
Increased Storage Loss	14	214	245	327	209	180	71	161
Regional Flow	6	13	18	24	23	24	22	27
Streams	75	107	142	212	210	217	197	217
Aquifer Outcrop	2	3	2	3	3	4	4	4
USCU	28	56	66	74	81	79	70	84
Total	**125**	**393**	**474**	**641**	**526**	**504**	**363**	**493**

For WY 12, we see similar results, but due to increased irrigation the contributions of each component were more prominent (Table 3.10). In WY 12, during the months of March to September, we see that contribution of discharge components were more than recharge

components. During the month of May 2012, out of 893 Mgal/d of irrigation, increased recharge contributed 252 Mgal/d and decreased discharge contributed 641 Mgal/d (Table 3.10).

Figure 3.5 shows percentage contribution of simulated increased recharge and decreased discharge components of UFA to irrigation pumpage for WY 12. The figures show that recharge and discharge from USCU, streams and increased storage loss are the major factors contributing to irrigation withdrawal in the study area. The contribution of increased recharge/decreased discharge through USCU was approximately 35%, from increased recharge/decreased discharge stream-aquifer flux was approximately 30% and contribution of increased storage loss ranged from 7% to 40% (Figure 3.5). The results clearly show that a major component of irrigation water withdrawal is derived from loss in stream-aquifer flux and storage loss.

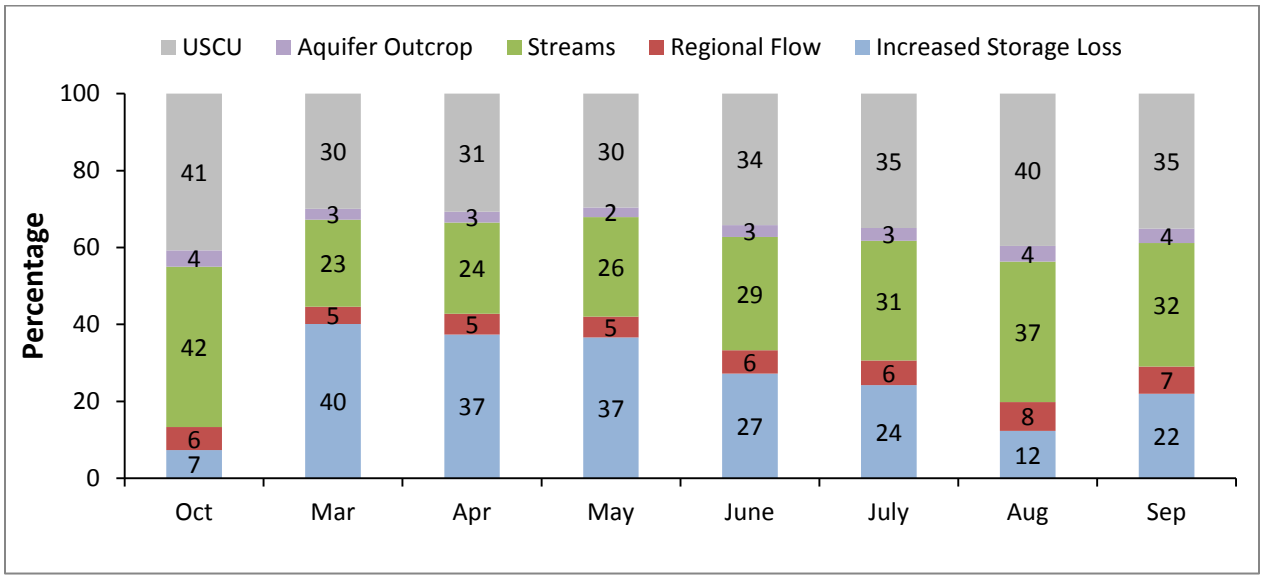

Figure 3.5 Percentage contributions by budget components (increased recharge and decreased discharge) of UFA to irrigation pumpage for water year 2012.

3.6.7 Critical Areas

Critical areas are identified as areas where GW levels are severely affected by irrigation withdrawals. Identification of critical areas is important to understand the locational impacts of irrigation pumpage on GW levels and also identify potential areas having greater impacts on stream-aquifer flux. It is important to note that identification of critical areas are based on difference in simulated GW levels for IR and NI scenarios, which are within an RMSE error level of 8.58 ft and hence should be considered in relation to that. It is to be understood that an RMSE error of 8.58 ft will be present in both the scenario runs and therefore comparison and difference in GW levels between the two scenarios is just for the sole purpose of identifying the areas where the effect of pumpage is the most and not to present an absolute value of drawdown.

Figures 3.6 and Figure 3.7 show decrease in GW levels for irrigated months during WY 11 and WY 12, respectively. In WY 11, we see that there is no significant decrease in GW levels except during the month of July 2011 (Figure 3.6).

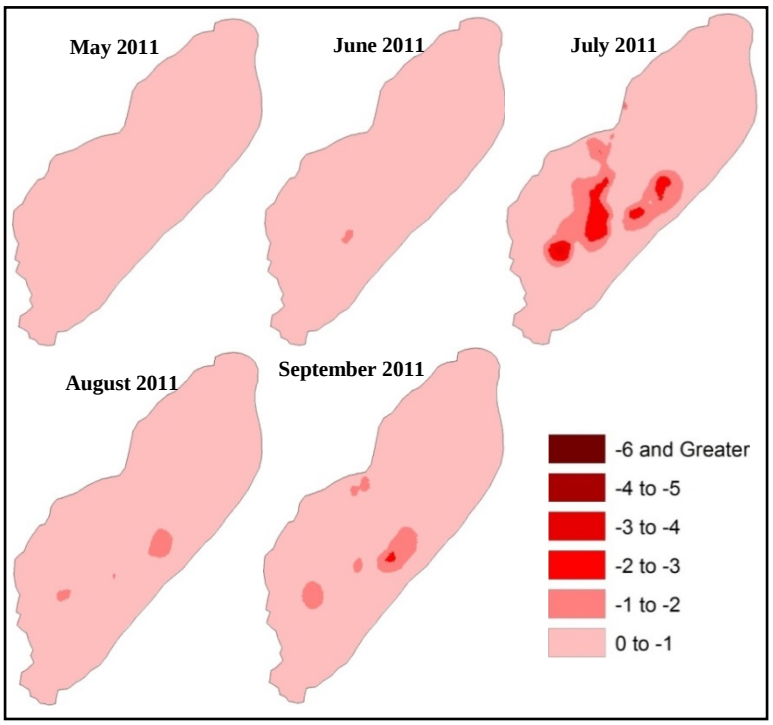

Figure 3.6 Groundwater level drawdown due to irrigation pumpage in WY 11.

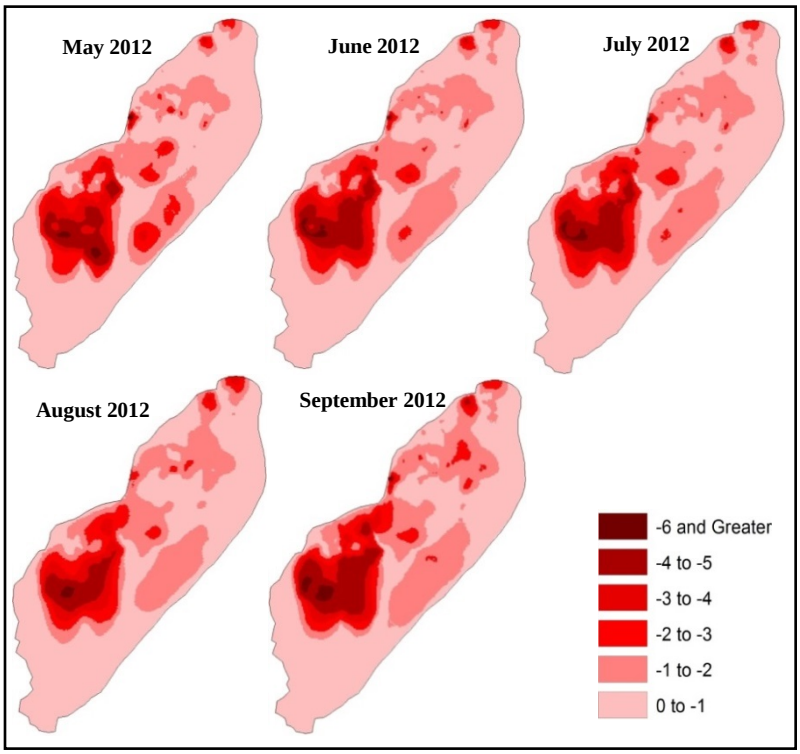

Figure 3.7 Groundwater level drawdown due to irrigation pumpage in WY 12.

In the month of July 2011, simulated GW levels decreased by 2ft to 4ft due to irrigation. In contrast to WY11, WY 12 showed greater decrease in groundwater levels due to increased pumpage in WY 12. GW levels decreased by as much as 6 ft in certain areas due to intense pumpage during all the irrigated months (Figure 3.7). The areas showing greater drawdown in GW levels coincide with the areas having intense irrigation. These areas were localized in GHZ of Upland Interstream, Interstream Karst and Upland inerstream Karst; severe drawdown was localized in the Upland Interstream GHZ. These areas are also within the vulnerable subwatersheds of Spring Creek which is on the critically endangered species list. Identification of these areas can help water managers issue restrictions on irrigation pumpage during droughts and this might help avoid the irrigation induced streamflow reduction.

3.7 Summary and Conclusion

This paper used the MODFE groundwater model to simulate and understand the effect of irrigation pumpage on GW levels, groundwater budget, and stream-aquifer flux for the drought period of 2010 to 2012. The inputs to the model include stream stage, infiltration, head in the USCU, and irrigation pumpage. The model simulated IR and NI scenarios and the outputs were compared to analyze the differences in groundwater levels, groundwater budget, and stream-aquifer fluxes to understand the effect of irrigation on them.

Results showed that GW levels and GWB in the UFA follow the seasonal precipitation patterns of the Southeast US. Infiltration increased during the late fall and decreased considerably during the summer months. The contribution of infiltration as a recharge component to the water budget varied from 2% to 11% for the WY 11. Irrigation for WY 11 varied largely on a monthly basis. Irrigation for WY 11 was far lower than the irrigation during

the March 2001-02 period (Jones and Torak, 2006) and WY 12. Irrigation pumpage was a major component in the entire GWB and its contribution varied from 1% to 7% for WY 11. Recharge and discharge through USCU also varied on a seasonal basis. Results showed that recharge and discharge through USCU and stream-aquifer flux were the major components of GWB. USCU was also the major source of recharge to the UFA and accounted for almost 66% of the total recharge to the UFA in WY 11. The entire contribution of stream-aquifer flux to the GWB was approximately 30% and also the major source of discharge from UFA. Recharge and discharge through streamflow changed significantly because of irrigation. Change in UFA storage (gain and loss) also followed seasonality. Storage loss was lower during the late winter and early spring than during the summer months. Irrigation resulted in increased storage loss from the aquifer except for the non-irrigated months. Analysis of change in groundwater component due to irrigation showed that that recharge to the UFA through stream increased by more than 10% due to irrigation, during the highly irrigated months. The contribution of flux from USCU and stream-aquifer flux to irrigation was approximately 35%, 30% respectively. The results clearly showed that irrigation water withdrawal was derived mainly from loss in stream-aquifer flux and storage.

Analysis of critical areas showed that, in the WY 11, there was no significant decrease in GW levels except during the month of July 2011. In contrast to WY11, WY 12 showed greater decrease in GW levels due to increased pumpage in WY 12. GW levels decreased by as much as 6 ft in certain areas due to intense pumpage during the irrigated months. The areas showing greater drawdown in GW levels coincide with the areas having intense irrigation. These areas are close to Spring Creek which is among the critically endangered species list. The results above exemplify that apart from seasonality, irrigation pumpage also has an important role in the

overall state of groundwater resources and stream-aquifer fluxes in the study area. The study showed that stream-aquifer flux, which is one of the most contentious issues in the tri-state conflict, was significantly impacted by irrigation during droughts. Addressing this irrigation induced flow reductions during droughts in the Flint River will be one of the major challenges in solving the tri-state conflict. Identification of critical areas therefore can help water managers issue restrictions (in those areas) on irrigation pumpage during droughts. The study clearly illustrated the effect of anthropogenic activities on groundwater resources in the study area.

Chapter 4

Effect of Simulated Irrigation Scenarios on Groundwater Resources during Droughts in the Lower Apalachicola-Chattahoochee-Flint River Basin

4.1 Abstract

El Niño Southern Oscillation (ENSO) induced droughts in the Southeast US have been the source of water conflicts in the region. These conflicts intensify every time there is a drought in the region. One of the issues regarding the conflict is the irrigation-induced streamflow depletion during droughts in southwest Georgia. Excessive irrigation during La Niña phases (drought) from the Upper Floridan Aquifer results in lowering of streamflow levels in the Flint River due to stream-aquifer connection. This leads to the failure of the state of Georgia to maintain minimum flow levels in the Flint River leading to endangered species, water quality and high temperature issues. This study was undertaken to study the impacts of increase/decrease in irrigation levels on groundwater levels and groundwater budget components using the groundwater model MODular-Finite Element Groundwater Model (MODFE). The model was run for the water year 2012 and simulated the groundwater budget components at irrigation levels of 50%, 75%, 100%, 125%, 150% and 200%. Changes in groundwater budget components were studied at different irrigation levels and their contributions to irrigation water withdrawal were also analyzed. Additionally, the effect of irrigation restrictions and acreage buyout in the vulnerable regions of Spring Creek subwatershed were also studied. Results show that increasing irrigation levels in the study area majorly affected storage loss and flux through the overburden

and stream-aquifer flux. During the months of May to September 2012 when irrigation was maximum, doubling of irrigation resulted in almost 50% increase in the recharge from streams to aquifer and 10% decrease from aquifer to streams. The results suggest linear relationship between irrigation water withdrawal and contribution of stream-aquifer flux to it. Results also showed that groundwater levels in the vulnerable subwatershed of Spring Creek were severely affected by increase in irrigation. Increasing irrigation levels to 200% resulted in groundwater levels to fall by as much as 11 ft in some areas in the Spring Creek subwatershed and by 5 ft in some areas on the east of Flint River. Analysis of acreage buyout suggested that restricting irrigation withdrawal in vulnerable subwatershed of Spring Creek can have significant impacts on stream-aquifer flux in the study area. The results in this study will be helpful in understanding the impacts of applying irrigation restrictions in the vulnerable regions and help avoid the irrigation-induced streamflow depletion in the Flint River.

4.2 Introduction

Climate change and climate variability affect water resources in the United States (Gleick and Adams 2000) and around the world. El Niño Southern Oscillation (ENSO) is one of the dominant forms of natural climate variability cycles in the world (Diaz and Markgraf, 1992). ENSO is the periodic warming and cooling of Pacific Ocean in the equatorial region and consists of three phases namely El Niño, La Niña and Neutral phase. El Niño represents the warming phase and La Niña refers to the cooling of Pacific sea surface temperatures off the coast of South America (Quinn 1994; Aceituno 1992). ENSO has been shown to have influence on extreme events and hydrology of watersheds around the world (Kahya and Drakup, 1993; Gurdak et al., 2007; Chiew et al., 1998; Rajagopalan and Lall, 1998; Piechota and Dracup, 1999).

The southeastern United States is a region with rapid population growth, increased agricultural production and is especially vulnerable to ENSO-induced climate variability (Enfield et al. 2001). The phase of La Niña is characterized by warmer and drier winters and is responsible for droughts in the Southeast United States (Kiladis and Diaz, 1989; Hansen and Maul, 1991; Schmidt and Luther, 2002). The Apalachicola-Chattahoochee-Flint River Basin (ACF), in the Southeast is particularly prone to droughts caused by ENSO. Irrigated agriculture in the ACF, especially in southwest Georgia, is heavily dependent on groundwater withdrawals from the Upper Floridan Aquifer (UFA). Since the early 1980's, a series of droughts have caused losses in agricultural productivity and have led to increased water conflicts in the region (Tri-State Water Conflict between the states of Alabama, Georgia and Florida) (Southern Environmental Law Center). During droughts, when groundwater levels are already low, excessive irrigation water withdrawal from the UFA results in further lowering of groundwater levels. Due to the hydraulic connection between the UFA and Flint River (FR), lowering of groundwater levels in UFA results in lowering of flow levels in the FR as well. This leads to the failure of the state of Georgia to maintain minimum flow levels in the FR and affects flow in the downstream Apalachicola River and Apalachicola Bay where it threatens the struggling oyster industry. Chapter 2 showed that groundwater levels (GW) are affected by droughts and their longevity. Subsequently, in Chapter 3, the combined effects of droughts and irrigation activities were studied. The results from the studies show that irrigation severely affects GW levels and groundwater budget components in the lower ACF. They also showed that as much as 30% of irrigation water withdrawal is contributed from stream-aquifer flux, and groundwater levels and stream-aquifer flux are majorly affected by irrigation in the lower ACF. This clearly suggests that increased irrigation in future has potential to further aggravate the crisis. Therefore, this

study was undertaken to understand the effects of possible future increases in irrigation pumpage on GW levels and its effects on stream-aquifer flux. Further, an attempt was made to study the effectiveness of possible future water restrictions based on the Flint River Drought Protection Act (FRDPA) (Georgia General Assembly). The FRDPA mandates the state to compensate farmers for not irrigating their crops during droughts to sustain flows in the FR. The buyback program was first used in the drought of 2000-01, but subsequently in 2012, the state declined to implement the program citing lack of funds and effectiveness of the policy (need a ref). Therefore, in this study, a cost benefit analysis of implementation of the buyback program was studied.

This study is part of a bigger project that aims at understanding the relationships between droughts, irrigation and its effects on stream-aquifer fluxes and GW levels. A groundwater model is used to study the effects of increased irrigation pumpage and irrigation restrictions on groundwater levels in lower ACF.

4.3 Study Area and the Upper Floridan Aquifer

The study area is in the lower Apalachicola-Chattahoochee-Flint (ACF) River Basin in the states of Alabama (AL), Florida (FL) and Georgia (GA). The climate in the study area is humid subtropical with an average annual precipitation of about 50 inches. The total area is approximately 4632 mi^2 with approximately 4000 irrigation wells pumping water from the UFA. The UFA is the major water bearing unit in the region. The UFA consists of 4 sections, the Surficial Aquifer System, UFA, Upper Semi-Confining Unit (USCU) and the Lower Confining Unit. The USCU is overburden overlying the UFA and acts as the major source of recharge to the aquifer (Torak and Painter, 2006).

4.4 Methodology

To study and understand the impacts of simulated irrigation levels on groundwater levels, a groundwater model developed by United States Geological Survery (USGS) named MODular Finite-Element model (MODFE; Cooley, 1992; Torak, 1993 a, b) was used. MODFE uses a finite element mesh that represents the geometry of the study area. The finite element mesh consists of elements, the intersection of which are called nodes. A finite element mesh developed by Jones and Torak (2006) was used for this study. The finite element mesh used for this study consisted of 37,587 elements and 18,951 nodes (Figure 4.1a).

4.4.1 Governing Groundwater Flow Equation

The basic governing equation for groundwater flow in MODFE is represented by the following two-dimensional equation:

$$\frac{\partial}{\partial x}\left(T_{xx}\frac{dh}{dx}+T_{xy}\ \frac{dh}{dx}\right)+\ \frac{\partial}{\partial y}\left(T_{yx}\frac{dh}{dx}+T_{yy}\ \frac{dh}{dx}\right)+R(H-h)+W+P=S\frac{\partial h}{\partial t} \qquad (1)$$

where, *(x,y)* are the cartesian coordinate directions, *t* is time, *S(x,y,t)* is the storage coefficient, *h(x,y,t)* is the aquifer hydraulic head, *W(x,y,t)* is the unit areal recharge or discharge rate (infiltration), *H(x,y,t)* is the hydraulic head of the USCU, *R(x,y,t)* is the vertical hydraulic conductance (vertical hydraulic conductivity divided by thickness) of USCU, *P(x,y,t)* are point source or sinks and symmetric transmissivity is written in matrix form as

$$\begin{bmatrix} T_{xx}\ (x,y,t) & T_{xy}\ (x,y,t) \\ T_{yx}\ (x,y,t) & T_{yy}\ (x,y,t) \end{bmatrix} \qquad (2)$$

The model solves for hydraulic head in the UFA using the governing equation and initial and boundary conditions. Further details about the model and solution methods can be found in MODFE manuals (Torak, 1992) and Jones and Torak (2006).

4.4.2 MODFE Inputs

Inputs to MODFE are made at the elements or at the nodal intersections of the finite element mesh. Input parameters such as aquifer properties (transmissivity), properties of the USCU, stream channel properties are time invariant and hence were retained from Jones and Torak (2006). Parameters such as infiltration, irrigation and municipal pumpage and head in the USCU were varied on a monthly basis. The various input parameters are summarized below.

4.4.3 Head at UFA Updip Limit

The Updip limit area (Figure 4.1a) is the area on the northwestern side of the model area where the UFA reaches the land surface and hence is under unconfined conditions. Groundwater levels here do not fluctuate on a yearly or seasonal basis (Jones and Torak, 2006), therefore, the boundary at the Updip was input as a specified head boundary where the heads remain constant throughout the period of simulation. For this study, the hydraulic head distribution from Jones and Torak (2006) was retained.

4.4.4 Infiltration

Infiltration rates to the UFA vary considerably on a seasonal basis. In the absence of an inbuilt infiltration calculation mechanism in MODFE, approximations were made to calculate infiltration rates. Hayes et al. (1983) showed that mean annual recharge to the UFA is about 10 inches per year (i.e. 20% of mean annual rainfall) and about 6 inches per year during late summer.

Infiltration rates were calculated on a seasonally varying conversion rate of 10%, 20% and 30% of precipitation, allowing MODFE to simulate variable infiltration rates corresponding

to different months in the year. A monthly precipitation conversion rate of 30% was used for fall and winter months (October to February) which are characterized by long duration precipitation from frontal passages (Jones and Torak, 2006).

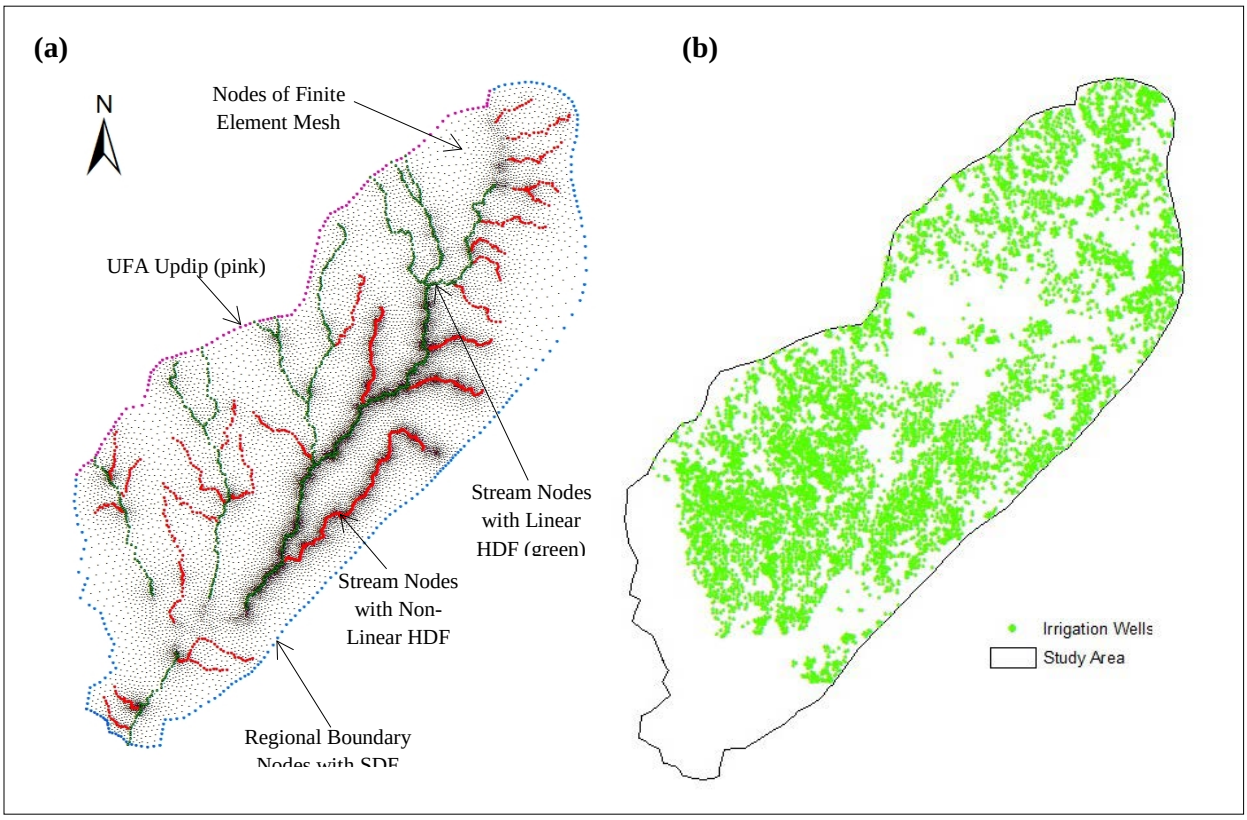

Figure 4.1 (a) The finite element mesh and the associated types of boundary nodes in the study area. **(b)** Location of irrigation wells in the study area.

A conversion rate of 10% was used to simulate infiltration rates during the summer months (April to August). Precipitation during the summer months is due to summer convective storms of high intensity but short duration (Jones and Torak, 2006). The months of March and September are transition months when both types of storms occur and hence a conversion rate of 20% of average monthly precipitation was used. Infiltration was derived from precipitation data collected from 14 rain gauge stations from National Climatic Data Center (Appendix C.1). It is It

is important to note that infiltration was applied as a source of recharge only at areas where the USCU is less than 30 ft or is absent. USCU greater than 30 ft acts as a source of recharge to the UFA, through a process called vertical leakage and therefore infiltration from the land surface acts as a source of recharge in areas where USCU is less than 30 ft (Jones and Torak, 2006).

4.4.5 Irrigation/Municipal Pumpage and Discharge through Springs

Irrigation pumpage is the major anthropogenic activity affecting the aquifer in the study area. Approximately 4000 irrigation wells pump water from the UFA supplying them to central pivot irrigation systems for agricultural use. Irrigation was calculated using monthly telemetered depth maps procured from USGS, Georgia Water Science Center. Irrigation flux was calculated by multiplying the depth value obtained from the maps to irrigated acreage in the study area, which was then assigned to the nearest node in the finite element mesh. Municipal pumpage of 26 Mgal/d was simulated for the entire period of simulation and was retained from Jones and Torak (2006). Off-channel spring discharge of 0.39 Mgal/d was also retained from Jones and Torak (2006) owing to unavailability of time varying data. The unavailability of industrial use and off-channel spring data is unlikely to introduce significant error in the model simulation as the combined withdrawal for industrial pumpage and springflow is extremely small compared to the total irrigation pumpage.

4.4.6 Regional Groundwater Flow

Flow across regional boundaries (except UFA updip) was simulated across the element sides at the model boundaries. Flow across an element defined by nodes *k* and *l*, at the boundary is expressed as:

$$Q_B = (1/2)\ \alpha\ L_{kl}\ (H_{Bi} - h_i),\ i = k\ or\ l \quad (3)$$

where, Q_B is the flow rate across the model boundary, L_{ki} is the length of the element side and α is defined as

$$\alpha = \frac{Kb}{L} \quad (4)$$

K and *b* are average hydraulic conductivity and thickness of the aquifer between the model boundary and external head (H_B). External head is the head at a distance of 3 miles from the model boundary that is used to calculate the flow across boundary. The model boundary is representative of a groundwater divide, therefore, the external head does not fluctuate appreciably on a monthly basis and hence is kept constant. Flow across the model boundary is therefore determined by the difference in groundwater levels at the boundary nodes (h_i) and the external head as in equation 4. Values of external head at the model boundary were interpolated from the potentiomentric surface maps of the UFA for May – June 2010 published by USGS (Ortiz, 2010). α values for regional boundaries were retained from Jones and Torak (2006)

4.4.7 Flow Across Streambeds

Flow across streambeds follows the same principle as flow across regional boundaries. However for flow across streambeds the α value is defined as

$$\alpha = \frac{K_r\ W_r}{b_r} \quad (5)$$

where, W_r and B_r is streambed width and thickness, respectively and K_r is vertical hydraulic conductivity of the streambed. Controlling head, H_{Bi}, in equation 3 is the stream stage (or lake level), for the associate node *i* (=*k or l*) of the element side on the boundary for calculation of

flow across streambeds. The equation 3 represents flow across streambeds that are linear and representative of streams that are perennial and have flow throughout the year.

However a non-linear form of the equation is used to simulate ephemeral or small streams. Ephemeral streams go dry when groundwater levels are lower than the altitude of the streambed. Flow across ephemeral streams is given by equation for node *i (=k or l)* on a streambed element

$$Q_{ri} = \begin{cases} C_{ri}\,(h_{ri} - h_i), & h_i > Z_{ri} \\ C_{ri}\,(h_{ri} - z_{ri}), & h_i > Z_{ri} \end{cases} \quad (6)$$

where, Q_{ri} is the volumetric flow rate, h_{ri} is the stream stage, z_{ri} os the altitude of streambed bottom and C_{ri} is the coefficient. α values were retained from Jones and Torak (2006), and were changed slightly for model calibration. Stream stage values (H_{Bi}) were calculated by interpolation of stream gauge data based on local variations in slope (obtained from contour maps) of the stream surface data. Stream gauge data was obtained from 13 stream gauging stations from U.S. Army Corps of Engineering, Mobile District, Alabama (Appendix B.1).

4.4.8 Vertical Leakage across USCU and Lake-Beds

Vertical leakage across streambeds were expressed by the function *R(H-h)* in equation 1 and is simulated in areas where the USCU thickness is more than 30 ft. The volumetric flow rate, Q_{ai}, across nodes *i* of the leakage is expressed as

$$Q_{ai} = \begin{cases} C_{ai}\,(H_i - h_i), & h_i > z_{ti} \\ C_{ai}\,(H_i - z_{ti}), & h_i > z_{ti} \end{cases} \quad (7)$$

where, C_{ai} is the nodal vertical leakage coefficients, z_{ti} is the nodal altitude of the top of UFA or base of USCU, h_i is the nodal hydraulic head in the UFA and H_i is the nodal head in the USCU.

Recharge to the aquifer from USCU is limited to a maximum rate of recharge by equation 7. Heads in the overlying USCU, H_i, were calculated as proportion saturation thickness of USCU which varies seasonally for each geo-hydrologic zone (GHZ). For the drought period of (La Niña event) May 2010 – September 2012, the saturation proportion of the USCU for each GHZ is the represented by the thickness of the sandy clay or clay layer in the geo-hydrologic zone that remains saturated even when the upper sandy layer completely dewaters (Torak and Painter, 2006). This lower clayey layer acts as a source of recharge to the UFA. Due to lack of USCU head data, the monthly drought period USCU head values by Jones and Torak (2006) (March 2001 – February 2002) were retained. More details about the model input parameters and simulation techniques can be found in the MODFE manual (Cooley,1992; Torak, 1993 a,b) and USGS scientific investigation reports by Jones and Torak (2006) and Torak et al (1996).

4.4.9 Analysis

In the previous chapter, the effect of irrigation on groundwater budget components was studied. The calibrated model from Jones and Torak (2006) was used. The model was validated in the previous chapter for the 2010-2012 period of simulation. In this study, the impacts of possible future increases in irrigation levels during droughts on groundwater levels and groundwater budget components in the study area were quantified. The model simulated the drought period of (La Niña) WY 2012.

In the first part of the study irrigation levels were increased to 125%, 150% and 200% of present and its effects on stream-aquifer flux, USCU recharge/discharge, storage loss and regional flow were studied. In addition to studying the effects of increased irrigation levels, effects of possible irrigation restrictions, to avoid the irrigation induced flow reductions in Flint

River, was also studied. Irrigation levels were reduced throughout the study area to 75% and 50% of present levels and the impacts on groundwater budget components, especially stream-aquifer flux and storage loss, were studied. Contribution of each budget component towards irrigation pumpage and groundwater drawdown at different irrigation levels was also studied. In the second part of the analysis, irrigation restrictions were applied in the vulnerable subwatershed of Spring Creek (SCW). The SCW, Ichawaynichaway Creek (ICH) and Kinchafoonee-Muckalee Creek (KMC) are classified as vulnerable as they harbor the federally protected endangered mussel species. In the previous chapter, we found that the subwatershed of Spring Creek (SCW) was responsible for most of the storage loss where groundwater levels fell by approximately 6 ft due to irrigation, more than any other area in the study area. Therefore, the goal here is to study contribution of the effect of irrigation restrictions in vulnerable subwatershed on groundwater budget components of the entire study area. Irrigation in the SCW subwatershed was lowered to 75%, 50% and 25% of the present levels and the contribution of UFA to streamflow was analyzed. Finally, impact of shutting irrigation in regions in accordance to the buyout program of the FRDPA was analyzed. During the 2001 drought the Georgia Environmental Protection Division (GAEPD) started a buyout program in which certain acres of land near to the creeks were bought to prevent irrigation in those areas. The areas were located in the SCW and hence in this study effect of such buyout program during drought periods were studied. In this study, irrigation was shut progressively starting from areas in the Spring Creek subwatershed and then in the Ichawaynochaway Creek and Kinchafoonee-Muckalee Creek, followed by regions on the east of the Flint River (Figure 4.2). Analysis was done on how the contribution of stream-aquifer flux changed with shutting of irrigation in the region. Irrigation was shut for the months of May to September 2012, corresponding to the months of high

irrigation. Apart from that, cost analysis was done based on 2001 acreage buyout costs of $150/acre and estimates were made on the cost of buying out irrigated acreage in the region.

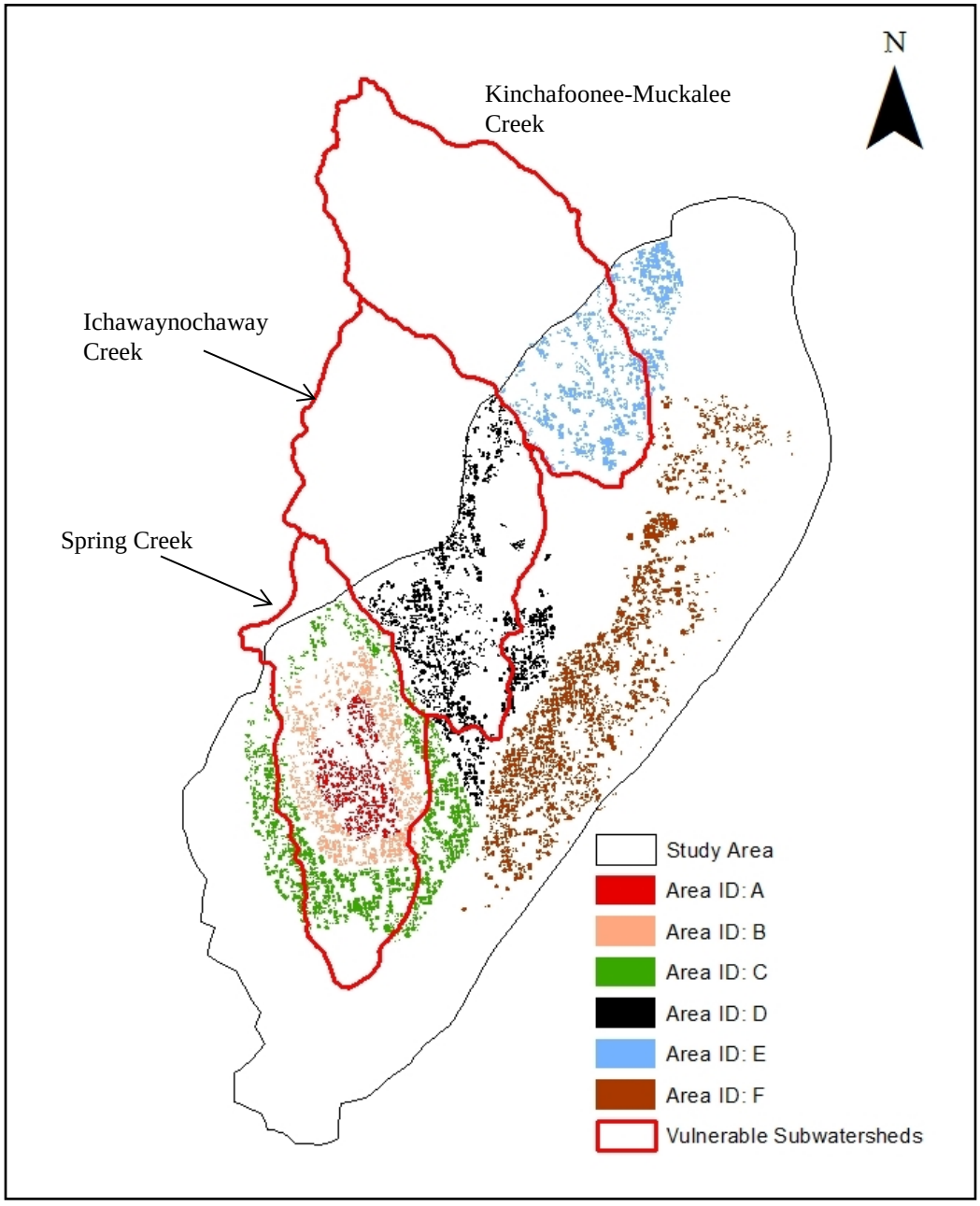

Figure 4.2 Area IDs used for analysis of the buyout program. Includes areas showing the vulnerable subwatersheds.

It is important to note that increase in irrigation levels were not associated with increase in irrigated acreage, rather increase in pumpage in the already existing wells. It is impossible to know how irrigated acreage might increase in future, therefore increasing irrigation levels in the existing wells present us with the opportunity to study the response of groundwater budget components to possible changes in irrigation water withdrawal in the study area.

4.5 Results

4.5.1 Stream-Aquifer Flux

Understanding the effects of irrigation sensitivity on groundwater budget will help in understanding the effects of increased irrigation on the GWC in the future. Irrigation sensitivity analysis also helps in understanding the effects of possible irrigation restrictions that might have to be imposed in future to help maintain flow levels in the study area. Groundwater levels and GWC in the study area follow the distinct seasonal precipitation patterns of the Southeast. Increased irrigation during the summer months combined with high evapotranspiration leads to lowering of groundwater levels and due to stream-aquifer connection also leads to lowering of flow levels in the Flint River (Torak and Painter, 2006; Mitra et al., 2014). Groundwater levels and streamflow reach yearly high in late winters due to high and steady rain and low evapotranspiration in winter months. Studies conducted by Mitra et al. (2014) and Torak and Painter (2006), showed that in the study area, groundwater component of storage, stream-aquifer flux and flux through the USCU are greatly affected by irrigation and contribute to irrigation pumpage in the region. The results in this section will therefore help elucidate the extent to which increased/decreased irrigation will affect the groundwater budget components in the study area.

Table 4.1 shows the changes in streamflow recharge to the UFA for the water year 2012. The table shows that recharge from stream to aquifer increased significantly with increase in irrigation in the study area. During the month of May 2012 when irrigation was maximum, doubling of irrigation resulted in almost 50% increase in the recharge from streams to aquifer (Table 4.1). This trend was similar during the months with high irrigation (i.e. May 2012 to September 2012). During the months with less or no irrigation also we see that increasing pumpage during the previous months leads to increase streamflow recharge to the aquifer due to lower groundwater levels (Table 4.1), though the increase in recharge is less than during irrigated months. During the month of August 2012, increasing irrigation to 200% increased streamflow recharge to aquifer from 54 Mgal/d to 74 Mgal/d, whereas, during December 2011 flow increased from 47 Mgal/d to 50 Mgal/d (Table 4.1). This clearly shows that increasing irrigation decreases recharge from stream to aquifer and the effect is more prominent during the irrigated months. Table 4.1 also shows that reducing irrigation in the study area results in decrease in flux from stream to aquifer. During May 2012, decreasing irrigation to 75% resulted in decrease of recharge by 7 Mgal/d and decreasing irrigation to 50% lead to a further decrease in recharge by 11 Mgal/d. During the non-irrigated month of December 2012, decreasing irrigation in the previous month did not lead to any significant change in streamflow recharge to aquifer.

Table 4.2 shows the changes in monthly discharge from aquifer to stream for the water year 2012 (WY 12). Discharge from aquifer to streams is one of the major discharge sources of the UFA accounting for as much as half of the entire discharge. Seventy-five percent irrigation levels led to the increase of discharge to the streams by as much as 47 Mgal/d to 50 Mgal/d during the months of high irrigation (May to September) which was approximately 2% to 3 % of the simulated discharge during the WY 12 (Table 4.2). Fifty percent irrigation levels almost

doubled the increase observed in the 75% irrigation level scenario. That is, during the months of high irrigation, the average contribution to the streamflow from UFA increased by an average 100 Mgal/d for 50% irrigation levels, whereas, the average increase was approximately 50 Mgal/d for the irrigation levels of 75% (Table 4.2). Discharge to streams increased by approximately 3% - 5% during the irrigated months of WY 12 for the irrigation levels of 50% (Table 4.2).

Table 4.1 Simulated monthly recharge to UFA from streams at different irrigation levels for the water year 2012.

Recharge to UFA from streams in Mgal/d												
Year	**2011**			**2012**								
IL*	**Oct**	**Nov**	**Dec**	**Jan**	**Feb**	**March**	**Apr**	**May**	**June**	**July**	**Aug**	**Sep**
50%	42	39	45	46	43	72	60	51	53	45	47	52
75%	44	39	46	47	43	75	64	55	57	49	51	57
100%	45	40	47	47	44	79	67	62	63	53	54	63
125%	47	41	47	48	44	84	71	70	70	58	59	68
150%	48	42	48	48	45	89	75	79	78	65	63	76
200%	52	44	50	50	46	99	85	100	94	82	74	92

**Irrigation Levels*

Increase in irrigation levels to 125%, 150% and 200% in the study area progressively resulted in the decrease in contribution of UFA to the stream. Increasing irrigation levels to 125%, 150% and 200% resulted in the lowering of discharge to the streams by approximately 47 Mgal/d, 92 Mgal/d and 178 Mgal/d, respectively, during the heavily irrigated months which was approximately 2%, 5% and 9% of the simulated discharge to streams for the WY12 (Table 4.2). Table 4.2 also shows that increasing irrigation during the month of October resulted in significantly lower contribution to the aquifer during subsequent winter months (November – February) owing to lowering of groundwater levels. This clearly shows that the effects of irrigation persist for at least 4 months, resulting in reduced contribution to stream from the UFA.

The results here exemplifies the effect of possible future irrigation increases on stream-aquifer flux, suggesting that stream-aquifer flux will continue to be significantly affected by increases in irrigation levels the lower ACF.

Table 4.2 Simulated changes in monthly discharge to streams from UFA at different irrigation levels for the water year 2012.

Discharge to Streams from UFA in Mgal/d														
	Year	**2011**			**2012**									**HIM***
	IL*	**Oct**	**Nov**	**Dec**	**Jan**	**Feb**	**Mar**	**Apr**	**May**	**June**	**July**	**Aug**	**Sep**	
Change in Discharge	**50%**	36	21	15	11	8	50	68	99	100	105	95	104	101
	75%	18	10	8	6	4	24	33	47	49	52	47	51	49
Discharge to Streams	**100%**	2121	2133	2123	2004	2047	1814	1943	1980	1956	1990	1967	1946	1968
Change in Discharge	**125%**	-19	-11	-8	-6	-4	-24	-33	-46	-46	-49	-45	-49	-47
	150%	-37	-22	-16	-11	-9	-47	-64	-90	-90	-96	-90	-96	-92
	200%	-72	-46	-33	-24	-19	-91	-125	-170	-174	-184	-175	-186	-178
Percentage Change in Discharge to Stream from UFA														
Percentage Change in Discharge	**50%**	2	1	1	1	0	3	3	5	5	5	5	5	5
	75%	1	0	0	0	0	1	2	2	2	3	2	3	3
	100%	0	0	0	0	0	0	0	0	0	0	0	0	0
	125%	-1	-1	0	0	0	-1	-2	-2	-2	-2	-2	-3	-2
	150%	-2	-1	-1	-1	0	-3	-3	-5	-5	-5	-5	-5	-5
	200%	-3	-2	-2	-1	-1	-5	-6	-9	-9	-9	-9	-10	-9

**Irrigation Levels*
* *High irrigated months*

4.5.2 Upper Semi-Confining Unit

Table 4.3 shows the changes in USCU flux to/from UFA at different irrigation levels for the WY 12. Recharge and discharge from USCU is one of the major factors contributing to irrigation pumpage in the study area (Torak and Painter, 2006). Since USCU is the major recharge factor to the UFA, changes in recharge/discharge to/from USCU due to increased irrigation will affect groundwater levels in the UFA.

Table 4.3 Simulated changes in monthly flux to/from USCU at different irrigation levels for the water year 2012.

USCU Recharge to UFA in Mgal/d														
	Year	**2011**			**2012**									**HIM***
	IL*	**Oct**	**Nov**	**Dec**	**Jan**	**Feb**	**March**	**Apr**	**May**	**June**	**July**	**Aug**	**Sep**	
Change in Recharge	**50%**	-25	-7	-5	-5	-4	-51	-65	-93	-89	-89	-78	-86	-87
	75%	-13	-4	-3	-3	-2	-26	-32	-46	-44	-44	-39	-42	-43
USCU Recharge	**100%**	2148	2314	2402	2363	2305	2267	2364	2379	2367	2373	2327	2318	2353
Change in Recharge	**125%**	13	4	3	2	2	25	32	45	43	43	38	41	42
	150%	26	8	6	5	5	49	64	88	85	85	75	82	83
	200%	51	17	13	10	9	98	127	172	167	167	147	161	163
USCU Discharge to UFA in Mgal/d														
Change in Discharge	**50%**	14	2	2	1	2	26	31	34	37	36	33	38	36
	75%	7	1	1	1	1	12	15	16	18	18	16	19	17
USCU Discharge	**100%**	930	984	947	968	961	941	868	844	833	829	839	855	840
Change in Discharge	**125%**	-6	-2	-1	-1	-1	-12	-14	-14	-16	-17	-15	-17	-16
	150%	-13	-3	-2	-2	-1	-24	-27	-28	-33	-33	-29	-34	-31
	200%	-26	-7	-5	-3	-3	-45	-51	-54	-62	-62	-56	-64	-60

**Irrigation Levels*
** High irrigated months*

Recharge from USCU to the UFA decreased with decrease in irrigation levels (Table 4.3). Table 4.3 clearly shows that reducing irrigation levels to 75% resulted in average reduction of recharge by 43 Mgal/d during the months of high irrigation and reducing by 87 Mgal/d when the irrigation levels were at 50%. Increasing irrigation levels led to increased recharge from the USCU to UFA. Increasing irrigation to 125% led to increased recharge by 25 Mgal/d in the month of March and 45 Mgal/d during May (Table 4.3). Increasing irrigation levels from 125% to 150% approximately doubled the increase in recharge from 42 Mgal/d to 83 Mgal/d. Further increase in irrigation levels to 200% led to further increase in recharge varying from 98 Mgal/d in the month of March to 172 Mgal/d in May (Table 4.3). The table also shows that during the winter months, irrespective of irrigation application, the change in recharge to UFA was not significant. It is important to note that the changes in recharge to the UFA from USCU are more

prominent during the months with high irrigation suggesting that excessive irrigation can also affect the levels in the USCU, which is the major source of recharge to the aquifer.

Discharge from UFA to USCU increased by an average of 17 Mgal/d and 36 Mgal/d, during the months with high irrigation, for irrigation levels of 75% and 50%, respectively (Table 4.3). Discharge decreased by 16 Mgal/d, 34 Mgal/d and 60 Mgal/d for the highly irrigated months when irrigation levels were increased to 125%, 150% and 200%, respectively (Table 4.3). The month of May showed the highest increase/decrease in recharge from/to USCU during the WY 12 (Table 4.3). The results clearly show that increase in irrigation leads to increase in recharge from the USCU to UFA and decrease in discharge from UFA to USCU, whereas, decreasing irrigation results in reversing the process.

4.5.3 Storage Loss

Storage loss in the UFA is an important component in the overall hydrologic budget of the UFA. The loss in storage in the UFA manifest in the lowering of groundwater levels in the UFA. However, this lowering also results in lowering of recharge to the streams from the UFA and thus affecting flow in the Flint River and its tributaries.

Table 4.4 shows that increasing/decreasing irrigation levels in study area has profound impacts on the storage of the UFA. Increasing irrigation levels to 200% increased storage loss from -693 Mgal/d to -1084 Mgal/d in the month of May, an increase of about 50% (Table 4.4). Similar results were seen during the rest of the months with irrigation as well, such as during the months from June to September increased in irrigation levels to 125%, 150% and 200% resulted in almost 14% to 17%, 28% to 34% and 58% to 72% decrease in storage levels (Table 4.4) respectively. Decreasing irrigation levels to 75% and 50% leads to reduced storage from –693

Mgal/d to -604 Mgal/d and -518 Mgal/d, respectively (Table 4.4) for May 2012. It is quite evident that in terms of absolute value, a certain percentage change in irrigation levels leads to greater change in storage loss followed by flux through the USCU and stream-aquifer flux, suggesting that increased irrigation pumpage majorly affects storage loss thus is responsible for lowering of groundwater levels as well (Table 4.2, Table 4.3, Table 4.4). We also see that changes in stream-aquifer flux exhibit a linear relationship with changes in irrigation suggesting a level of predictability.

Table 4.4 Simulated monthly storage loss at different irrigation levels for the water year 2012.

Storage Loss in Mgal/d													
Year	**2011**			**2012**									**HIM**
IL*	**Oct**	**Nov**	**Dec**	**Jan**	**Feb**	**Mar**	**Apr**	**May**	**June**	**July**	**Aug**	**Sep**	
50%	-170	-141	86	96	119	-195	-428	-518	-338	-348	-187	-210	-320
75%	-174	-122	100	107	127	-249	-491	-604	-393	-395	-206	-252	-370
100	-177	-103	115	119	137	-305	-557	-693	-452	-446	-228	-298	-423
125%	-181	-82	130	131	147	-363	-625	-786	-514	-499	-252	-348	-480
150%	-184	-61	146	143	157	-423	-694	-882	-578	-555	-279	-400	-539
200%	-192	-16	180	168	180	-545	-837	-1084	-714	-675	-338	-511	-665
Percentage Change in Storage Loss													
50%	-4	37	-25	-19	-13	-36	-23	-25	-25	-22	-18	-30	-24
75%	-2	19	-13	-10	-7	-18	-12	-13	-13	-11	-10	-15	-12
100	0	0	0	0	0	0	0	0	0	0	0	0	0
125%	2	-20	13	10	7	19	12	13	14	12	11	17	13
150%	4	-41	27	20	15	39	25	27	28	25	22	34	27
200%	9	-84	57	41	32	79	50	56	58	51	48	72	57

**Irrigation Levels*

** High irrigated months*

Changing irrigation levels did not have significant impacts on other budget components such as recharge/discharge from aquifer outcrop area or regional flow. Though the changes in flow were not significant, it was generally seen that increasing irrigation levels resulted in

increased recharge from aquifer outcrop and regional boundaries to the UFA owing to lowering of groundwater levels in the study area.

4.5.4 Groundwater Levels

Figure 4.3 shows the lowering of groundwater levels for May 2012 due to increased/decreased irrigation levels in the study area compared to no irrigation. In the previous chapter, vulnerable areas were identified based on the lowering of groundwater levels. The area corresponding to the subwatershed of Spring Creek is the area where irrigation pumpage is highly concentrated and where the drawdown was the highest. During the summer of 2012 increasing irrigation levels in the study area progressively led to lowering of groundwater levels. Increasing irrigation levels to 200% resulted in groundwater levels to fall by as much as 11 ft in some areas in the Spring Creek subwatershed and by 5 ft in some areas on the east of Flint River (Figure 4.3). Irrigation levels of 125% and 150% led to groundwater level drawdown of approximately 8 ft in some areas of the Spring Creek (Figure 4.3). Increasing irrigation actually led to increased drawdown in the areas east of the Flint River, suggesting that future irrigation levels can lead to lowering in groundwater levels in this region as well. Since, this region also bears direct hydraulic connection to the Flint River, lowering of groundwater levels in this region can result in lowering of UFA recharge to streams from this area as well. It is to be noted that increase in irrigation levels were not due to increase in irrigated acreage, rather greater pumpage from existing wells and thus the results suggests that significant increase in irrigation levels even without increase in irrigated acreage can lead to drawdown in surrounding areas as well. Lowering of irrigation levels to 75% and 50% led to drawdown of as much as 5 ft feet to 3 ft, respectively, in the Spring Creek watershed (Figure 4.3). In the rest of the study area

groundwater levels do not fluctuate significantly with increase or decrease in irrigation levels. The results clearly show that the vulnerable Spring Creek watershed is the most affected by increase in irrigation withdrawals. The watershed also harbors federally protected endangered mussel species, therefore any fluctuations in flow due to changes in irrigation and groundwater levels can be of concern.

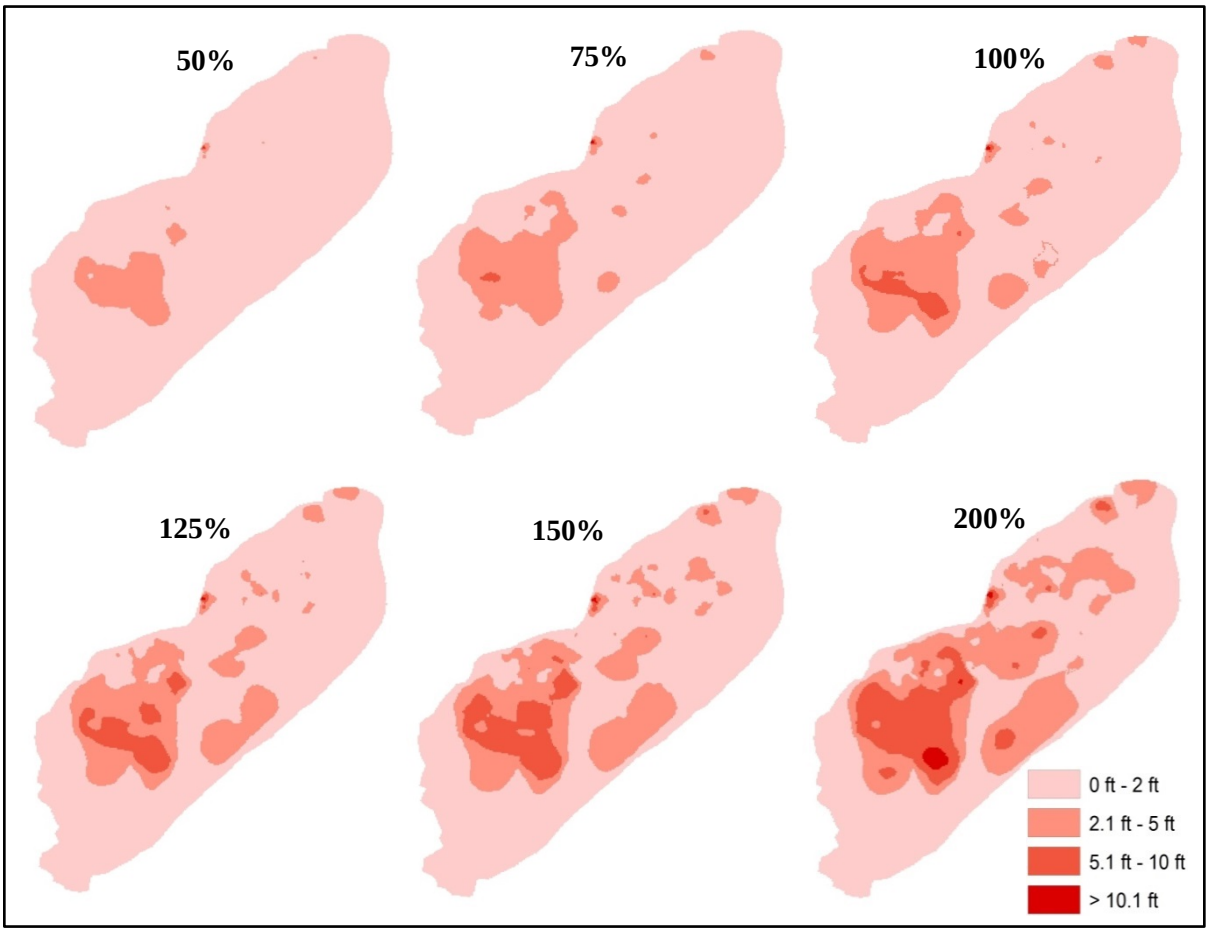

Figure 4.3 Groundwater level drawdown at different levels of irrigation for May 2012.

4.5.5 Contribution to Irrigation Withdrawal

Figures 4.4 (a), 4.4 (b) and 4.4 (c) show the contribution of stream-aquifer flux, flux thorough USCU and increased storage loss towards irrigation water withdrawal for the months of May, June and July.

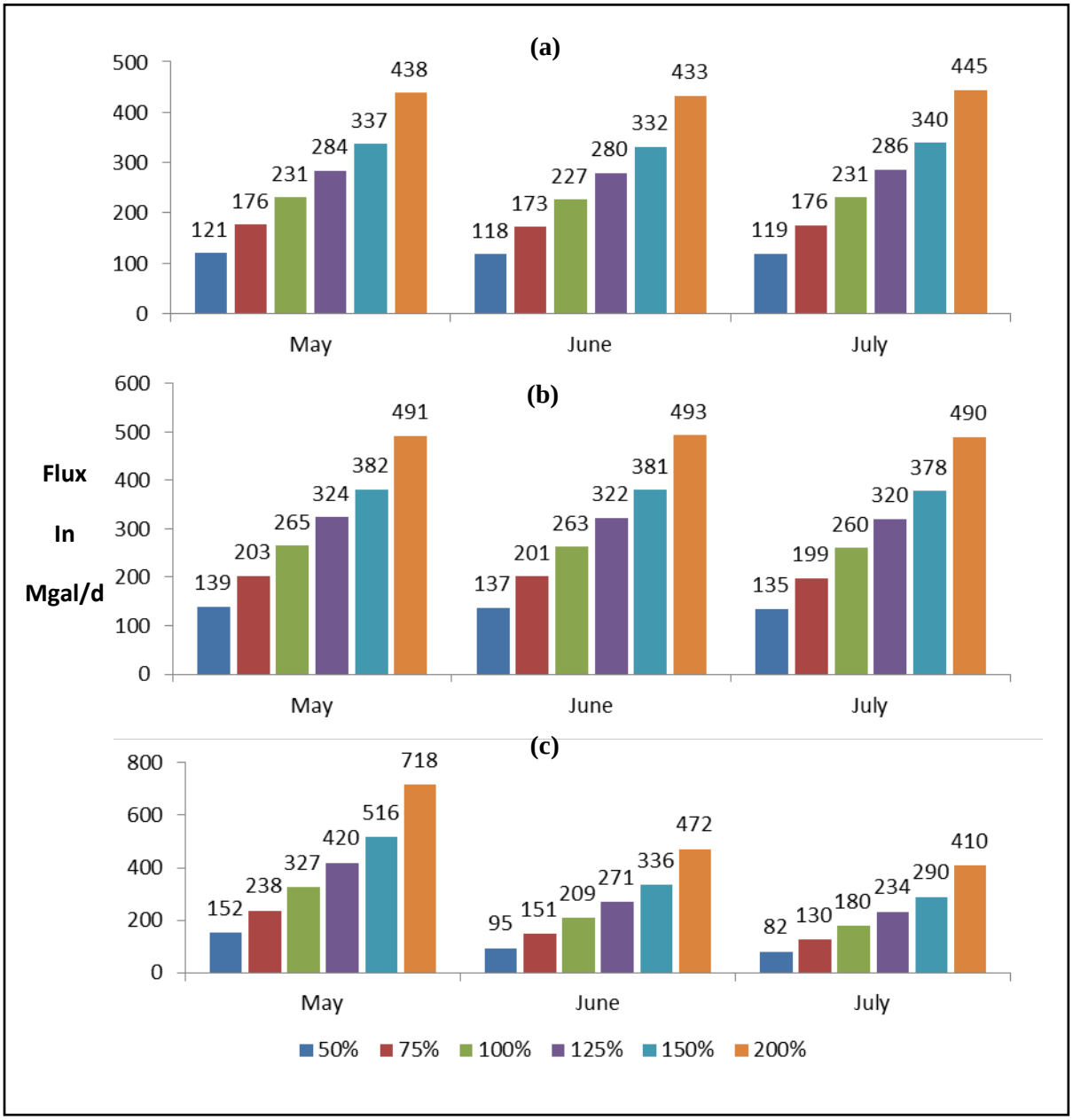

Figure 4.4 Contribution of budget components to irrigation water withdrawal **(a)** Contribution through stream-aquifer flux, **(b)** Contribution through USCU flux and **(c)** Contribution through increased storage loss.

Increasing irrigation levels to 125%, 150% and 200% led to significant increase in contribution of stream-aquifer towards irrigation withdrawal (Figure 4.4a). Increasing irrigation to 200% led to almost doubling of contribution of stream-aquifer flux from 231 Mgal/d to 438 Mgal/d in the months of May suggesting linearity (Figure 4.4a). This linearity was consistent in all the months.

Decreasing irrigation levels by 25% and 50% also led to the decrease in contribution of stream-aquifer flux by approximately 25% and 50% (Figure 4.4a). The linearity relationships were also valid for the months of June and July (Figure 4.4a). This linear relationship was also found to be consistent for contribution through flux across USCU towards irrigation water withdrawal. In the month of May increasing irrigation withdrawals to 150% and 200% led to an increase in contribution from USCU from 265 Mgal/d to 382 Mgal/d and 491 Mgal/d (Figure 4.4b). Contribution from USCU and through increased storage loss varied based on increases in irrigation levels. Increasing irrigation levels to 200% more than doubled the contribution of storage loss to irrigation water withdrawal from 327 Mgal/d to 718 Mgal/d in the month of May (Figure 4.4c). This suggests that at higher irrigation levels storage loss majorly contributes to irrigation water withdrawal in the study area.

Figure 4.5 shows the percentage contribution of each component towards irrigation water withdrawal at different irrigation levels for the month of May 2012. The figure clearly shows that increasing irrigation levels increases the percentage contribution of storage loss towards irrigation withdrawal (Figure 4.5). The percentage contribution of storage loss increased from 34% for the irrigation level of 50% to 40% at 200% irrigation levels (Figure 4.5). This suggests that increasing irrigation (to 200%) in the study area results in water loss primarily through storage loss, followed by stream-aquifer flux. The percentage contribution of stream-aquifer flux

varied slightly between 27% to 24% for different irrigation levels suggesting that changes in stream-aquifer flux bear a linear relationship with irrigation withdrawal at all irrigation levels (Figure 4.5). This suggests a potential of being able to forecast the reduction in flow levels in the Flint River with different possible irrigation scenarios which can be helpful in determining the amount of irrigation levels that will help maintain the flow levels in the FR during droughts. USCU flux also exhibited linear relationship with at different irrigation levels in the study area.

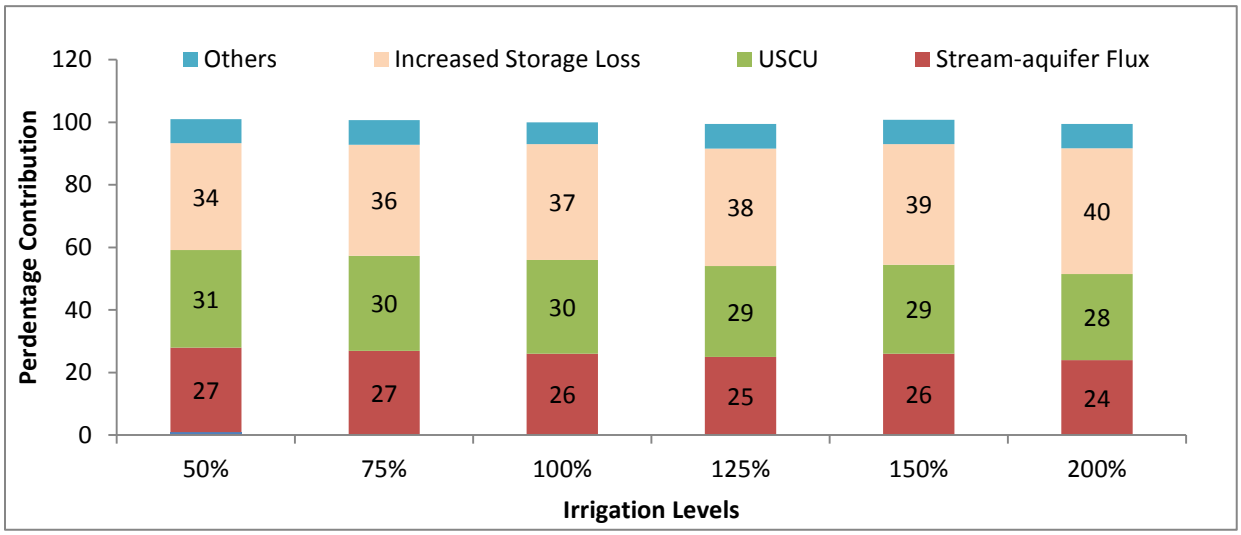

Figure 4.5 Percentage contributions of groundwater budget components to irrigation withdrawal in the month of May at different irrigation levels. "Others" in the figure indicate flux through regional boundary and aquifer updip limit.

4.5.6 Decreased Irrigation Intensity in Spring Creek Subwatershed

Table 4.5 and Table 4.6 show the changes in streamflow discharge to aquifer and storage loss by application of different irrigation levels in the vulnerable Spring Creek subwatershed (SCW) respectively for the heavily irrigated months of May to September. Irrigation levels of 75% and 50% in the SCW result in a percentage increase of approximately 1% to 3% in streamflow discharge to UFA (Table 4.5) for the months of May to September. This is

approximately half the value in Table 4.2, showing the effect of irrigation restrictions in the entire study area on discharge to streams from UFA for the similar months. Table 4.2 shows that irrigation levels of 75% and 50% in the entire study area resulted in increase in discharge to streams from the UFA by approximately 2% and 5% for the months of May to September. This suggests that irrigation restrictions in the SCW accounts for almost half of the increase in discharge to stream as it would by application of similar restrictions (percentage terms) in the entire study area.

Table 4.5 Changes in discharge to streams from UFA at different irrigation levels in the Spring Creek subwatershed.

Streamflow Discharge in Mgal/d					
IL*	**May**	**June**	**July**	**Aug**	**Sep**
25%	2074	2045	2085	2049	2039
50%	2040	2014	2052	2021	2006
75%	2008	1984	2021	1993	1976
100%	1980	1956	1990	1967	1946
Percentage Change					
IL	**May**	**June**	**July**	**Aug**	**Sep**
25%	5	5	5	4	5
50%	3	3	3	3	3
75%	1	1	2	1	2
100%	0	0	0	0	0

**Irrigation Levels*

Lowering of irrigation levels to 25% in the vulnerable areas resulted in increase in discharge to streams by approximately 5% (Table 4.5) which is similar to the increase obtained at 50% irrigation levels for the entire study area (Table 4.2). This suggests that reducing irrigation levels to 25% in the SCW region can help in similar recovery as reducing irrigation levels to 50% in the entire study area. Furthermore, it can be hypothesized that changing irrigation levels in the SCW regions would greatly impact the flow in the vulnerable creek.

Storage loss is another component that changes significantly by the application of irrigation restrictions in the SCW region. Lowering of irrigation levels to 75% and 50% in the vulnerable areas resulted in a decrease in storage loss of approximately 6% and 12% respectively (Table 4.6) as against 13% and 25% in the entire study area (Table 4.4) for the same months. Lowering of irrigation levels to 25% in the vulnerable areas results in decreased storage loss of upto 18% in the months of May to September (Table 4.6). The results here clearly suggest that application of irrigation restrictions in the vulnerable subwatershed of Spring Creek can help in major recovery of the groundwater budget components.

Table 4.6 Changes in storage loss from UFA at different irrigation levels in the Spring Creek subwatershed.

Storage Loss in Mgal/d					
IL*	**May**	**June**	**July**	**Aug**	**Sep**
25%	-571	-372	-377	-206	-243
50%	-609	-395	-397	-210	-258
75%	-650	-422	-420	-218	-277
100%	-693	-452	-446	-228	-298
Percentage Change					
IL	**May**	**June**	**July**	**Aug**	**Sep**
25%	-18	-18	-15	-10	-18
50%	-12	-13	-11	-8	-13
75%	-6	-7	-6	-4	-7
100%	0	0	0	0	0

**Irrigation Levels*

4.5.7 Analysis of Acreage Buyout

Buying out of irrigated acreage was first done by the Georgia, during 2001-02 droughts, to avoid the irrigation induced streamflow reduction. In 2002, Georgia paid $150 per acre for the buyout plan. The Georgia Environmental Protection Division (GAEPD) intended to reduce withdrawal in the vulnerable subwatersheds of Spring Creek (SCW) and Ichawaynochaway

(ICH) Creek through the buyout program and to reduce irrigation withdrawal by as much as 20% in these subwatersheds during the 2002 drought. Therefore, this section presents the results of possible future irrigation buyout program according to the FRDPA and its impacts on water stream-aquifer flux. Figure 4.6(a) and Figure 4.6(b) shows the changes in stream-aquifer flux by increasing the buyout areas and thereby shutting of irrigation withdrawal in those areas for May and June 2012. Shutting irrigation in area A, B and C encompassing the SCW subwatershed resulted in an increase in recharge to streams from UFA from 1980 Mgal/d to 2064 Mgal/d in May 2012, which is approximately half of the total recovery possible (Figure 4.6a). It will also be safe to say that this increase in recharge would be contributed majorly to the Spring Creek. Further we see that shutting irrigation in the area D (ICH subwatershed) increased discharge to streams to 2078 Mgal/d (Figure 4.6a). We also see that shutting irrigation in the ICH and the Kinchafoonee-Muckalee Creek (KMC) subwatersheds did not result in substantial increase in recharge to the streams from the aquifer. That is SCW accounted for around 84 Mgal/d of increased recharge whereas the KMC and ICH subwatersheds combined accounted for only 21 Mgal/d (Figure 4.6).

The trends were similar in Figure 4.6b for June 2012 where we see that the slope of the curve representing the recharge to streams was steeper suggesting greater increase in contribution to stream in those regions per percentage increase in irrigated acreage. Figure 4.6a and Figure 4.6b also suggest that shutting of irrigation in the area results in decrease in contribution from the stream to the aquifer, though the decrease is not significant enough. Results here clearly suggest that restricting irrigation withdrawal in SCW subwatershed can have significant impacts on stream-aquifer flux in the study area and it can be hypothesized that the Spring Creek is majorly impacted by irrigation water withdrawals. It is important to note that in

the analysis in this section the changes in stream-aquifer flux in the entire study area is studied and is not representative of particular streams.

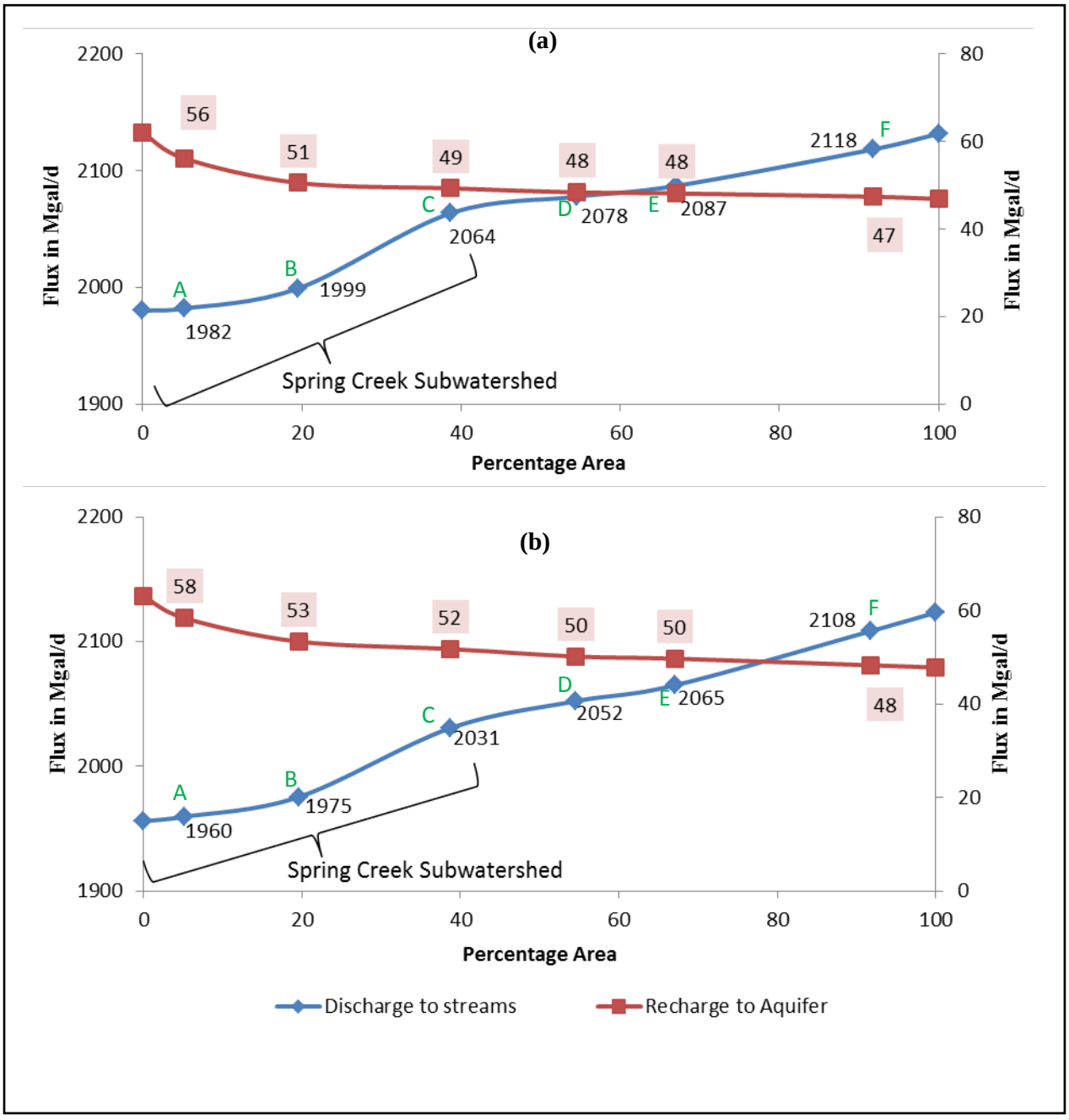

Figure 4.6 Changes in stream-aquifer flux with acreage buyout program (a) for May 2012 (b) June 2012.

Table 4.7 shows the cost estimates of buyout of irrigated acreage with different prices per acre. Table 4.7 shows that with a price of approximately $150/acre the cost of buying out the irrigated acreage in the SCW subwatershed would cost around $ 29 million that will contribute to almost half of the total increase in recharge to the streams from the aquifer (Figure 4.6 a,b). Stopping irrigation pumpage in the 3 vulnerable subbasins of SCW, ICH and MC would cost approximately $ 50 million with $150/acre prices and the estimate for the entire study area would be around $ 74 million.

Table 4.7 Cost analysis of irrigation acreage buyout.

Area ID*	Cumulative Acreage (Acres)	Percentage Acreage (%)	Cost (Millions of Dollars)		
			at $150/ac	at $200/ac	At $300/ac
NI	0	0	0	0	0
A	25608	5	4	5	8
B	96520	20	14	19	29
C	190971	39	29	38	57
D	269182	55	40	54	81
E	330848	67	50	66	99
F	452989	92	68	91	136
Irri	493401	100	74	99	148

**Refer to Figure 4.2.*

4.6 Summary and Conclusion

This study uses the MODFE model to simulate and understand the effects of simulated irrigation pumpage on GW levels, groundwater budget and stream-aquifer flux for the water year 2012 (a drought year). The model inputs include infiltration, stream stage, irrigation pumpage and head in the USCU. The model simulated the groundwater components at irrigation levels of 50%, 75%, 100%, 125%, 150% and 200%. Percentage change in groundwater budget components were studied at different irrigation levels and their contribution to irrigation water

withdrawal was also analyzed. Additionally, the effect of irrigation restrictions and acreage buyout in the vulnerable regions of Spring Creek subwatershed were studied.

Results show that that recharge from stream to aquifer increased significantly with increase in irrigation in the study area. During the months of May to September 2012 when irrigation was maximum, doubling of irrigation resulted in almost 50% increase in the recharge from streams to aquifer. During the months with little or no irrigation, we see that increasing pumpage during the previous months leads to increase streamflow recharge to the aquifer due to lower groundwater levels. Increase in irrigation levels to 125%, 150% and 200% in the study area progressively resulted in the decrease in contribution of UFA to the stream. Increasing irrigation levels to 125%, 150% and 200% resulted in the lowering of discharge to the streams by approximately 47 Mgal/d, 92 Mgal/d and 178 Mgal/d, respectively, during the heavily irrigated months which was approximately 2%, 5% and 9% of the simulated discharge to streams for WY12. Increasing irrigation during the month of October resulted in significantly lower contribution to the aquifer during subsequent winter months (November – February) owing to lowering of groundwater levels. This clearly shows that the effects of irrigation persist for at least 4 months, resulting in reduced contribution to stream from the UFA. The results exemplify the effect of possible future irrigation increases on stream-aquifer flux, suggesting that stream-aquifer flux will continue to be significantly affected with increase in irrigation levels in the lower ACF. Increasing/decreasing irrigation levels in study area has profound impacts on the storage of the UFA. Increasing irrigation levels to 200% increased storage loss from -693 Mgal/d to -1084 Mgal/d in the month of May, an increase of about 50%.

During the summer of 2012, increasing irrigation levels in the study area progressively led to lowering of groundwater levels. Increasing irrigation levels to 200% resulted in

groundwater levels to fall by as much as 11 ft in some areas in the Spring Creek subwatershed and by 5 ft in some areas on the east of Flint River. Irrigation levels of 125% and 150% led to groundwater level drawdown of approximately 8 ft in some areas of the Spring Creek. Increasing irrigation actually led to increased drawdown in the areas east of the Flint River, suggesting that future irrigation levels can lead to lowering in groundwater levels in this region as well. Since, this region also bears direct hydraulic connection to the Flint River, lowering of groundwater levels in this region and result in lowering of UFA recharge to streams from this area as well.

Analysis of contribution of each component to pumpage at different irrigation levels suggested linear relationship which suggests a potential of being able to forecast the flow levels in the FR with different possible irrigation scenarios which can be helpful in determining the amount of irrigation levels that will help maintain the flow levels in the FR during droughts. Analysis of acreage buyout suggested that restricting irrigation withdrawal in SCW subwatershed can have significant impacts on stream-aquifer flux in the study area and it can be hypothesized that the Spring Creek is greatly impacted by irrigation water withdrawals. The results also show that irrigation restrictions in the SCW subwatershed accounts for almost half of the total recovery possible if similar restrictions are applied throughout the study area.

The results indicate that future increases in the irrigation will affect stream-aquifer flux in the region. Application of irrigation restrictions in the vulnerable regions can helpful in avoiding irrigation induced streamflow depletion in some of the most affected streams in the study area.

Chapter 5

Conclusions

Summary and Conclusions

Recurring climate variability induced droughts and resulting ongoing water disputes in the Southeast United States have brought to the forefront the pressing water management issues which cannot be ignored. In an area with an ever increasing population and increased irrigated agriculture from groundwater resources, stresses on water resources will increase in future. Therefore, identification and understanding the effects of climate variability induced droughts on hydrologic cycle components and its interaction with anthropogenic activities can provide vital information in solving the present and future water issues and resolving the water disputes.

This study focused on the effect of climate variability induced droughts on groundwater levels and the combined impacts of droughts and increased irrigation pumpage on groundwater budget components in the Upper Floridan Aquifer in the southwest Georgia. The study had three major objectives mentioned earlier and the most important finding for each of the objectives are listed below.

5.1.1 Objective 1

Quantify the effect of ENSO-induced climate variability on groundwater levels under different overburden conditions..

Wavelet analysis techniques were used to identify teleconnections between ENSO and groundwater levels under different overburden conditions. Mann-Whitney test was used to quantify the effect of ENSO- induced droughts and groundwater level anomalies. Further, short and long term droughts were studied and their respective recovery periods were calculated. The major conclusions were:

1. Wavelet analysis indicated that wells representing shallow and moderately deep overburden conditions respond to ENSO-induced climate variability, whereas, wells in deep overburden condition do not.
2. Mann-Whitney test results validated the findings of wavelet analysis. GW levels were higher than long-term average during El Niño phases while lower than average during La Niña phases except for well under deep overburden conditions.
3. Analysis for recharge and non-recharge periods indicated that ENSO- induced anomalies were approximately 2.5 times greater during the recharge season than during for the non-recharge season.
4. Comparison of La Niña phases representing severe (2000–01) and average conditions indicated that during recharge and non-recharge seasons average GW levels dropped approximately twice during the severe La Niña as compared to the average La Niña event.
5. Recovery times for the severe La Niña during 2000–01 were significantly longer than those during the short La Niña of 1988–89 (22 months vs. 2 months).
6. Therefore, the study suggests that GW levels should also be used (in combination with precipitation deficit, soil moisture, stream flows and others) as an indicator of drought in this area and the role of irrigation cannot be ignored during prolonged drought events.

5.1.2 Objective 2

Quantify how pumping for irrigation exacerbates the effect of La Niña (droughts) on groundwater levels and groundwater budget components.

The MODFE model was used to analyze the effect of irrigation on groundwater levels and groundwater budget components during the 2010 – 2012 La Niña phase. Groundwater budget components such as stream-aquifer flux, recharge/discharge through the Upper Semi Confining Unit and regional boundary flows were studied. In addition to those areas critical areas were analyzed. The major conclusions were:

1. Stream-aquifer flux and the Upper Semi Confining Unit is the major source of discharge and recharge, respectively, to the Upper Floridan Aquifer.
2. Irrigation caused significant changes in recharge/discharge through stream aquifer flux and storage loss in the Upper Floridan Aquifer.
3. Irrigation pumpage caused recharge to the Upper Floridan Aquifer through stream-aquifer flux to increase by more than 10% during the highly irrigated months.
4. Loss in streamflow, recharge/discharge through Upper Semi Confining Unit and storage losses were the major budget components contributing to irrigation pumpage in the study area.
5. Results clearly suggest that irrigation withdrawal results in lowering of streamflow levels in the Flint River and its tributaries.
6. In Water Year 2012 groundwater levels decreased by as much as 6 ft in certain areas due to intense pumpage during the irrigated months. The areas showing greater drawdown in groundwater levels coincide with the areas having intense irrigation. These areas are close to Spring Creek which is on the critically endangered species list.

5.1.3 Objective 3

Analyze the effects of simulated irrigation levels on groundwater levels and groundwater budget components during a La Niña event.

The MODFE model was used to simulate the effect of elevated irrigation levels on groundwater levels and groundwater budget components in the study area during the drought period of 2012.

Effects of possible irrigation restrictions on stream-aquifer flux in the vulnerable subwatershed of Spring Creek for drought periods were analyzed. The major conclusions were:

1. Recharge from stream to aquifer increased and discharge to streams from aquifer decreased significantly with increase in irrigation in the study area.
2. Doubling of irrigation resulted in almost 50% increase in the recharge from streams to aquifer.
3. Doubling of irrigation levels led to a decrease in discharge from aquifer to streams by as much as 9% during the months of high irrigation.
4. Doubling of irrigation levels resulted in groundwater levels to fall by as much as 11 ft in some areas in the Spring Creek subwatershed and by 5 ft in some areas on the east of Flint River.
5. Analysis of contribution of each component to pumpage at different irrigation levels suggested linear relationship, which suggests a potential of being able to forecast the flow levels in the FR with possible irrigation scenarios which can be helpful in determining the amount of irrigation levels that will help maintain the flow levels in the FR during droughts.

6. Analysis of acreage buyout suggested that restricting irrigation withdrawal in Spring Creek subwatershed can have significant impacts on stream-aquifer flux in the study area and it can be hypothesized that the Spring Creek is majorly impacted by irrigation water withdrawals.

Chapter 6

Future Research

This study analyzed the effect of ENSO-induced droughts and irrigation withdrawal on groundwater levels in the Upper Floridan Aquifer. The study showed that irrigation pumpage during droughts affect groundwater levels and stream-aquifer flux in the Upper Floridan Aquifer. Recommendations for possible future work are presented below:

1. In this study the effect of ENSO tele-connections was studied on groundwater levels, however, the effect of other climate variability cycles such as Atlantic Multidecadal Oscillation and Pacific Decadal Oscillation and their interaction with ENSO would provide useful information regarding the severity and persistence of droughts and their effect on groundwater levels in the study area.
2. In this study, the reduction in stream-aquifer flux due to irrigation pumpage for the entire study area was analyzed. Analyzing individual stream sections and identifying streams that are more sensitive to irrigation pumpage can be helpful in future in formulating policies related to irrigation restrictions in the study area to help maintain the flow levels during droughts.
3. This study identified teleconnections with ENSO and groundwater levels in the Upper Floridan Aquifer. The information can be used to develop methodologies for possible short-term (3-6 months) forecasting of groundwater levels in the study area during

droughts that will give prior information of the status of groundwater levels and possible streamflow depletion during droughts.

References

Aceituno, P., 1992. El Niño, the southern oscillation, and ENSO: Confusing names for a complex ocean-atmosphere interaction. *Bulletin of the American Meteorology Society,* 73, 483–485.

Allen, M. R., and Smith, L. A., 1996. Monte Carlo SSA: Detecting irregular oscillations in the presence of coloured noise, *Journal of Climate*, 9, 3373–3404.

Barsugli, J. J., Whitaker, J. S., Loughe, A. F., Sardeshmukh, P. D., and Toth., Z., 1999. The effect of 1997/98 El Nino on individual large scale weather events. *Bullentin of American. Meterological. Soc*iety, 80, 1399-1411.

Berri, J. G., and Flamenco, E. A., 1999. Seasonal volume forecast of the Diamante river, Argentina, based on El Nino observations and predictions. *Water Resources Resesearch*, 35(12), 3803-3810.

Cane, M. A., 2005. The evolution of El Niño, past and future. *Earth Planet Sci. Lett*., 230(3-4), 227-240.

Charles, C. D., Hunter, D. E., and Fairbanks, R. G., 1997. Interaction between the ENSO and the Asian monsoon in a coral record of tropical climate. *Science,* 277(5328), 925.

Chen, W. Y., 1982. Assessment of Southern Oscillation Sea-Level Pressure Indices. *Mon. Wea. Rev.*, 110, 800–807.

Chiew, F.H.S., Piechota, T.C., Dracup, J.A., and McMahon, T.A., 1998. El Niño/Southern Oscillation and Australian rainfall, streamflow, and drought: links and potential for forecasting. *Journal of Hydrology,* 204, 138–149.

Climate Research Committee and National Research Council. 1995. Natural Climate Variability on Decade-to-Century Time Scales. Washington, DC: National Academy Press.

Cooley, R.L., 1983, Analysis of an incongruity in the standard Galerkin finite-element method. *Water Resources Research*, 19(1), 289 – 291.

Cooley, R.L., 1992, A MODular Finite-Element model (MODFE) for areal and axisymmetric ground-water flow problems, Part 2 — Derivation of finite-element equations and

comparisons with analytical solutions: U.S. Geological Survey Techniques of Water-Resources Investigations, Book 6, Chap. A4, 108 p.

Coulibaly, P., and Baldwin, C. K., 2005. Nonstationary hydrological time series forecasting using nonlinear dynamic methods. *Journal of Hydrology*, 307(1-4), 164-174.

Diaz, H. F., and Markgraf, V., 1992. El Niño: historical and paleoclimatic aspects of the Southern Oscillation, *Cambridge University Press*.

Enfield, D.B., Mestas-Nuez, A.M., and Trimble, P.J., 2001. The Atlantic multi-decadal oscillation and its relation to rainfall and river flows in the continental US. *Geophysical Research Letters*, 28(10), 2077-2080.

Eltahir, E. A. B., 1996. The role of vegetation in sustaining large scale atmospheric circulations in the tropics. *J . Geophys Res*., 101, 42-55.

Fraedrich, K., and Muller, K., 1992. Climate anomalies in Europe associated with ENSO extremes. *Int. J. Climatol*., 12(1).

Gershunov, A., and Barnett, T.P., 1998a. ENSO influence on intraseasonal extreme rainfall and temperature frequencies in the contiguous United States: Observations and model results. *Journal of Climate*, 11(7), 1575-1586.

Gershunov, A., and Barnett, T.P., 1998b. Interdecadal modulation of ENSO teleconnections. *Bulletin of American Meteorological Society*, 79, 2715–2726.

Glantz, M., 2001. Currents of Change: Impacts of El Niño and La Niña on Climate and Society, Second edition. *Cambridge University Press*, Cambridge, UK.

Gleick PH, Adams DB (2000) Water: the potential consequences of climate variability and change for the water resources of the United States: the report of the Water Sector Team of the National Assessment of the Potential Consequences of Climate Variability and Change for the U.S. Global Research Program. Pacific Institute for studies in Development, Environment, and Security, Oakland, CA, p 15.

Grinsted, A., Moore, J., and Jevrejeva, S., 2004. Nonlinear processes in geophysics application of the cross wavelet transform and wavelet coherence to geophysical time series. *Nonlinear processes in geophysics*, 11(5/6), 561-566.

Gurdak, J. J., Hanson, R. T., McMahon, P. B., Bruce, B. W., McCray, J. E., Thyne, G. D., and Reedy, R. C., 2007. Climate Variability Controls on Unsaturated Water and Chemical Movement, High Plains Aquifer, USA. *Vadose Zone Journal*, 6, 533–547.

Hansen, D. V., and Maul, G. A., 1991. Anticyclonic current rings in the eastern tropical Pacific Ocean. *Journal of Geophysical Research*, 96(C4), 6965-6979.

Hansen, J., Jones, J., Irmak, A., and Royce, F., 2001. El Niño-southern oscillation impacts on crop production in the southeast United States. *ASA Special Publication*, 63, 55-76.

Hanson, K., and Maul, G.A., 1991. Florida precipitation and the Pacific El Niño, 1895– 1989. *Florida Scientist*, 54 (3/4), 160–168.

Halpert, M. S., and Ropelewski, C. F., 1992. Surface temperature patterns associated with the Southern Oscillation. *J. Clim*., 5(6), 577-593.

Hayes, L.R., Maslia, M.L., and Meeks, W.C., 1983, Hydrology and model evaluation of the principal artesian aquifer, Dougherty Plain, southwest Georgia: Georgia Geologic Survey Bulletin 97, 93 p.

Hickey, B., 1975. The relationship between fluctuations in sea level, wind stress and sea surface temperature in the Equatorial Pacific. *J. Phys. Oceanogr*., *5*, 460-475.

Huang, J., Higuchi, K., and Shabbar, A., 1998. The relationship between the North Atlantic Oscillation and the ENSO, *Geophys. Res. Lett*., 25, 2707– 2710.

IPCC (Intergovernmental Panel on Climate Change). 2001. Climate Change 2001: Impacts, adaptations, and vulnerability. In Contribution of working group II to the third assessment report of the Intergovernmental Panel on Climate Change. Cambridge: *Cambridge University Press*.

Johnson, N. T., Martinez, C. J., Kiker, G. A., and Leitman, S., 2013. Pacific and Atlantic sea surface temperature influences on streamflow in the Apalachicola–Chattahoochee–Flint river basin. *Journal of Hydrology*, 489, 160–179.

Jones, L.E., and Torak, L.J., 2006. Simulated effects of seasonal ground-water pumpage for irrigation on hydrologic conditions in the lower Apalachicola–Chattahoochee–Flint River Basin, southwestern Georgia and parts of Alabama and Florida, 1999–2002: *U.S. Geological Survey Scientific Investigations Report 2006-5234*, 115 p., a Web-only publication at http://pubs.usgs.gov/sir/2006/5234/.

Kahya, E., and Dracup, J. A., 1993. US streamflow patterns in relation to the El Niño/Southern Oscillation. *Water Resources Research*, 29(8), 2491-2503.

Keener, V.W., Ingram, K.T., Jacobson, B., and Jones, J.W., 2007. Effects of El-Niño/ Southern Oscillation on simulated phosphorus loading. *Transactions of the ASABE*, 50(6), 2081–2089.

Keener, V.W., Feyereisen, G.W., Lall, U., Jones, J.W., Bosch, D.D., and Lowrance, R., 2010. El-Niño/Southern Oscillation (ENSO) influences on monthly NO3 load and concentration,

stream flow and precipitation in Little River Watershed, Tifton, Georgia. *Journal of Hydrology*, 381, 352-363.

Kiladis, G.N., and Diaz, H.F., 1989. Global climate anomalies associated with extremes in the Southern Oscillation. *Journal of Climate*, 2 (9), 1069–1090.

Kinnaman, S.L., and Dixon, J.F., 2011, Potentiometric surface of the Upper Floridan aquifer in Florida and parts of Georgia, South Carolina, and Alabama, May – June 2010: U.S. Geological Survey Scientific Investigations Map 3182, 1 sheet.

Kulkarni, J.R., 2000. Wavelet analysis of the association between the southern oscillation and the Indian summer monsoon. *International Journal of Climatology*, 20, 89–104.

Martinez, C. J., 2011. What does the 2010-2011 La Nina mean for the Southeastern USA? An Apalachicola-Chattahoochee-Flint river basin drought early warning system fact sheet. WWW document available at http://www.drought.gov/imageserver/NIDIS/DEWS/ACFRB/2010_2011laninafactsheet.pdf

McCabe, G. J., and Dettinger, M. D., 1999. Decadal variations in the strength of ENSO teleconnections with precipitation in the western United States. *International Journal of Climatology*, 19(13), 1399-1410.

Mitra, S., Srivastava, P., Singh, S., and Yates, D., 2014. Effect of ENSO-Induced Climate Variability on Groundwater Levels in the Lower Apalachicola-Chattahoochee-Flint River Basin. *Transactions of the ASABE*, 57(5), 1393-1403.

Molnar, P., and Cane, M. A., 2007. Early Pliocene (pre-Ice Age) El Niño-like global climate: Which El Niño. *Geosphere.*, 3(5), 337.

NCDC. 2014. National Climate Data Center. WWW document available at http://www.ncdc.noaa.gov.

Newman, M., Compo, G. P., and Alexander, M. A., 2003. ENSO-Forced Variability of the Pacific Decadal Oscillation. *J. Climate*, 16, 3853–3857.

Nicholls, N., Lavery, B., Friedericksen, C., Drodowsky, W., and Torok, S., 1996. Recent apparent changes in relationships between the ENSO and Australian rainfall and temperature. *Geophys. Res. Letters*, 23, 3357-60.

NOAA (National Oceanic and Atmospheric Administration), WWW document available at http://www.pmel.noaa.gov/tao/elnino/nino-home.html

NOAA CPC (National Oceanic and Atmospheric Administration Climate Prediction Center). 2012. ENSO index. Camp Springs, MD: Climate Prediction Center. (http://www.cpc.ncep.noaa.gov/products/analysis_monitoring/ensostuff/ensoyears.shtml)

Philander, S. G. H., and Rasmusson, E. M., 1985. The Southern Oscillation and El Niño. *Advances in Geophysics*, 28(A), 197-215.

Postel, S. L., G. C. Daily, and Ehrlich, P.R., 1996. Human appropriation of renewable fresh water. *Science*, 271(5250), 785-788.

Quinn, W. H., Zopf, D. O., Short, K. S., and Yang, R. T. Kuo., 1978. Historical trends and statistics of the Southern Oscillation, El Nino, and Indonesian droughts. *Fish. Bull*., 76, 663–678.

Quinn, W.H., 1994. Monitoring and predicting El Niño invasions. *Journal of Applied Meteorology*, 9, 20–28.

Rajagopalan, B., and Lall, U., 1998. Interannual variability in western US precipitation. *Journal of Hydrology*, 210, 51–67.

Rasmusson, E. M., and Carpenter, T. H., 1982. Variations in Tropical Sea Surface Temperature and Surface Wind Fields Associated with the Southern Oscillation/El Niño. *Mon. Wea. Rev.*, **110**, 354–384.

Rasmusson, E. M., and Wallace, J. M., 1983. Meteorological aspects of the El Niño/southern oscillation. *Science*, 222(4629), 1195-1202.

Redmond K. T., and Koch, R. W., 1991. Surface climate and streamflow variability in western United States and their relationship to large-scale circulation indices. *Wat. Resources Res*., 27(9), 2381–2399.

Ropelewski, C.F., and Halpert, M.S., 1986. North American precipitation and temperature patterns associated with the El Niño/Southern Oscillation. *Monthly Weather Review*, 114, 2352– 2362.

Ropelewski, C. F., and Halpert, M. S., 1987. Global and regional scale precipitation patterns associated with the El Nino Southern Oscillation. *Mon. Weather Rev.*, 115 (8), 1601-1626.

Ropelewski, C.F. and Jones, P.D., 1987. An extension of the Tahiti-Darwin Southern Oscillation Index. *Monthly Weather Review*, **115**, 2161-2165.

Roy, S.S., 2006. The impacts of ENSO, PDO, and local SSTs on winter precipitation in India. *Physical Geography*, 27(5), 464-474.

Schmidt, N., Lipp, E.K., Rose, J.B., and Luther, M., 2001. ENSO influences on seasonal rainfall and river discharge in Florida. *Journal of Climate*, 14 (4), 615–628.

Schmidt, N., and Luther, M. E., 2002. ENSO impacts on salinity in Tampa Bay, Florida. *Estuaries and Coasts*, 25(5), 976-984.

Sharda, V., Srivastava, Puneet, Ingram, K., Chelliah, M., and Kalin, L., 2012. Quantification of El Niño Southern Oscillation (ENSO) Impact on Precipitation and Stream flows for Improved Management of Water Resources in Alabama. *Journal of Soil and Water Conservation*, 67(3), 158-172.

Simpson, H. J., and Colodner, D. C., 1999. Arizona precipitation response to the Southern Oscillation: A potential water management tool. *Wat. Resources Res*., 35(12): 3761-3769.

Southern Environmental Law Center. 2012. WWW document available at https://www.southernenvironment.org.

The Flint River Drought Protection Act. Georgia General Assembly Legislation, WWW document available at http://www.legis.ga.gov/legislation/en-US/display/20132014/SB/213.

Tootle, G.A., Piechota, T.C., and Singh, A., 2005. Coupled oceanic-atmospheric variability and US streamflow. *Water Resources Research*, 41. W12408, doi:10.1029/2005WR004381.

Torak, L.J., 1993a, A MODular Finite-Element model (MODFE) for areal and axisymmetric ground-water flow problems, Part 1— Model description and user's manual: U.S. Geological Survey Techniques of Water-Resources Investigations, Book 6, Chap. A3, 136 p.

Torak, L.J., 1993b, A MODular Finite-Element model (MODFE) for areal and axisymmetric ground-water flow problems, Part 3 — Design philosophy and programming details: U.S. Geological Survey Techniques of Water- Resources Investigations, Book 6, Chap. A5, 243 p.

Torak, L.J., and Painter, J.A., 2006, Geohydrology of the lower Apalachicola–Chattahoochee–Flint River Basin, southwestern Georgia, northwestern Florida, and southeastern Alabama: *U.S. Geological Survey Scientific Investigations Report 2006-5070*, 80 p.

Torrence, C., and Compo, G. P., 1998. A practical guide to wavelet analysis. *Bulletin of the American Meteorological Society*, 79(1), 61-78.

Trenberth, K. E., and Stepaniak, D. P., 2001. Indices of El Niño evolution. *J. Clim.*, 14.

Trenberth, K.E., and Hoar, T. J., 1996. The 1990-1995 El Niño Southern Oscillation event: Longest on record. *Geophysical Research Letters*, 23, 57-60.

Troup, A. J., 1965. The 'southern oscillation'. *Q.J.R. Meteorol. Soc.*, 91, 490–506.

USCOE. 2013. US Army Corps of Engineers, Mobile Distrct, Mobile, Alabama. WWW document available at http://water.sam.usace.army.mil/gage/acfhist.htm.

Walker, G. T., and Bliss, E. W., 1926. On correlation coefficients, their calculation use (with discussion). *Quarterly Journalof the Royal Meteorological Society.*, 52, 73–84.

Walker, G. T., 1924. Correlation in seasonal variations of weather. IX. A further study of world weather. *Memoirs of the Indian Meteorological Department*, 24(9), 275–332.

Wang, Y., and Wang, B., 1996. Temporal structure of the Southern Oscillation as revealed by waveform and wavelet analysis. *Journal of Climate*, 9, 1586–1598.

Wolter, K., and Timlin, M. S., 1993. Monitoring ENSO in COADS with a seasonally adjusted principal component index, in *Proc. 17th Climate Diagnostics Workshop*., 52–57.

Zienkiewicz, O.C., 1977, The finite element method: New York, McGraw-Hill, 787 p.

Zhang, Y., Wallace, J.M., Battisti, D.S., 1997. ENSO-like interdecadal variability: 1900-93. *Journal of Climate*, 10, 1004-1020.

Appendix A

Groundwater Observation Wells from USGS.

A. 1. USGS long term observation wells

Table A.1. List of long-term groundwater observation wells (with their coordinates in degree decimals) used for Wavelet Analysis and Mann-Whitney tests.

Site Name	Latitude	Longitude
06F001	30.90	-84.90
09F520	30.96	-84.60
09G001	31.07	-84.52
10G313	31.09	-84.44
08G001	31.11	-84.68
07H002	31.17	-84.83
11J012	31.30	-84.32
13J004	31.36	-84.12
08K001	31.38	-84.65
12K014	31.44	-84.19
13K014	31.45	-84.12
11K015	31.45	-84.27
10K005	31.48	-84.46
11K003	31.49	-84.26
13L012	31.52	-84.11
12L030	31.53	-84.17
15L020	31.53	-83.82
12L028	31.55	-84.20
13L049	31.59	-84.09
12M017	31.64	-84.16
13M006	31.73	-84.01

A.2. USGS groundwater observation wells for model calibration

Table A.2. List of groundwater observation wells (with their coordinates in degree decimals, observation, observation dates and model simulated values) used for groundwater level calibration. The observed and simulated values are in feet and the date format is month/day/year.

Site Name	Longitude	Latitude	Date	Observed	Simulated
08D006	-84.67	30.71	7/19/2011	77.81	77.56
08D005	-84.71	30.73	7/19/2011	75.21	79.72
07D005	-84.80	30.73	7/18/2011	86.88	77.48
08D003	-84.75	30.74	7/18/2011	67.13	79.64
08D002	-84.73	30.74	7/18/2011	89.31	79.93
08D001	-84.74	30.75	7/18/2011	72.52	79.26
08D090	-84.67	30.75	7/19/2011	74.62	78.05
08D007	-84.67	30.75	7/19/2011	74.15	78.05
07E009	-84.75	30.76	7/18/2011	73.56	78.45
07E062	-84.81	30.76	7/18/2011	58.79	77.01
08E024	-84.73	30.76	7/19/2011	89.72	78.92
07E001	-84.77	30.76	7/18/2011	69.57	77.53
07E008	-84.76	30.76	7/18/2011	72.81	77.53
09E521	-84.61	30.77	7/19/2011	95.64	75.64
08E019	-84.73	30.77	7/19/2011	82.32	78.15
08E022	-84.72	30.77	7/19/2011	67.53	77.76
08E021	-84.72	30.77	7/19/2011	69.60	77.76
07E045	-84.83	30.78	7/21/2011	76.49	75.50
08E038	-84.67	30.79	7/31/2011	75.43	76.99
09E009	-84.56	30.80	7/18/2011	77.66	79.32
08E031	-84.65	30.80	7/19/2011	84.25	76.87
06E023	-84.92	30.80	7/21/2011	72.25	76.41
08E039	-84.68	30.80	7/31/2011	76.39	76.27
07E046	-84.79	30.80	7/21/2011	74.16	76.51
08E035	-84.74	30.81	7/20/2011	75.81	76.63
08E034	-84.71	30.82	7/20/2011	75.83	76.87
07E007	-84.79	30.84	7/21/2011	72.17	77.69
06E019	-84.91	30.85	7/21/2011	74.95	76.55
09E006	-84.57	30.86	7/19/2011	66.71	78.88

Site Name	Longitude	Latitude	Date	Observed	Simulated
08E037	-84.69	30.87	7/20/2011	74.71	78.94
07E044	-84.76	30.87	7/20/2011	61.23	78.69
09E005	-84.57	30.87	7/19/2011	77.21	78.05
09E004	-84.59	30.87	7/19/2011	79.40	77.57
09E003	-84.59	30.87	7/19/2011	78.93	77.57
08E032	-84.63	30.84	7/19/2011	71.49	77.03
08F018	-84.74	30.88	7/20/2011	76.70	79.67
08F499	-84.63	30.88	7/20/2011	77.65	77.79
07F006	-84.85	30.88	7/21/2011	73.30	76.92
06F007	-84.92	30.89	7/21/2011	66.30	78.07
08F009	-84.64	30.89	7/20/2011	76.87	78.57
08F017	-84.68	30.90	7/21/2011	82.56	80.01
06F001	-84.90	30.90	7/20/2011	70.44	78.15
06F005	-84.92	30.92	7/21/2011	81.69	79.90
08F012	-84.65	30.92	7/20/2011	76.80	80.86
07F002	-84.83	30.94	7/20/2011	65.78	81.19
09F005	-84.61	30.95	7/21/2011	77.25	80.18
06F084	-84.93	30.95	7/21/2011	87.87	85.31
08F513	-84.68	30.95	7/20/2011	78.91	83.53
09F520	-84.60	30.96	7/31/2011	77.29	80.58
09F004	-84.51	30.96	7/21/2011	78.27	80.86
07F003	-84.76	30.97	7/20/2011	71.55	86.04
10F004	-84.44	30.97	7/21/2011	90.44	84.09
07F004	-84.78	30.99	7/20/2011	79.82	90.28
10F001	-84.48	31.00	7/21/2011	85.25	82.09
07G007	-84.83	31.00	7/20/2011	97.95	92.29
07G028	-84.84	31.00	7/20/2011	84.50	93.17
10G001	-84.39	31.02	7/21/2011	107.12	88.90
08G005	-84.69	31.03	7/21/2011	90.11	93.26
11G021	-84.31	31.04	7/21/2011	103.12	97.06
07G026	-84.85	31.05	7/20/2011	91.02	98.68
09G010	-84.57	31.05	7/21/2011	84.44	86.94
07G005	-84.79	31.05	7/20/2011	89.83	100.24
08G013	-84.64	31.05	7/21/2011	88.12	93.96
06G008	-84.97	31.06	7/21/2011	95.52	95.97
06G006	-84.99	31.07	7/21/2011	96.65	97.46
09G001	-84.52	31.07	7/31/2011	90.68	80.81
11G002	-84.34	31.08	7/21/2011	99.45	95.65
10G313	-84.44	31.09	7/31/2011	84.03	88.41
07G027	-84.86	31.09	7/20/2011	118.95	107.62
08G001	-84.68	31.11	7/31/2011	108.08	112.43
06H013	-84.94	31.13	7/19/2011	123.30	131.80

Site Name	Longitude	Latitude	Date	Observed	Simulated
10H006	-84.43	31.13	7/21/2011	91.17	89.79
07H008	-84.84	31.14	7/20/2011	122.78	125.48
09H012	-84.56	31.15	7/18/2011	90.30	104.17
08H010	-84.68	31.16	7/18/2011	113.23	125.47
07H002	-84.83	31.17	7/31/2011	153.85	138.10
06H009	-84.95	31.19	7/19/2011	147.88	148.50
07H012	-84.76	31.19	7/19/2011	140.86	136.96
06H022	-84.89	31.20	7/19/2011	147.27	151.79
05H008	-85.01	31.20	7/19/2011	153.92	147.79
12H008	-84.22	31.22	7/21/2011	120.74	123.31
10H009	-84.50	31.23	7/31/2011	121.85	111.03
08H009	-84.68	31.24	7/18/2011	142.60	144.21
07H026	-84.77	31.24	7/19/2011	136.00	146.76
07H025	-84.84	31.25	7/19/2011	149.52	152.92
05J007	-85.00	31.26	7/19/2011	172.54	168.74
06J009	-84.90	31.29	7/19/2011	174.28	160.05
13J001	-84.04	31.29	7/21/2011	151.07	154.47
11J012	-84.32	31.30	7/31/2011	114.13	117.84
10J003	-84.39	31.30	7/19/2011	123.40	126.81
07J012	-84.78	31.32	7/18/2011	158.37	162.71
13J014	-84.00	31.34	7/20/2011	167.80	163.08
13J004	-84.12	31.36	7/31/2011	136.05	145.65
11J003	-84.34	31.36	7/19/2011	140.66	137.84
14J019	-83.88	31.37	7/20/2011	177.99	180.88
14J022	-83.93	31.37	7/20/2011	169.47	179.64
08K001	-84.65	31.38	7/31/2011	196.59	195.07
12K001	-84.16	31.38	7/20/2011	132.70	139.32
14K008	-83.98	31.40	7/20/2011	182.97	176.38
11K016	-84.35	31.41	7/19/2011	138.59	149.19
12K009	-84.18	31.43	7/19/2011	134.71	142.19
14K013	-83.92	31.43	7/20/2011	178.82	188.38
12K014	-84.19	31.44	7/31/2011	132.21	144.19
13K017	-84.06	31.44	7/18/2011	148.11	157.33
12K013	-84.16	31.45	7/20/2011	148.65	141.69
11K033	-84.35	31.45	7/20/2011	163.27	157.00
12K010	-84.19	31.45	7/19/2011	141.77	147.02
12K110	-84.17	31.47	7/20/2011	140.42	145.42
14K012	-83.91	31.48	7/21/2011	198.58	197.16
12K115	-84.16	31.48	7/20/2011	141.55	144.21
11K043	-84.32	31.49	7/18/2011	156.73	162.81
12K173	-84.23	31.48	7/20/2011	154.68	152.66
10K005	-84.46	31.48	7/31/2011	157.80	176.86

Site Name	Longitude	Latitude	Date	Observed	Simulated
11K003	-84.26	31.49	7/31/2011	156.46	155.84
09K012	-84.53	31.49	7/18/2011	177.59	181.79
12K180	-84.16	31.50	7/31/2011	142.41	144.30
12K141	-84.22	31.50	7/31/2011	153.08	155.14
12L373	-84.17	31.50	7/31/2011	142.94	146.42
12L370	-84.18	31.51	7/31/2011	141.49	150.09
12L352	-84.22	31.51	7/19/2011	153.84	157.13
14L013	-83.95	31.51	7/21/2011	205.27	195.54
12L277	-84.21	31.51	7/31/2011	152.89	155.06
12L353	-84.23	31.51	7/19/2011	154.17	159.22
12L272	-84.20	31.51	7/19/2011	148.42	155.92
13L012	-84.11	31.52	7/31/2011	146.99	151.84
12L351	-84.21	31.52	7/19/2011	153.26	157.35
12L030	-84.17	31.53	7/31/2011	148.29	150.42
12L344	-84.22	31.53	7/19/2011	156.39	160.58
15L020	-83.82	31.53	7/31/2011	202.24	202.52
09L029	-84.51	31.55	7/18/2011	198.30	194.76
11L020	-84.31	31.55	7/19/2011	183.00	177.99
11L111	-84.37	31.56	7/20/2011	189.70	186.11
14L006	-83.93	31.57	7/22/2011	218.90	212.44
12L029	-84.15	31.58	7/31/2011	150.75	159.65
11L092	-84.28	31.58	7/19/2011	188.83	184.20
13L049	-84.09	31.59	7/31/2011	162.18	167.35
10L004	-84.48	31.59	7/18/2011	211.77	209.56
11L112	-84.34	31.60	7/20/2011	197.18	201.83
13L047	-84.01	31.61	7/18/2011	198.68	205.98
14L014	-83.92	31.62	7/22/2011	231.79	226.33
12M017	-84.16	31.64	7/31/2011	189.46	188.68
16M027	-83.72	31.64	7/18/2011	199.49	211.22
11M025	-84.35	31.64	7/21/2011	235.03	230.86
15M005	-83.82	31.65	7/22/2011	242.18	223.86
15M013	-83.76	31.66	7/19/2011	230.72	218.43
15M004	-83.83	31.69	7/21/2011	253.13	230.73
13M056	-84.03	31.69	7/20/2011	214.40	219.95
11M017	-84.26	31.70	7/21/2011	230.56	217.62
11M041	-84.36	31.71	7/21/2011	266.01	254.35
13M027	-84.10	31.71	7/20/2011	205.52	218.13
13M066	-84.11	31.73	7/20/2011	212.63	220.27
13N007	-84.07	31.87	7/20/2011	251.63	260.10
13M086	-84.06	31.75	7/20/2011	213.11	228.64
10N024	-84.43	31.76	7/21/2011	293.10	297.12
13N003	-84.12	31.80	7/20/2011	241.88	236.92

Site Name	Longitude	Latitude	Date	Observed	Simulated
12N004	-84.17	31.87	7/20/2011	256.51	258.49
15P018	-83.83	31.95	7/19/2011	264.78	274.31
13P019	-84.03	31.99	7/19/2011	285.81	264.98
15Q016	-83.85	32.03	7/31/2011	247.91	289.28

Appendix B

Stream Gauging Stations from USGS

B. 1. USGS streamflow gauging stations for stream-stage calculation

Table B.1. List of stream gauge stations from USGS (with coordinates in degree, minutes and seconds) used for stream stage calculation in MODFE.

Site ID	Latitude	Longitude
02343801	31°15'33"	85°06'37"
02350512	31°43'30"	84°01'07"
02350900	31°45'52"	84°15'12"
02351890	31°46'34"	84°08'22"
02352500	31°35'39"	84°08'39"
02353000	31°18'25"	84°20'20"
02353265	31°31'37"	84°34'58"
02353500	31°22'58"	84°32'47"
02354500	31°21'02"	84°28'57"
02354800	31°17'38"	84°29'31"
02355350	31°13'03"	84°28'15"
02357000	31°02'25"	4°44'24"
02358000	30°42'03"	84°51'33"

B. 2. USGS streamflow gauging stations for stream-aquifer flux calibration

Table B.2. List of stream gauge stations from USGS (with coordinates in degree, minutes and seconds) used for calibration of stream-aquifer flux. The streamflow values are in cubic feet per second (cfs).

Station Number	Latitude	Longitude	Streamflow (cfs)	Date
02355600	31.20	-84.50	0.00	7/23/2011
02355880	31.09	-84.33	0.00	7/21/2011
02355950	30.94	-84.52	0.00	7/21/2011
02356600	31.21	-84.73	0.00	7/23/2011
02356970	31.11	-84.78	0.00	7/23/2011
02350220	31.96	-83.88	41.80	7/21/2011
02350300	31.91	-83.86	0.00	7/23/2011
02350360	31.84	-83.86	7.43	7/23/2011
02350509	31.76	-83.98	1.21	7/24/2011
02350524	31.72	-83.99	3.72	7/24/2011
02350527	31.67	-84.00	7.56	7/22/2011
02352980	31.33	-84.33	0.32	7/22/2011
02356220	31.31	-84.75	0.00	7/22/2011
02356640	31.17	-84.74	126.00	7/23/2011
02356290	31.37	-84.88	10.40	7/22/2011
02356460	31.28	-84.82	43.80	7/22/2011
02351900	31.73	-84.13	160.00	7/21/2011
02351930	31.65	-84.11	105.00	7/23/2011
02357050	30.98	-84.75	81.20	7/24/2011
02357150	30.90	-84.75	158.00	7/23/2011
02356100	31.41	-84.78	2.96	7/22/2011

Appendix C

Raingauges from National Climate Data Center (NCDC)

C. 1. Raingauge station from NCDC for infiltration calculation

Table C.1. List of raingauges (with their coordinates in degrees, minutes and seconds) from NCDC for the calculation of infiltration.

Station Name	Latitude	Longitude
Albany	31.58	84.16
Cordele	31.96	83.78
Americus	32.07	84.22
Colquitt	31.17	84.72
Butler	32.55	84.23
Milledgeville	33.08	83.23
Cairo	30.88	84.21
Ashburn	31.70	83.65
Haddock	33.03	83.42
Crisp Co. Power Dam	31.85	83.95
Woodruff Dam	30.70	84.86
Danville	32.60	83.24
Macon	32.83	83.65
Camilla	31.23	84.20